UNIVERSITY OF NAPLES "FEDERICO II"

FACULTY OF ENGINEERING

Ph.D. THESIS IN MATERIALS AND STRUCTURES ENGINEERING

BIOMATERIALS

XXVI CYCLE (2011-2014)

DEVELOPMENT OF NOVEL HYALURONIC ACID BASED SYSTEMS TOWARDS REGENERATIVE MEDICINE AND DRUG DELIVERY

Luisa Russo

PhD Coordinator

Ch.mo Prof. G. Mensitieri

Supervisor

Ch.mo Prof. P.A. Netti

ABSTRACT

Hyaluronic acid (HA) is a natural linear glycosaminoglycan that, thanks to its peculiar properties such as biocompatibility, resorbability and the possibility for an easy chemical functionalization, currently represents one of the most attractive building block for the preparation of advanced biomaterials for many biomedical applications.
The overall aim of this thesis was to design, prepare and characterize advanced HA based systems for applications in regenerative medicine and drug delivery.
However although HA is an excellent biomaterial, due to its hydrophilic nature, native HA is unsuitable to encapsulate hydrophobic drugs.
Furthermore native HA exhibits physico-chemical properties incompatible to form stable structures to be used in vivo for regenerative medicine and drug delivery applications. Infact when HA is injected in physiological environment, it is subjected to a degradation process due to its high hydrophilicity and to the action of an enzyme known as hyaluronidase.
For these reasons in this study in order to obtain HA stable nanostructures, able to incorporate hydrophobic drugs, two strategies were developed. The first strategy was to realize nanostructured systems in which HA was anchored onto nanoparticles, based on hydrophobic polymers, containing drugs; the second strategy was to modify HA molecules with hydrophobic groups. Moreover to obtain a HA stable structure at macroscale for regenerative medicine application, HA molecules were modified by a crosslinking reaction.

In particular in the first part of the thesis the design, the preparation and the characterization of HA-coated biodegradable nanoparticles (NPs) as new drug carriers for tumor targeting were reported. In particular the idea was to bind a HA shell to a biodegradable core (Polylactic-coglycolic acid (PLGA) particle) by means of a physical binding using an anphiphilic polymer, known as Pluronic ®, that acts as a bridge between the hydrophobic PLGA and the hydrophilic HA.
One of the most challenge in the design of nanoparticles is an efficient targeting. NPs can passively accumulate into tumors, taking advantage of enhanced permeation and retention (EPR) effect. However, NPs *in vivo* efficacy can be hampered by lack of cell internalization and/or by the fact that the loaded drugs may be released before

nanoparticles uptake. HA is an attractive material for tumor targeting delivery since it can specifically bind to the cancer cells overexpressing at their surface CD44, an HA binding receptor. Thanks to this specific interaction, HA binding to the tumor cells and its subsequently internalization are strongly enhanced. In light of this the HA based nanoparticles realized in this project can be efficiently internalized by the tumors cells by means of both a passive and an active targeting strategy.

NPs were prepared by a single emulsion technique and characterized for their morphology, size, and surface charge. HA based nanoparticles shown a spherical shape and a size ranging from 170 to 300 nm. Bare PLGA particles shown immediate aggregation phenomena; HA addition allowed to obtain stable NPs size for more than 10 days. Furthermore Irinotecan, a widely employed chemotherapeutic drug, was chosen to load NPs, and its *in vitro* release kinetics were assessed. The results demonstrated that nanoparticles were able to sustain Irinotecan release for at least 24 days.

The second part of the thesis deals with the development of amphiphilic hyaluronic acid derivative towards the design of micelles for the sustained delivery of hydrophobic drugs and for the viscosupplementation. The new syntetized amphiphilic HA derivative is an octenyl succinic anhydride (OSA) modified HA, obtained through a simple reaction in an aqueous medium involving exclusively HA hydroxyl groups. In this way it was possible to overcome the problems related to the HA modifications that involve carboxylic groups, which result in an alteration of the distribution of negative charges along the polymer backbone at physiological pH and probably affect fundamental biological and pharmacological HA properties.

A morphological, dimensional, calorimetric and rheological studies of this novel HA derivatives were conducted. Furthermore the ability of this novel amphiphilic HA derivative to self-assemble into micelles and to act as a solubility enhancer and as a modulator of release kinetics of a hydrophobic anti-inflammatory drug was demonstrated. In particular from morphological analysis it resulted that micelles are spherical objects with diameters around 100 nm. Differential scanning calorimetric (DSC) analysis revealed that the ability of HA to sequester water seems to be enhanced

by the introduction of lipophilic functions within HA molecules, resulting in a further decrease of the fraction of free water able to freeze compared to the unmodified HA.
Moreover in the perspective of using the novel OSA derivatives as viscosupplementation product, the rheological features assume a crucial role since they must properly restore the biomechanical functions of the normal synovial fluid. From a rheological point of view OSA-HA solutions appeared to be an appropriate tool to be used in viscosupplentation therapy owing to their suitable viscoelastic features; infact the OSA-HA solutions exhibit a rheological behavior similar to the human synovial fluid, that is viscous at low frequencies and prevalently elastic at high frequencies and characterized by the presence of crossover frequency.
Concerning release studies, the results indicated that OSA-HA is able to self-assemble into micelles, load a hydrophobic drug and release the active molecule with controlled kinetics. In particular, the analysis of release profiles shown that drug diffusion into the gel is faster compared to gel/drug dissolution with the dissolution contribution becoming more and more relevant as the OSA-HA concentration increases.

In the third part of this thesis the optimization and the characterization of HA hydrogels for regenerative medicine were reported. HA hydrogels, produced crosslinking HA molecules with divinyl sulfone (DVS) and based on a simple, reproducible and safe process that does not employ any organic solvents, were developed. Owing to an effective purification step, the resulting homogeneous hydrogels do not contain any detectable residual crosslinking agent and are easier to inject through a fine needle.
HA hydrogels were characterized in terms of their viscoelastic and network structural properties. They exhibit a rheological behavior typical of a strong gel and show improved viscoelastic properties by increasing HA concentration and decreasing HA/DVS weight ratio. Furthermore it was demonstrated that processes such as sterilization and extrusion through clinical needles do not imply significant alteration of viscoelastic properties. Moreover the crosslinks appear to compact the network, being a reduction of the mesh size by increasing the crosslinker amount.
In vitro and in vivo HA hydrogel degradation tests demonstrated that these novel hydrogels show a good stability against enzymatic degradation, that increases by increasing HA concentration and decreasing HA/DVS weight ratio.

Finally the hydrogels show a good biocompatibility confirmed by in vitro and in vivo tests.

In conclusion, HA coated nanoparticles composed of a hydrophilic shell and hydrophobic inner core were developed. These nano-sized particles could be suitable tools for applications in drug delivery and in particular for cancer therapy, taking advantage of both passive accumulation in tumor tissues via the EPR effect and active targeting by the strong receptor-binding affinity of HA to CD44 receptor.
Furthermore soft nanostructures, based on an amphiphilic HA derivative, were developed. These HA derivatives represent novel and promising biomaterials for the realization of systems able to self-assemble into micelles, sustain the delivery of an anti-inflammatory hydrophobic drug, release the active molecule with a controlled kinetic and at the same time able to act as a viscosuplementation agent for the treatment of joints affected by osteoarthritis.
Moreover HA crosslinked hydrogels were developed; these systems represent promising injectable biomaterials for application in regenerative medicine.

TABLE OF CONTENTS

LIST OF FIGURES

LIST OF TABLES

LIST OF EQUATIONS

CHAPTER 1

Introduction: Hyaluronic Acid

In the last years increased attention has been paid on the use of hyaluronic acid or hyaluronan (HA) in the biomaterial field thanks to its peculiar properties such as biocompatibility, nonimmunogenicity, biodegradability and viscoelasticity.

HA was discovered in 1934 by Karl Meyer and John Palmer in the vitreous humour of bovine eyes [1]. The name *hyaluronic acid* originates from *hyaloid* (vitreous) and *uronic acid* [2].

It is a linear polyanionic polymer composed of repeating disaccharide units of D-glucuronic acid (GlcUA) and *N*-acetyl-D-glucosamine (GlcNAc), that are linked together through alternating beta-1,3 and beta-1,4 glycosidic bonds.

It belongs to the class of glycosaminoglycans (GAGs) and specifically it presents the most simple structure being the only one not covalently associated with a core protein and non-sulfated [3].

HA is a primary component of the extra-cellular matrix of the mammalian connective tissues. It is an important structural element in the skin and is present in high concentration in the synovial joint fluids, vitreous humor of the eyes, hyaline cartilage, disc nucleus and umbilical cord [4-8].

HA plays a major role in several functions in vivo such as lubrification of arthritis joints, viscoelastic properties of soft tissues and it is involved in important cell functions such as cell motility, cell matrix adhesion and cell organization [9-13].

Thanks to its biocompatibility, physical, chemical properties and due to the ease of chemical functionalization, HA has generated increasing interest among researchers and it is already used in several biomedical applications [3-14] such as regenerative medicine and drug delivery.

Herein an overview of the most important physical-chemical and structural properties of HA including some chemical modifications of the biopolymer to obtain HA derivatives

was shown. Moreover some examples of applications in biomedical field (such as cosmetic surgery, ophthalmology, otolaryngology, orthopedic surgery, tissue engineering, drug delivery) were reported.

1. 1 GENERAL FEATURES AND BIODISTRIBUTION

1.1.1 Origin

The HA production methods are based on extraction from animal sources or on microorganism fermentation.

The traditional method for HA production is based on extraction from animal sources such as rooster comb; this procedure, however, is expensive and requires an extensive purification of the crude product [15-16]. Furthermore the use of animal-derived biomolecules for biopharmaceutical applications is facing growing opposition because of the risk of cross-species viral and other adventitious agent contaminations.

For these reasons alternatives to the animal extraction of HA were gradually replacing by industrial techniques based on microorganism fermentation emerged in the 1990's.

In large industrial quantities, HA is produced by fermentation of strains of bacteria *Streptococci* such as *Streptococcus equi*, *Streptococcus zooepidemicus*, *Streptococcus equisimilis, Streptococcus pyogenes and Streptococcus uberis*.

However *Streptococcus* requires an expensive and very difficult fermentation, the use of substantial volumes of organic solvents, and finally the HA product can contain endo- and exotoxins.

The HA industrial manufacturing is recently devoted to the fermentation of *Bacillus subtilis* [6]. *Bacillus subtilis* represents a valid alternative to Streptococcus HA production because it is a non-pathogenic microorganism and the final HA product does not contain any endo- or exotoxins; moreover it's possible to have a better control on HA molecular weight (MW) and also *Bacillus subtilis* grows on minimal media in contrast to Streptococcus that requires more expensive and complex media for growth.

In this Ph.D. project, HA obtained by *Bacillus subtilis* fermentation and provided by Novozymes Biopolymer A/S, was used for its environmentally friendly production process and its ultra-purity.

1.1.2 Biodistribution and biological functions

HA is widespread in nature having been found in vertebrate soft tissues such as joints, synovial fluid (SF), skin, vitreous humour of the eye, umbilical cords, roster combs [17], in algae [18], in mollusks [19], and also in cultured eukaryotic cell lines, and certain prokaryotes, where it occurs as a mucoid capsule surrounding the cell [16] (table 1.1).

In the human body the largest amount of HA (7-8 g of hyaluronate per average adult human, or approximately 50% of the total in the body) resides in the skin, where it is present in both the dermis and the epidermis (0.5 mg/g wet tissue). It's well known that in a 70-kg individual there are around 15 g of hyaluronan, 5 g of which is turned over (degraded and synthesized) every day.

Tissue or fluid	Concentration (µg/ml)
Rooster comb	7500
Human umbilical cord	4100
Human synovial fluid	1400-3600
Bovine nasal cartilage	1200
Human vitreous body	140-340
Human dermis	200-500
Human epidermis	100
Rabbit brain	65
Rabbit heart	27
Human thoracic lymph	0.2-50
Human urine	0.1-0.3
Human plasma	0.01-0.1

Table 1.1: HA occurrence in different animal tissues and fluids

HA is involved in several functions in vivo. In the skin HA exhibits important structural and biological functions. As regards to the HA structural properties, it provides a matrix substrate for the distribution and organization of important molecules of the ECM such as proteoglycans (PG), fibrin, fibronectin, collagen and elastin [20] (Figure 1.1).

Furthermore it maintains tissue hydration [21] thanks to its ability to retain water and also it ensures at the same time space and cohesion between the cells in the skin, allowing the diffusion of both nutrients and waste products [22].

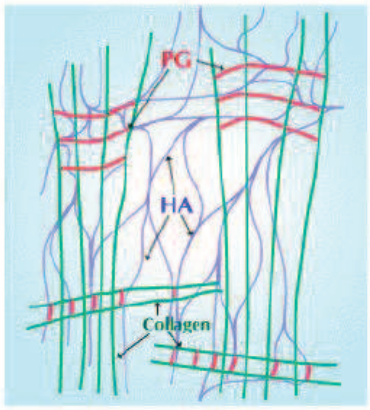

Figure 1.1: Organization of proteoglycans and collagen in HA matrices

http://www.glycoforum.gr.jp/science/hyaluronan/HA02/HA02E.html

Moreover it was demonstrated that HA provides to the elimination of free radicals generated by the ultraviolet rays from sunlight. The ultraviolet light inflicts oxidative stress on cells and may damage their genetic material, thus causing degeneration and death.

In cartilage, despite its relatively low content, HA functions as an important structural constituent of the matrix, forming an aggregation center for Aggrecan, a large chondroitin sulfate proteoglycan that retains its macromolecular assembly in the matrix due to specific HA–protein interactions [23].

In the synovial fluid, there is an elevated concentration of high MW HA which serves as shock absorber and provides necessary lubrication for the joints, reducing friction of the moving bones and thus diminishing wear. Under inflammatory conditions, such as osteoarthritis or rheumatoid arthritis, high MW HA is degraded by reactive oxygen species (ROS), which reduces its viscosity and its lubricant and shock absorbing properties, leading to deteriorated joint movement and pain [24].

HA is also involved in embryogenesis and is associated with cancer invasiveness and metastasis [25]. Moreover, HA has a wide MW, ranging from 1000 to 10,000,000 Da, and it playes different roles in the body depending on its MW. For example, high MW

HA, is space-filling, anti-angiogenic, and immunosuppressive, whereas the intermediate-sized polymers comprising 25–50 disaccharides are inflammatory, immunostimulatory, and highly angiogenic. Smaller HA oligosaccharides seem to function as endogenous danger signals. Some of the variably sized fragments trigger different signal transduction pathways [26].

HA is also known to play a role in promoting cell proliferation, differentiation and migration [27-28] by binding with cells with specific interactions. These processes infact are mediated by proteins, known as hyaladherins, that act as cellular receptors for HA. Examples of HA receptors are cluster determinant 44 (CD44) [29], receptor for hyaluronate-mediated motility (RHAMM) [30], HA receptor for endocytosis (HARE) [31-32], and lymphatic vessel endothelial hyaluronan receptor-1 (LYVE-1) [33]) that can recognize and bind HA selectively. Within these receptors, CD44 and RHAMM have attracted much attention because they are involved in metastasis [34-37]. In particular CD44 is the best characterized transmembrane HA receptor; it is expressed on the surface of several cells such as leucocytes, fibroblasts, keratinocytes and epithelial and endothelial cells [38], and it is also involved in different cellular processes (cell adhesion, migration, proliferation and activation as well as HA degradation and uptake) [39].

RHAMM was found on cell surfaces and also in the cytosol and nucleus [39]. It was demonstrated that it's involved in regulating cellular response to growth factors and in cell migration, particularly for fibroblasts and smooth cells [40].

1.2 Physical and chemical properties of HA

HA is a linear polysaccharide composed of repeating disaccharide unit of D-glucuronic acid and N-acetyl-D-glucosamine, that are linked together through alternating β-1,4 and β-1,3 glycosidic bonds [2, 41-42] (Figure 1.2).

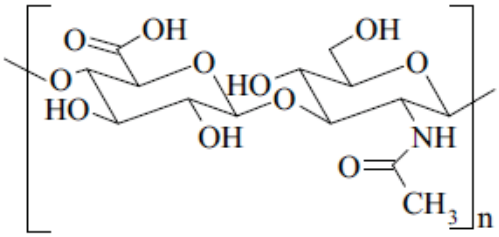

Figure 1.2: Molecular structure of the HA repeating unit

The number of repeating disaccharide units in a HA molecules can reach 10000 or more, that generates large molecules of up to several million daltons in weight and up to 10 μm in length.

One of the main properties of HA, that makes this molecule attractive for several biomedical applications, is its capacity to retain water being a highly hydrophilic polymer [43]. In aqueous solution, due to the combination of different interactions (intra and intermolecular hydrogen bonding, hydrogen bonding with the solvent and intermolecular non-polar/hydrophobic interactions), HA exhibits preferred structures known as the primary, secondary and tertiary structures [44-46].

The primary structure is related to the sequence of HA disaccharide units. The secondary structure in HA solutions is due to the formation of intramolecular hydrogen bonding (including interaction between D-glucuronic acid and N-acetyl-D-glucosamine and between two neighboring disaccharide units [24, 47-49]), and between the HA molecule and the solvent (Figure 1.3).

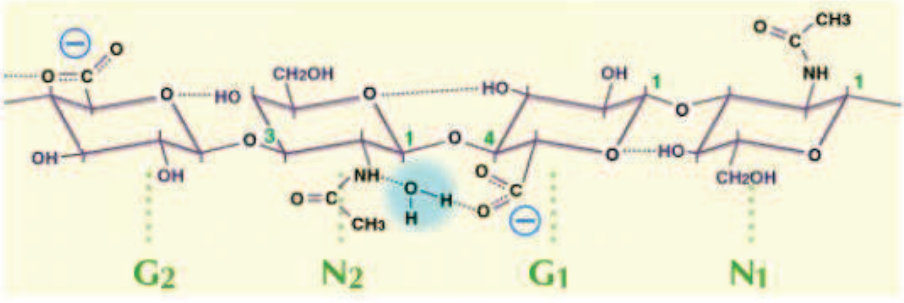

Figure 1.3: Intramolecular hydrogen bonding and hydrogen bonding with the solvent in aqueous HA solutions.

http://www.glycoforum.gr.jp/science/hyaluronan/HA02/HA02E.html

The sugar rings are relatively fixed in their shape; instead in correspondence of oxygen atom between two neighboring disaccharide units, it's possible a rotation of 180 degree. In particular each disaccharide unit could in principle rotate of 360 degree, but the configurations are limited by the presence of intramolecular hydrogen bonding and hydrogen bonding with the solvent. Due to this twist in the chains, the molecule assumes a two-fold helix structure (Figure 1.4).

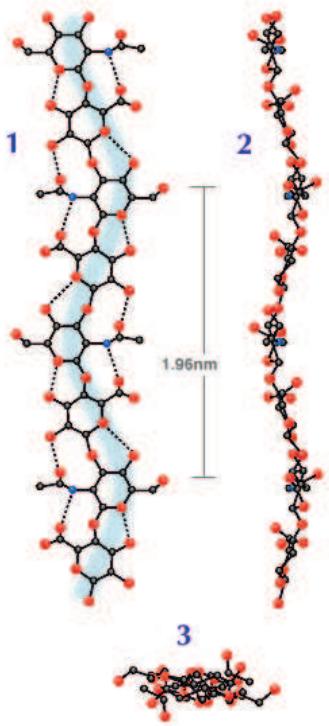

Figure 1.4: Plan (1) and elevation (2) computer drawn projections of HA and view along the two-fold helix axis

http://www.glycoforum.gr.jp/science/hyaluronan/HA02/HA02E.html

Due to the presence of intermolecular nonpolar/hydrophobic interactions and intermolecular hydrogen bonding between neighboring HA chains, HA shows also a tertiary structure. Infact the axial hydrogen atoms of about 8 CH groups on the alternating sides of the secondary structure create secondary hydrophobic faces that energetically favor the formation a meshwork-like β -sheet tertiary structure as a result of molecular aggregation. The hydrophobic and hydrogen bonding interactions, countering electrostatic repulsion, allow HA molecules to aggregate leading to the formation of molecular networks (matrices) of HA. This structure is rigid and very

stable, even if it has some degree of flexibility and a large number of conformations are possible. It is also to be noticed that the tertiary structure of hyaluronan is sensitively dependent on the environment, it varies with pH and ionic strength, a behavior typical of a flexible polyelectrolytes. In particular it was demonstrated that HA chains contract with increasing ionic strength and decreasing pH [42].

Significative informations about the conformation of HA molecules in water can be obtained by dynamical mechanical analysis. This allows to obtain the viscoelastic properties of the materials by measuring the response of a sample when it is deformed under small periodic oscillation in shear [50].

Moreover the knowledge of HA solution viscoelastic properties allows to get informations on the solution structure thus giving the possibility to engineer the solution performance for the specific biomedical application.

From this analysis it is possible to obtain the dependence of the elastic modulus, G'(ω) and the viscous modulus G"(ω) upon frequency, the so called mechanical spectra. In particular G' gives information about the elasticity or the energy stored in the material during deformation, whereas G" describes the viscous character or the energy dissipated as heat.

The ratio between the viscous modulus and the elastic modulus is expressed by the loss tangent:

$$\tan\delta = \frac{G''}{G'} \qquad (1.1)$$

where δ is the phase angle. The loss tangent is a measure of the ratio of energy lost to energy stored in the cyclic deformation. The phase angle, δ, is equal to 90° for a purely viscous material, 0° for a pure elastic material, and 0°< δ <90° for viscoelastic materials [51]. The information on the HA structural properties can be obtained by analyzing the mechanical spectra of HA solution [52].

HA based materials exhibit different viscoelastic properties. They can indeed behave as diluite solutions (Figure 1.5) or entangled solutions (Figure 1.6) depending of the concentration and MW of HA.

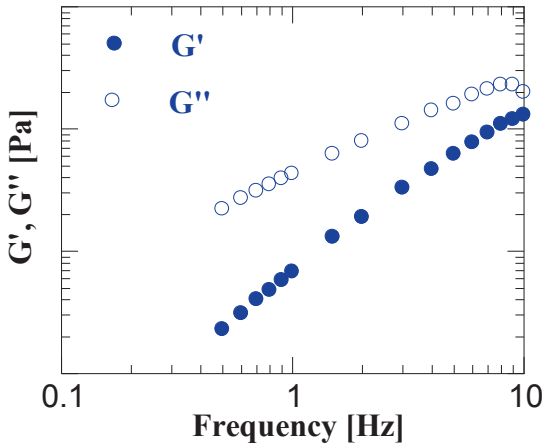

Figure 1.5: Mechanical spectra of HA solutions at low molecular weight

Low MW HA solutions [150 KDa] behave as diluite solutions as reported in figure 1.5. The mechanical spectra is characterized by a loss modulus greater than elastic modulus in all frequency range; these results suggest that no topological interaction, such as entanglement, occurs among HA chains, so HA molecules can flow as individual flow unit.

Due to the expansion of HA random coil in water, the molecular weight increases also at low concentration leading to a different rheological behavior. Indeed even at low concentration high molecular weight solutions exhibit entangled network.

The solution shows a viscous behaviour at low frequency (G''>G') and a prevalently elastic one at high frequencies (G'>G''), as reported in Figure 1.6. The limit between the two regions is represented by the crossover frequency, usually expressed as ω_c.

This behaviour can be explained by considering that at low frequency entanglements among the chains occur and the molecular chains can release stress by disentanglement and molecular rearrangement during the period of oscillation, and hence, the solution shows viscous behavior (G''>G'); instead at high frequency molecular chains cannot disentangle during this short period of oscillation, and therefore, they behave as a temporary cross-linked network, and the elastic behavior (G' > G'') is prevalent [5-6, 53].

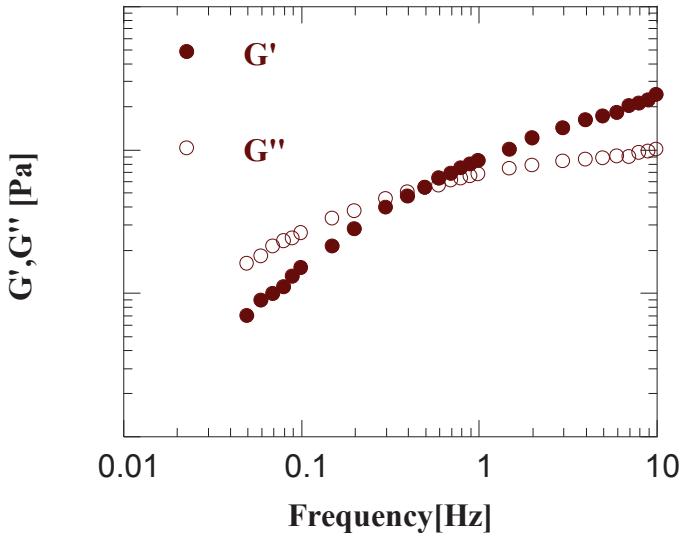

Figure 1.6: Mechanical spectra of HA solutions at high molecular weight

Moreover by increasing HA concentration, the viscoelasticity of the solutions increases [54-57]. The viscoelastic properties of HA in aqueous solution are also influenced by the presence of small molecular agent [58-60]. For example, the presence of phospholipids, guanidine, and sodium chloride leads to decreases in both elastic and viscous moduli. The effect of these compounds on the viscoelasticity is due to the disruption of intermolecular interactions and reduction in the entanglement between HA molecules [61].

1.3 Degradation

1.3.1 Enzymatic degradation

In physiological environment HA is subjected to a degradation process due to the action of three type enzymes, hyaluronidase (or hyase), b-d-glucuronidase, and β-N-acetyl-hexosaminidase [62-63]. As regards to hyaluronidase, the degradation mechanism is based on the cleaving high molecular weight HA into smaller oligosaccharides. On the other hand b-d-glucuronidase, and β-N-acetyl-hexosaminidase further degrade the oligosaccharide fragments by removing nonreducing terminal sugars [39].

Thanks to the hyaluronidase action, HA is used in combination with drugs to improve their dispersion and delivery. Infact hyaluronidase action allows to decrease the viscosity of HA, that is a component of interstitial barrier; in this way it's possible to improve tissue permeability [64].

1.3.2 Ultrasonic degradation

The treatment of HA by means of sonication causes HA degradation. In particular it was demonstrated that there is a linear relationship between the reaction time and the reciprocal of the square of HA molecular weight [65-68].
Furthermore HA high molecular weight chains appear to degrade more slowly than HA low molecular weight chains. It is important to underline that ultrasonic treatment does not allow complete degradation of HA in monomers, regardless ultrasonic energies and HA molecule type [69-70].

1.3.3 Ph-dependent and thermal degradation

Temperature and pH are also factors that can imply degradation of HA. In particular it was demonstrated that at alkaline pH HA degrades randomly, because there is the cleaving of hydrogen bonding that takes part in structural organization of HA, resulting in a flexible random coil [71]. Furthermore HA solutions in acid media are subjected to degradation [72].
Thermal degradation of HA solutions also occurs. It was proved that the viscosity decreases in function of time and exponentially in function of the temperature [73-74].

1.4 HA derivatives

Thanks to its above mentioned physical-chemical properties and to its large-scale production, in the last decades HA has been used in several applications. At the same time, however, the enlarged use of this biopolymer has led to consider some disadvantages such as its short *in vivo* residence time, due to the degradation catalyzed by hyaluronidase [75], and its poor mechanical properties. To overcome these drawbacks, various chemical modifications of the HA structure have been developed to synthesize new HA derivatives which are less susceptible to chemical and enzymatic

hydrolysis and show enhanced mechanical properties [76]. Chemical modifications of HA target three different functional groups: the primary and secondary hydroxyl groups, the glucuronic acid carboxylic group and the N-acetyl group (after deacetylation). Usually hydroxyls are modified through etherification, divynilsulfone crosslinking, esterification and bis-epoxide crosslinking, whereas carboxylates are modified by carbodiimide-mediated reactions, esterification and amidation. When modifying HA, it has to be taken into account that modifications carried on the -COOH can alter the HA biological behavior in the body because the carboxylic groups are the recognition sites for hyaluronidase and HA receptors [77]. For this reason, in many case low degree of modification are preferred to preserve the HA biological characteristic.

HA can be modified through two main ways, conjugation or crosslinking; in the first case, a compound is grafted onto HA chain, whereas in the second case different HA chains are linked together (Figure 1.7). Crosslinked HA are also commonly referred to as hylans and can reach very high molecular weight (up to $23x10^6$ Da) and prolonged *in vivo* residence time (1.5-9 days) [24, 78].

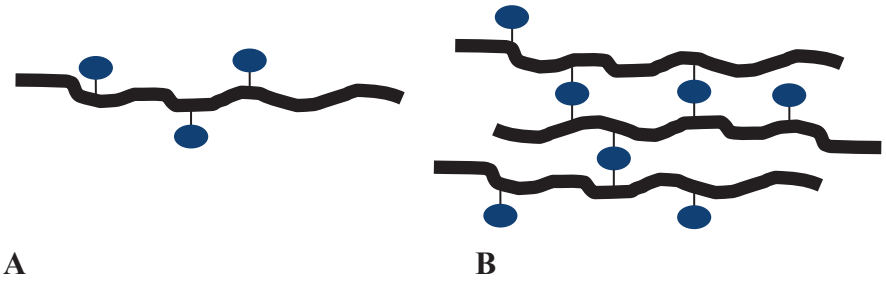

Figure 1.7. Chemical conjugation (A) and chemical crosslinking (B) of a polymer

To crosslink or conjugate HA polymers, numerous methods have been developed in organic solvents, such as dimethylformamide (DMF) or dimethylsulfoxide (DMSO). In this case, the native HA, which is in the form of a sodium salt, needs to be in its acidic form or a tetra-butylammonium salt (HA-TBA) for solubilization in organic solvents. However this requires additional steps of physical and chemical treatments that can induce HA chain hydrolysis [79-81].

Recently, a new appealing classification for HA derivatives has been proposed, it considers two different categories, “monolithic” and “living” HA derivatives [82-83]. The first arise when the chemical modification gives a final structure that cannot form

new covalent bonds in the presence of cells or tissues and can only be pre-fabricated in different forms. On the contrary, living HA derivatives can be further modified or crosslinked in the presence of cells or tissues enabling a change in their physical form during *in vivo* or *in vitro* use.

Figure 1.8 shows an hypothetical structure of an HA octasaccharide, containing some chemical modifications targeting the carboxylic acid or the primary hydroxyl group of the N- acetylglucosamine. Some of these modifications are monolithic, like the benzyl ester, the HYADD type amide, the divinyl sulfone (DVS) and the butane-1,4-diol diglycidyl ether (BDDE), while the others are examples of living HA derivatives.

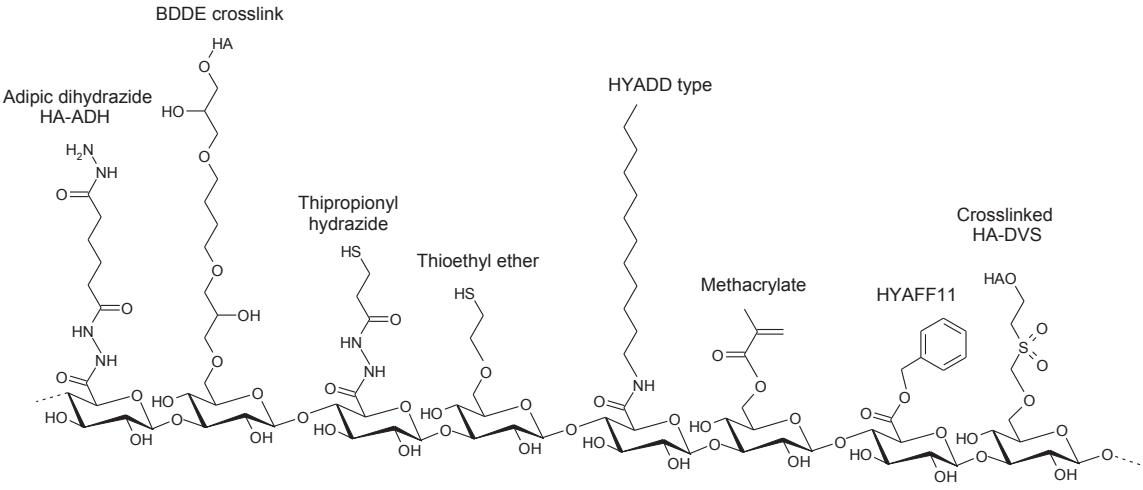

Figure 1.8. An hypothetical HA octasaccharide showing some chemical modifications.

Concerning the modification of the carboxylic group of the glucuronic acid, one of the most widely used reaction is the amidation [84-85], that usually need an activator agent. 1-ethyl-3-[3-(dimethylamino)-propyl]-carbodiimide (EDC) is one of the preferred among the carbodiimide based activator agents because of its water solubility. EDC reacts with the HA carboxylic acid forming an O-acyl isourea-HA intermediate, which in turn react with the chosen amine to form the amide bond. However the O-acyl isourea intermediate is very reactive and can hydrolyze and then rearrange into a stable N-acyl urea by-product. In this regard, Bullpitt reported the use of N-hydroxsuccinimide (NHS) and 1-hydroxybenzotriazole (HOBt) with EDC to form a less hydrolyzable intermediate thus preventing the formation of the N-acylurea by-product [39]. One of main

advantages of the amidation using EDC is that it can be performed in water using the native HA. However, some authors have developed dimethyl sulfoxide (DMSO) methodologies on the acidic form of the HA to minimize the EDC hydrolysis thus reaching substitution degrees of up to 60-80% [39, 86]. Kuo *et al.* demonstrated that carbodiimides can also be used as the reagent, not only as the activator agent, and using biscarbodiimides managed to crosslink HA and form stable bis(N-acylurea) crosslinked gels [87]. Nonetheless, using dihydrazides, like the adipic hydrazide (ADH) no crosslinking was observed, but only single functionalization (Figure 1.8 for HA-ADH) [88].

EDC-hydrazide chemistry has also been to introduce thiol groups on the HA chain (Figure 1.8). This result was accomplished by EDC-mediated reaction of HA with disulfide containing dihydrazide, followed by reduction with dithiothreitol (DTT) [89].

Amidation using CMPI (2-chloro-1-methylpyridinium iodide) as the activator agent is usually performed in DMF, thus HA have to be converted into the tetrabutylammonium salt (HA-TBA) through additional steps of preparation and purification [90]. With this method high degree of substitution up to 100% can be achieved, therefore it is higly effective. In addition, if no amine is added to the reaction medium, the CMPI-activated HA reacts with its own hydroxyl groups, forming an auto-crosslinked HA gel through ester crosslink between the HA chains [91]. These crosslinked HA products have been prepared by Fidia and are referred to as Auto Crosslinked Polysaccharide (ACP) gels. In gels of this kind, no bridge molecules are present, thus during their *in vivo* degradation, only natural components of HA are released [91].

The amidation of the -COOH of the glucuronic acid with alkylamides having long carbon chain (Figure 1.8) has also led to a class of amphiphilic HA amide derivatives called HYADD® and patented by Fidia [92].

A further chemical modification that involves carboxylic group is the esterification; this can be performed using epoxides, diazomethane or by alkylation using alkyl halides or tosylate activation. These reactions are usually performed in an organic solvent, such as DMF, on the TBA salt of HA. Among the ester derivatives of HA, HYAFF is particularly interesting. These are a class of hyaluronan derivative polymer, patented by Fidia, obtained by esterifying the free carboxyl group with different types of alcohol (aliphatic, aryliphatic, cycloaliphatic, and others). These derivatives are

characterized by a reduced hydrophilic character that results in a decreased solubility in water and slightly increased in the structural rigidity of the macromolecule, caused by the interaction of hydrophobic group organized in hydrophobic patches. The benzyl ester of hyaluronan (Figure 1.8), called HYAFF11®, has been well-characterized from both the chemical–physical and biological point of view [93]. It has been showed that the numerous hydrophobic benzyl groups along the polymeric chain are probably organized in hydrophobic patches. This gives the molecule a more rigid structure and reduces its ability to interact freely with water molecules. Amphiphilic ester derivatives have also been synthesized in which a rather small proportion of the carboxylic groups (~10% mol) was esterified by long alkyl chains ($C_{12}H_{25}$ or $C_{18}H_{37}$) [82]. In this case an alkyl halide (dodecyl or octadecyl bromide) reacts with the HA carboxylic groups, preliminarily transformed into its TBA salts to be solubilized in DMSO.

For what concerns chemical modifications involving the -OH groups, one of the most common is the formation of ether using epoxides, DVS or ethylene sulfide. Among the epoxides, the most used is the BDDE (figure 1.8) which was patented for this reaction in 1986 by Malson and Lindqvist [94]. Nowadays BDDE is widely used for crosslinked HA hydrogels; the reaction consists of the epoxide ring opening to form ether bonds with the HA hydroxyl groups. Crosslinked HA hydrogels are also obtained using DVS, as reported in Figure 1.8, in this case, it has been demonstrated through histological assay that, even if the starting material is highly toxic, HA-DVS hydrogels are biocompatible [95].

Thiol groups can be added to the HA chain not only by modifying the –COOH, as previously mentioned, but also through reaction at the hydroxyl group. Indeed, Serban, Yang and Prestwich have used ethylene sulfide to synthesize 2-thioethyl ether HA derivatives (Figure 1.8) performing the reaction at pH 10 overnight and at pH 8.5 for 24 h after addiction of DTT.

The –OHs can also be converted into esters by reaction with activated compounds. For example it is possible to graft acyl-chloride activated carboxylate compound onto the hydroxyl groups of HA by chloroacylation with thionyl chloride. This reaction is performed at room temperature in an organic solvent, such as DMSO. Thus it is also possible to graft poly(lactic acid) (PLA) oligomers to the HA chain by first convert the

HA to a more hydrophobic salt like the cetyltrimethyl-ammonium bromide (CTA) salt, which is easier to prepare than HA–TBA [96].

Methacrylated HA is another type of esterification of the –OH groups of HA (Figure 1.8). It is usually performed using methacrylic anhydride in ice cold water for 12 h at pH 8–10. The obtained derivatives can be crosslinked by free-radical polymerization using UV-light (365nm) and a photo-initiator to obtain HA hydrogels.

HA can also be modified by oxidation with sodium periodate of the hydroxyl groups of the glucuronic acid moiety of HA to dialdehydes, thereby opening the sugar ring. This derivative has been employed to graft peptides to the HA by reaction with the aldehyde groups [97], or to crosslink with HA–hydrazide derivatives [98].

Eventually, even the N-acetyl group of the N-acetyl glucosamine can be a modification site after deacetylation [99]. In this way an amino group is recovered that can then react with an acid using the same amidation methods described before. However deacetylation can induce chain fragmentation. Platt and Szoka mention the possibility of using enzymes for HA deacetylation, which was previously performed on the N-acetylglucosamine moiety of heparin and heparan sulfate [100].

1.5 Applications

In the last decades, HA thanks to its peculiar properties, exposed before, have attracted a great deal of attention and have been extensively used in several biomedical applications such as regenerative medicine and drug delivery (table 1.2).

Biomedical Applications of HA	**HA role**
Viscosurgery	Tissue protection and lubrification
Tissue engineering	Scaffold to mimic extracellular matrix environment for tissue regeneration
Viscosupplementation	Tissue fluid replacement or supplementation
Viscoaugmentation	Tissue filling and augmentation
Drug delivery	Biocompatible nanocarrier for the controlled release of therapeutic drugs and agents

Table 1.2: Biomedical applications of HA based products

1.5.1 Ophthalmology

HA is one of the major components of the eye tissues and in particular of the vitreous body [5]. It is commonly used in ophthalmology and in particular in cataract surgery as Ophtalmic Viscoelastic Device (OVD) due to its peculiar viscoelastic properties. It is injected in the eyes during the procedures of the opaque lens removal and substitution with an artificial lens. HA provides a barrier and acts as a shock absorber between the tissues and the tools in order to protect the delicate eyes tissues, and keeps the space during surgical manipulations.

In general, an OVD requires specific rheological properties; it should be cohesive and have a high viscosity at low shear rates in order to maintain the space and to avoid ocular tissue collapse during the operation; on the other side it should be dispersive and have a viscosity which decreases rapidly with the deformation rate to ensure easy injection of OVD and adherence to tissues during the operation [101-103].

In order to fulfill the requirements for OVD as mentioned above, different strategies have been applied. Many products have been produced by varying molecular weight of the HA chain, obtaining OVD with cohesive or dispersive properties. Other OVD's have been realized by the combination of HA with other polymers such as chondroitin sulfate (named Viscoat) or a new binary combination with hydroxypropylmethyl cellulose (HPMC, named VISC26) [104], which seems to represent the formulation that better fulfill the OVD requirements showing both cohesive and dispersive properties.

In this case, the rheological synergy between HA and HPMC due to secondary interactions leads to a virtual increase of molecular weight and consequently high viscosity at low shear rate (cohesive properties), and at the same time it shows a decrease of viscosity at high shear rate due to the weakening of intermolecular interactions between the chains (dispersive properties).

1.5.2 Otolaryngology

The vocal folds (VF) are composed of twin infoldings of mucous membrane stretched horizontally across the larynx. They vibrate, modulating the flow of air being expelled from the lungs during phonation [105-107].

HA is one of the main components of ECM [3, 10, 108-109] of VF and plays an important role in phonation process because it directly affects their viscosity. In fact the energy involved in the process of the phonation can be divided in: 1) the energy to initiate phonation, known as phonation threshold pressure (*PTP*), and 2) the energy to sustain phonation (*Ep*). Both energies strongly depend on viscosity of vocal folds tissue. In particular *PTP* can be expressed by:

$$PTP = VDW/T \tag{1.2}$$

where V is the mucosal wave velocity, D is the tissue damping coefficient (which is proportional to tissue viscosity), W is the prephonatory glottal width, and T is the thickness of vocal folds. Moreover *Ep* can be expressed by:

$$Ep = (LT/D)\eta'\omega^2\xi^2 \tag{1.3}$$

where L, T and D are the length, thickness and depth of the vocal folds, respectively, η' is the tissue viscosity, ω is the angular frequency of oscillation and ξ is the vibrational amplitude [10, 110-111].

The viscoelasticity of VF depends on the ability of HA chains to dissipate energy during the phonation process. For this reason HA based products have been used in VF augmentation.

VF augmentation is used in therapy of scarring and paralysis of the vocal folds. During the phonation process the vocal folds are brought together near the centre of the larynx by muscle attached to the vocal folds basis. As air is forced through the vocal folds, they vibrate and produce sound. When vocal folds do not move well enough to be close to each other, a gap exists between them and the air leaks out too quickly thus causing the voice to sound breathy and weak. In this case to fill the gap, an augmentation substance is injected in the VF to achieve complete glottal closure.

However, the use of HA in VF augmentation is limited by its short residence time within vocal folds. In order to overcome this obstacle, derivatives of HA, obtained by chemically crosslinking the HA molecule, have been used as VF augmentation substances [112]. Furthermore it is seen that the HA based materials implies a durable tissue augmentation by attracting fibroblasts, which generated new collagen and ECM macromolecules [10, 113-114].

1.5.3 Orthopedic surgery

One of the main applications of HA is in the viscosupplementation of the joints affected by arthritis [115].

HA is present in high concentration in the ECM of joint tissues, including SF and the outer layer cartilage (figure 1.9) [116]. Thanks to its viscoelastic properties and its extraordinary capability to retain water, SF serves as lubricant and shock absorber [39, 117].

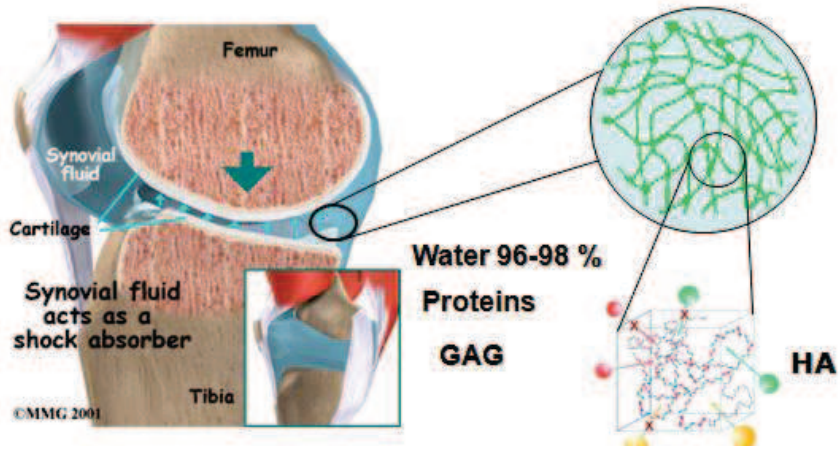

Figure 1.9: Schematic representation of joint tissue including synovial fluid and outer layer cartilage, that are characterized by a high HA concentration

When the joint is affected by osteoarthritis and rheumatoid arthritis there is a reduction of HA molecular weight [118-119] and concentration [120] in SF, which result in a decline in its viscoelastic properties [13]. The decrease of SF viscoelastic properties involves the degeneration of joints that become stiff and painful [7].

The purpose of viscosupplementation by intra-articular injection of HA is to restore the rheological properties (viscosity and elasticity) of synovial fluids [121] by normalizing the concentration and molecular weight of HA [122]. Furthermore viscosupplementation not only allows restoring its mechanical properties, it has also been observed to allow an induction of the synthesis of high-molecular weight (HMW) HA by synoviocytes [123].

Currently, several viscosupplementation products based on HA are commercially available. Some of them are characterized by HA with low molecular weight (HYALGAN® and ARTZ®), or intermediate molecular weight (ORTHOVISC®) but lower than that of the hyaluronan in normal healthy synovial fluid, and other are made of cross-linked HA (HYLAN®, DUROLANE®, SYNVISC®) [124].

Possible adverse events during the treatment of osteoarthritis by using HA based viscosupplementation products are joint infection, aseptic arthritis, and inflammation, even if in rare cases, being directly dependent upon the number of injections [125-127]. However, viscosupplementation with low MW HA preparations may have slightly higher risks and less benefits than viscosupplementation with high MW HA, because the relatively low MW HA preparations require more injections which may incur higher costs and chance of infection.

Recently, a series of derivatives have been obtained via amidation of the polymer carboxyl groups by long chain alkyl amine [99]. This covalent anchoring of hydrophobic side chains onto the hydrophilic polysaccharides results in an amphiphilic derivative. These derivatives show the associative behavior in water characteristic of amphiphilic species [80] and, given their appropriate viscoelasticity, can be considered promising candidates for use in viscosupplementation [13].

Moreover viscosupplementation products have shown their efficacy also in degenerative arthritis of the hip, ankle, shoulder and carpo-metacarpal joint of the thumb [128-141].

1.5.4 Tissue engineering

HA is a versatile macromolecule that shows great potential for tissue engineering (TE) applications [142] because of its non-immunogenic properties [143-144], widespread availability, and ease of chain size manipulation. The inclusion of HA has created

biocompatible biomaterials and engineered tissues that can be degraded controllably and can facilitate angiogenesis, osteointegration, and cell phenotype preservation.

HA is highly soluble in water and is quickly degraded in vivo by hyaluronidase; the short residence time of HA could be an obstacle to the structural integrity. In order to overcome this problem, different strategies have been used to stabilize HA as reported before, such as crosslinking or changes to the molecule chain of HA. Some of crosslinking methods include water-soluble carbodiimide crosslinking [145], polyvalent hydrazide crosslinking [146], DVS crosslinking [147], disulfide crosslinking [148], and photocrosslinking hydrogels through glycidyl methacrylate–HA conjugates [149].

As regards to the derivatives of HA, different esters and amides of HA have been used for tissue engineering approaches. For example a series of derivatives commonly used as polymeric scaffolds are HYAFF® obtained from esterification of the carboxyl groups of hyaluronic acid with different alcohol residue [80]. On the other side amides of HA, HYADD®, have been proved as bioactive and suitable vehicle to carry cells for tissue engineering procedures [150].

In the tissue engineering field, HA and its derivatives have also been blended with other polymers such as polylactic-*co*-glycolic acid (PLGA) [151], polyethylene glycol (PEG) [152] and collagen.

HA derivatives and their blends have been used as scaffolds for the regeneration of several tissues such as skin, cartilage, fibrocartilage, bone, intervertebral disc, adipose tissues, vascular tissues and heart valves.

Because HA is present in high concentrations in the skin and has both structural and regulatory functions during the wound healing process [153], it has been considered as an appropriate candidate to support skin tissue regeneration. It was demonstrated that crosslinked HA hydrogel films accelerate the process of the wound healing [10]. It was proposed that it is possible due to creation of a hydrated and non-immunogenic environment, suitable for tissue repair.

Moreover in skin tissue engineering to obtain epidermal and dermal-like tissues layers, three-dimensional scaffolds made up of benzyl esters of hyaluronan (HYAFF11®) and cultured in vitro with keratinocytes and fibroblasts, have been used [10, 154-155].

HYAFF11®, in the form of sponges, was proved to be effective in adipose tissue regeneration in a nude mouse model [156-158]. In particular, sponges with small and

large pore sizes were obtained using a salt leaching technique. A hydrophilic HA coating was added to the scaffold structure with the main aim to facilitate the process of cell (preadipocyte) seeding, through a fast medium absorption. The coating was realized by immersion of HYAFF11® sponges in an aqueous solution of HA biopolymer at a known concentration, and were subsequently freeze-dried [11].

For engineering fibro-cartilaginous tissues such as the central part of the meniscus, porous three dimensional composite scaffolds, based on HYAFF11® reinforced with polycaprolactone (PCL) [159], realized by phase separation technique and seeded with human chondrocytes, have been produced.

HA derivatives have also been used as scaffolds for the regeneration of nucleus pulposus (NP) tissue engineering. In particular, a dodecylamide of HA, HYADD3®, has been proved as bioactive and suitable vehicle to carry cells for NP tissue engineering, while a crosslinked HA ester, HYAFF120®, showed interesting results if used as an injectable acellular material [160].

Benzyl derivatives of HA (Hyalograft® C and HYAFF11®) were also used as scaffolds for tissue engineering of cartilage [161]. It was demonstrated that cell seeded HYAFF11® scaffolds, when implanted in mice, develop into tissues resembling hyaline cartilage. It was noticed that both collagen type I and type II were present in the newly formed tissue even if collagen type I is considered a negative phenotypic marker, indicative of dedifferentiated chondrocytes.

Recently, human clinical results for Hyalograft® C scaffolds have revealed more optimistic findings. It was reported that after implantation of the Hyalograft®, the grafts had integrated surrounding cartilage, and developed tissue in the locations of damaged tissues [162].

1.5.5 Dermal fillers

HA based dermal fillers (DF) in recent years aroused big interest in the area of cosmetic surgery for the rejuvenation of the dermis [4].

HA is an important structural element in the skin. Its concentration in the dermis decreases with the age promoting the formation of wrinkles [163]. With the use of DF it is possible to replace them, achieving a natural and younger appearance (Figure 1.10).

There are several kinds of HA-based DF in commerce, but there is no ideal DF for all indications. They differ with regards to their physical and chemical properties, for example particle size, polymer concentration, density of cross-linking agents, viscosity, extrusion force, stress applied etc. HA based dermal fillers are usually based on bacterial fermented or rooster combs derived-HA, cross-linked with BDDE and thus have a HA concentration in the range 20-25 mg/ml.

HA based DF differ significantly in their rheological properties depending on the site of the application. They can exhibit a behavior of strong gels, weak gels and entanglement network.

Figure 1.10: Schematic representation of skin layers before and after DF injection

Among the most used in commerce are Restylane, Perlane, Juvederm Voluma, Teosyal Deep Lines and Teosyal Ultra Deep which behave as strong gels; Belotero Basic, Belotero Intense, Juvederm Ultra 3 and Juvederm Ultra 4 behave as weak gels; Belotero Soft shows a mechanical spectrum that is typical of entanglement networks [164].

One of the most important aspects of the clinical use of DF is their persistence in the human body. The performance of dermal filler in vivo seems to be directly affect by materials physical properties. In particular the clinical data appear to correlate with the concentration of the polymer and with the product between the concentration and the percent elasticity, so these should be crucial parameters for the clinical performance of DF.

1.5.6 Drug delivery

Biological and chemical properties of HA qualify this macromolecule as a prospective carrier of drugs particularly for local application and/or targeting to lymphatic system [165]. Furthermore, it is immunologically inert and safely degraded in lysosomes of

many cells. HA can be conjugated directly to the drug or used to prepare nano- and micro-sized systems such as microcapsules, nano- and micro-particles and injectable devices for optimized drug delivery [166].

HA has been extensively studied in ophthalmic [167-171], nasal [172] and parenteral drug delivery [173-178]. As vehicle for the controlled and localized delivery of active molecules, HA has been employed alone or in combination with natural polymers such as collagen [179], gelatin [180], chitosan [181] and synthetic polymers such as PLGA [182], poly(ethylene oxide)-*b*-poly(propylene oxide)-*b*-poly(ethylene oxide) (PEO-PPO-PEO).

Thermosensitive and mucoadhesive polymeric platforms are potentially useful as vehicles for sustained delivery of proteins such as insulin or of topically active drugs in ophthalmology obtained by blending HA with poloxamers or pluronics [183-184]. Moreover the grafting of pluronic onto HA has been developed to be used for ophthalmic drug delivery systems (DDS).

Recent studies demonstrated the promising potential of HA as a stable and effective nano-sized DDS for cancer treatment.

Since HA has multiple functional groups available for chemical conjugation, several HA-drug conjugates have been developed as macromolecular chemotherapeutic prodrugs in which the conjugated drugs become active upon release from the HA backbone [88, 185-187]. In this case HA nanoparticles are formed by the self-assembly of the hydrophobically modified HA derivatives.

Otherwise, HA has been chemically anchored onto various nanoparticles containing chemotherapeutic agents such as doxorubicin [188-189]. Infact HA shows a high affinity to tumor cells since it can specifically bind to the cancer cells overexpressing CD44 receptor.

These systems exhibit prolonged circulation in blood and preferential accumulation at tumor tissues when they are systemically administrated in vivo [190-192]. This passive tumor targeting phenomenon of self-assembled HA nanoparticles, called the enhanced permeability and retention (EPR) effect, is attributed to the presence of leaky tumor vessels and the lack of an effective lymphatic drainage system in tumors [193-195].

Moreover HA microspheres were reported to be promising also for the delivery of plasmid DNA and monoclonal antibodies in gene transfer [196].

THE Ph.D. PROJECT

Objectives and challenges

Hyaluronic acid (HA) currently represents one of the most attractive building block for the preparation of advanced biomaterials for many biomedical applications, as described in details in the introduction chapter.

Therefore the overall objective of this thesis was to design and develop advanced HA based systems for applications in regenerative medicine and drug delivery.

Although HA is an excellent biomaterial, HA native shows physico-chemical properties incompatible to form in vivo stable structures at macro and micro scale to use it for regenerative medicine and drug delivery. Infact when HA native is injected in physiological environment, a fast degradation process often occurs because from a side it has a high affinity for water molecules and from the other side it is degraded in vivo by hyaluronidase. For this reason, different strategies such as crosslinking or coniugation, have been developed to stabilize HA and obtain a material less susceptible to chemical and enzymatic hydrolysis, showing enhanced mechanical properties. However the modifications methods currently available to crosslink or conjugate HA molecules present some drawbacks. In particular some modifications involve HA carboxyl groups resulting in an alteration of the distribution of negative charges along the polymer backbone at physiological pH and probably affecting fundamental biological and pharmacological HA properties. Moreover another drawback is the use of organic solvent in the modification reaction that implies environmental issues, limits the upscalability of the preparation methods and often requires converting HA into its tetraalkylammonium salt or preparing reactive HA intermediates that makes more complex the preparation methods and often results in HA degradation.

Furthermore native HA, because of its hydrophilic nature, is unsuitable for the encapsulation of hydrophobic drugs. In order to overcame this problem, in literature two strategies were adopted. The first strategy, used to incapsulate hydrophobic drugs in HA based nano-sized drug carriers, was to realize nanostructured systems in which HA was anchored onto various nanoparticles, based on hydrophobic polymers, containing drugs. However HA was binded to the nanoparticles by means of a chemical reaction.

The second strategy was to modify HA molecules with hydrophobic groups, obtaining a more favourable starting material for the production of stable nanostructures and the durable encapsulation of hydrophobic drugs.
However the current methods used for the preparation of amphiphilic HA involve modification to HA carboxyl groups and were developed in organic solvents.

Part 1)

Therefore the aim of the first part of this work was to formulate HA-coated biodegradable nanoparticles for the intracellular targeting of chemotherapeutic(s).
In particular the idea was to bind the HA shell to a biodegradable core (Polylactic-coglycolic acid (PLGA) particle) by means of a physical binding using an amphiphilic polymer that acts as a bridge between the hydrophobic PLGA and the hydrophilic HA. In this way it was possible to obtain nanocarriers in a simple way avoiding the problems related to a chemical reaction as mentioned before.
Furthermore one of the most challenge in the design of nanoparticles is an efficient targeting. Nanoparticles can passively accumulate into tumors, taking advantage of enhanced permeation and retention (EPR) effect. However, nanoparticle *in vivo* efficacy can be hampered by lack of cell internalization and/or by the fact that the loaded drugs may be released before nanoparticles uptake. To overcome these limitations in recent years the research has been devoted to the preparation of nanoparticles functionalized with antibodies, nucleic acids, proteins, and various ligands, such that they can bind in a specific way to the tumor cells, and can be internalized by means of receptor-mediated endocytosis. Of the different ligands studied, antibody fragments have been extensively used for nanoparticles funzionalization. However, the use of antibodies for therapeutic purposes suffers from their sometimes potent immunogenicity and as a consequence the binding affinity for the target is often deteriorated.
It is well known that HA is an attractive material for tumor targeting delivery since it can specifically bind to the cancer cells overexpressing at their surface CD44, an HA binding receptor. Thanks to this specific interaction, HA binding to the tumor cells and its subsequently internalization are strongly enhanced.

In light of this the HA based nanoparticles realized in this project can be efficiently internalized by the tumors cells by means of both a passive and an active targeting strategy.
Furthermore another important challenge in the design of nanopaticles for drug delivery is the particles aggregation. PLGA is the mainly polymer used in drug delivery for its peculiar properties of biocompatibility and biodegradability, but nanoparticles of PLGA, besides the fact that had no targeting groups for specific tumor cells, often are subjected to a phenomenon of aggregation. The idea to create a HA shell around the biodegradable core of nanoparticle, allows to improve the nanoparticles dimensional stability, taking advantage of electrostatic repulsion due to the negative charge of HA.

Part 2)

The aim of the second part of this work was to design a delivery system based on an amphiphilic HA derivative able to self-assemble into micelles, load a hydrophobic drug and release the active molecule in situ with controlled kinetics. The novel syntetized amphiphilic HA derivative is an octenyl succinic anhydride (OSA) modified HA, obtained through a simple reaction in an aqueous medium, and which involves exclusively HA hydroxyl groups, overcoming the problems mentioned before. In particular theses derivatives present great potential since, firstly no organic solvents are used in the reaction, thus avoiding environmental issues and allowing the upscalability of the preparation method; secondly, the reaction does not involve HA carboxyl groups which can neutralize negative charges along the polymer backbone. Actually, it is important to maintain the charge distribution that can confer an electrostatically-induced stability in the perspective of using the self-assembling properties of these derivatives toward the design of micelles for the drug delivery of poorly soluble drugs.
Furthermore the idea of this work was also to combine a local/controlled delivery of a hydrophobic anti-inflammatory drug and HA viscosupplementation.
Intra-articular injection of HA (viscosupplementation) is one of the most used therapies for the treatment of knee osteoarthritis and its goal is to restore the elastic and viscous properties of the synovial fluid (SF). Pathologic alterations occurring in joint diseases,

indeed, lead to a decrease in SF of HA molecular weight and concentration, and consequently a decline in SF viscoelastic properties. The beneficial improvements in SF viscoelastic properties and joint functions derive from both the intrinsic viscoelastic properties of HA and its potential stimulatory effect on the synthesis of high molecular weight HA by synoviocytes.

Moreover, to stimulate the production of healthy HA and facilitate the homeostasis in the joint region, oral administration of anti-inflammatory drugs is often necessary in combination, or as an alternative to HA viscosupplementation. However, the prolonged use of such drugs can cause important systemic adverse effects and, therefore, intra-articular injections of anti-inflammatory drug/s are often practiced.

So the idea of this study was to design a delivery system able to prolong the release of an anti-inflammatory drug into the joint cavity and, at the same time, able to restore the viscoelastic features of pathologic SF.

Part 3)

The aim of the third part of this work was to produce stable structures at macroscale obtained crosslinking HA molecules to form injectable hydrogels for regenerative applications.

The design of HA hydrogels requires to consider many parameters such as HA source, HA concentration, buffer environment for the hydrogel, nature of the crosslinking agent, crosslinking agent/HA weight ratio. However, regardless of these elements, the purity of the HA raw material and the safety of the crosslinking technology are crucial elements in achieving a hydrogel that can be safely administered to patients.

For these reasons in this work HA produced by fermentation of the novel, superior and safe strain, namely *Bacillus subtilis*, has been used to produce hydrogels. This production technology affords a HA product with unique advantageous properties such as reproducible molecular weight. In addition, the higher purity of *Bacillus-subtilis* derived HA compared to the available sources of HA offers the possibility of heat sterilization with minor degradation under given conditions and allows its use with various ingredients without degradation or decrease in viscosity.

Moreover the hydrogels were obtained by means of a crosslinking reaction with divinyl sulfone (DVS) that involves hydroxyl groups of HA molecular backbone, avoiding the problems related to the modification reactions involving HA carboxyl groups.

The hydrogels were produced with on a simple, reproducible and safe process that does not employ any organic solvents. Owing to an effective purification step, the resulting homogeneous hydrogels do not contain any detectable residual crosslinking agent.

Moreover the injectability of the hydrogel through pharmaceutical needles is a fundamental property to consider in the design of hydrogel to be used in regenerative medicine. In particular it's important to optimize gel preparation to obtain a material with tailored properties, i.e. a good injectability profile while maintaining the mechanical properties.

So in this frame the aim was to produce cross-linked HA hydrogels with improved properties, such as higher homogeneity and increased softness compared to the standard DVS crosslinked HA-hydrogels and an easier syringeability.

REFERENCES

[1] Meyer K., Palmer J. The polysaccharide of the vitreous humor. J. Biol. Chem., 1934; 107, 629-634.

[2] Weissman B., Meyer K. The structure of hyalobiuronic acid and of hyaluronic acid from umbilical cord. J. Am. Chem. Soc., 1954; 76(7), 1753-1757.

[3] Kogan G., Soltes L., Stern R., Gemeiner P. Hyaluronic acid: a natural biopolymer with a broad range of biomedical and industrial applications. Biotechnol Lett., 2007; 29, 17–25.

[4] Monheit G.D., Coleman K.M. Hyaluronic acid fillers. Dermatologic Therapy, 2006; 19(3), 141–150.

[5] Borzacchiello A., Netti P.A., Ambrosio L., Nicolais L. Hyaluronic acid derivatives mimic the rheological properties of vitreous body. New Frontiers in Medical Sciences: Redefining Hyaluronan, 2000; 195-202.

[6] Borzacchiello A., Ambrosio L. Network formation of low molecular weight hyaluronic acid derivatives. Journal of Biomaterials Science Polymer Edition, 2001; 12(3), 307-316.

[7] Barbucci R., Lamponi S., Borzacchiello A., Ambrosio L., Fini M., Torricelli P., Giardino R. Hyaluronic acid hydrogel in the treatment of osteoarthritis. Biomaterials, 2002; 23(23), 4503-4513.

[8] Xuejun X., Borzacchiello A., Netti P.A., Ambrosio L., Nicolais L. Hyaluronic Acid Based Semi Interpenetrating Materials. J. Biomater. Sci. Polymer Edn, 2004; 15(9), 1223-1236.

[9] Mori M., Yamaguchi M., Sumitomo S., Takai Y. Hyaluronic-based biomaterials in tissue engineering. Acta Histochem. Cytochem, 2004; 37(1), 1-5.

[10] Borzacchiello A., Mayol L., Gaerskog O., Dahlqvist A., Ambrosio L. Evaluation of injection augmentation treatment of hyaluronic acid based materials on rabbit vocal folds viscoelasticity. Journal of Materials Science: Materials in Medicine, 2005; 16(6), 553-557.

[11] Borzacchiello A., Mayol L., Ramires P.A., Di Bartolo C., Pastorello A., Ambrosio L., Milella E. Structural and rheological characterization of hyaluronic acid-based scaffolds for adipose tissue engineering. Biomaterials, 2007; 28, 4399–4408.

[12] Fusco S., Borzacchiello A., Miccio L., Pesce G., Rusciano G., Sasso A., Netti P.A. High frequency viscoelastic behaviour of low molecular weight hyaluronic acid water solutions. Biorheology, 2007; 44(5-6), 403-418.

[13] Borzacchiello A., Mayol L., Schiavinato A., Ambrosio L. Effect of hyaluronic acid amide derivative on equine synovial fluid viscoelasticity. Journal of biomedical materials research, 2010; 92A(3), 1162-1170.

[14] Liao Y. H., Jones S. A., Forbes B., Martin G.P., Brown M.B. Hyaluronan: Pharmaceutical Characterization and Drug Delivery. Drug Delivery, 2005; 12, 327–342.

[15] Widner B., Behr B., Von Dollen S., Tang M., Heu T., Sloma A., Sternberg D., DeAngelis P.L., Weigel P.H., Brown S. Hyaluronic acid production in bacillus subtilis. Appl. Environ. Microbiol., 2005; 71, 3747-3752.

[16] O'Regan M., Martini I., Crescenzi F., De Luca C., Lansing M. Molecular mechanisms and genetics of hyaluronan biosynthesis. Int J Biol Macromol, 1994; 16(6), 283-286.

[17] Balazs E.A., Leshchiner E., Larsen N.E., Band P. Applications of hyaluronan and its derivates. Biotechnological polymers, 1993; 41-65.

[18] De Angelis P.L. Hyaluronan synthases: fascinating glycosyltransferases from vertebrates, bacterial pathogens, and algal viruses. Cell Mol Life Sci, 1999; 56(7-8), 670-682.

[19] Volpi N. Maccari F. Purification and characterization of hyaluronic acid from the mollusc bivalve Mytilus galloprovincialis. Biochimie, 2003; 85(6), 619-625.

[20] Chen W.Y.J., Abatangelo G. Functions of hyaluronan in wound repair. Wound Rep. and Reg., 1999; 7(2), 79-89.

[21] Bettelheim F.A., Popdimitrova N. Hyaluronic acid-synergetic glycosaminoglycan. Curr. Eye Res., 1992; 11(5), 411-419.

[22] Yates J.R. Mechanism of water uptake by skin. In Biophysical properties of the skin, 1971; 14, 485-512.

[23] Felszeghy Sz.; Meszar Z.; Prehm P.; Modis L. The expression pattern of hyaluronan synthase during human tooth development. Archives of Oral Biology, 2005; 50, 175—179.

[24] Šoltés L., Mendichi R. Molecular characterization of two host–guest associating hyaluronan derivatives. Biomed. Chromatogr., 2003; 17(6), 376–384.

[25] Kogan G., Šoltés L., Stern R., Schiller J., Mendichi R. Hyaluronic acid: its function and degradation in in vivo systems. Studies in natural products chemistry, 2008; 34, 789-882.

[26] Stern R., Asari A.A., Sugahara K.N. Hyaluronan fragments: an information-rich system. Eur. Jour. Cell. Biol., 2006; 85(8), 699–715.

[27] Goldberg R.L., Toole B.P. Hyaluronate inhibition of cell proliferation. Arthritis Rheum, 1987; 30(7), 769–778.

[28] Alho A.M., Underhill C.B. The hyaluronate receptor is referentially expressed on proliferating epithelial cells. J Cell Biol, 1989; 108(4), 1557–1565.

[29] Aruffo A., Stamenkovic I., Melnick M., Underhill C.B., Seed B. CD44 is the principal cell surface receptor for hyaluronate, Cell, 1990; 61(7), 1303–1313.

[30] Entwistle J., Hall C.L., Turley E.A. HA receptors: regulators of signaling to the cytoskeleton. J. Cell. Biochem., 1996; 61(4), 569 –577.

[31] Asayama S., Nogawa M., Takei Y., Akaike T., Maruyama A. Synthesis of novel polyampholyte comb-type copolymers consisting of a poly(L-lysine) backbone and hyaluronic acid side chains for a DNA carrier. Bioconj. Chem., 1998; 9(4), 476 –481.

[32] Takei Y., Maruyama A., Ferdous A., Nishimura Y., Kawano S., Ikejima K., Okumura S., Asayama S., Nogawa M., Hashimoto M., Makino Y., Kinoshita M., Watanabe S., Akaike T., Lemasters J.J., Sato N. Targeted gene delivery to sinusoidal endothelial cells: DNA nanoassociate bearing hyaluronan–glycocalyx. FASEB J., 2004; 18(6), 699–701.

[33] Schledzewski K., Falkowski M., Moldenhauer G., Metharom P., Kzhyshkowska J., Ganss R.,. Demory A., Falkowska-Hansen B., Kurzen H., Ugurel S., Geginat G., Arnold B., Goerdt S. Lymphatic endothelium-specific hyaluronan receptor LYVE- 1 is expressed by stabilin-1^{+}, F4/80^{+}, $CD11b^{+}$ macrophages in malign ant tumors and wound healing tissue in vivo and in bone marrow cultures in vitro :implications for the assessment of lymphangiogenesis. J. Pathol., 2006; 209(1), 67–77.

[34] Toole B.P. Hyaluronan in morphogenesis. Journal of Internal Medicine, 1997; 242(1), 35–40.

[35] Ahrens T., Assmann V., Fieber C., Termeer C.C., Herrlich P., Hofmann M., Simon J.C. CD44 is the principal mediator of hyaluronic-acid-induced melanoma cell proliferation. Journal of Investigative Dermatology, 2001; 116, 93–101.

[36] Noble P.W. Hyaluronan and its catabolic products in tissue injury and repair. Matrix Biology, 2002; 21(1), 25–29.

[37] Toole B.P., Wight T.N., Tammi M.I. Hyaluronan-cell interactions in cancer and vascular disease. Journal of Biological Chemistry, 2002; 277, 4593–4596.

[38] Isacke C.M., Yarwood H. The hyaluronan receptor, CD44. Int J. Biochem. Cell Biol., 2002; 34(7), 718-721.

[39] Leach J.B., Schmidt C.E. Hyaluronan. Encyclopedia of biomaterials and biomedical engineering, 2004; 1, 779-789.

[40] Cheung W.F., Cruz T.F., Turley E.A. Receptor for hyaluronan-mediated motility (RHAMM), a hyaladherin that regulates cell responses to growth factors. Biochem. Soc. Trans., 1999; 27(2), 135-142.

[41] Linker A., Meyer K. Production of Unsaturated Uronides by Bacterial Hyaluronidases. Nature, 1954; 174, 1192–1193.

[42] Lapcik L.J., Lapcik L., De Smedt S., Demeester J., Chabrecek P. Hyaluronan: Preparation, Structure, Properties and Applications. Chemical Reviews, 1998; 98(8), 2663-2684.

[43] Laurent T.C., Fraser J.R.E. Hyaluronan. Faseb J., 1992; 6, 2397-2404.

[44] Scott J.E., Cummings C., Brass A., Chen Y. Secondary and tertiary structures of hyaluronan in aqueous solution, investigated by rotary shadowing-electron microscopy

and computer simulation Hyaluronan is a very efficient network-forming polymer. Biochem. J., 1991; 274, 699-705.

[45] Scott J.E. Supramolecular organization of extracellular matrix glycosaminoglycans, in vitro and in the tissues. The FASEB Journal, 1992; 6(9), 2639-2645.

[46] Scott J.E., Cummings C., Brass A., Chen Y. Secondary and tertiary structures of hyaluronan in aqueous solution, investigated by rotary shadowing-electron microscopy and computer simulation. Hyaluronan is a very efficient network-forming polymer. Biochem. J. 1991; 274, 699-705.

[47] Scott J.E. The periphery of the developing collagen fibril. Quantitative relationships with dermatan sulfate and other surface-associated species. Biochem. J., 1984; 218, 229–233.

[48] Scott J.E., Heatley F. Hyaluronan forms specific stable tertiary structures in aqueous solution: a CNMR study. Proc. Natl. Acad. Sci., 1999; 96(9), 4850–4855.

[49] Day A.J., Sheehan J.K. Hyaluronan: polysaccharide chaos to protein organisation. Curr. Opin. Struct. Biol., 2001; 11(5), 617–622.

[50] Ferry J.D. Viscoelastic Properties of Polymers. Wiley, 1970; p. 671.

[51] D'Errico G., De Lellis M., Mangiapia G., Tedeschi A., Ortona O., Fusco S., Borzacchiello A., Ambrosio L. Structural and Mechanical Properties of UV-Photo-Cross-Linked Poly(N-vinyl-2-pyrrolidone) Hydrogels. Biomacromolecules, 2008; 9(1), 231–240.

[52] Ambrosio L., Borzacchiello A., Netti P.A., Nicolais L. Rheological Study On Hyaluronic Acid And Its Derivative Solutions. J.M.S.-Part A: Pure Appl. Chem., 1999; 36(7-8), 991-1000.

[53] Carlfors J., Edsman K., Petersson R., Jörnving K. Rheological evaluation of Gelrite® in situ gels for ophthalmic use. European Journal of Pharmaceutical Sciences, 1998; 6(2), 113-119.

[54] Gibbs D.A., Merrill E.W., Smith K.A., Balazs E.A. Rheology of hyaluronic acid. Biopolymers, 1968; 6(6), 777–791.

[55] Kobayashi Y., Okamoto A., Nishinari K. Viscoelasticity of hyaluronic-acid with different molecular weights. Biorheology, 1994; 31(3), 235–244.

[56] Karim S. The determination of the viscosity-average molecular weight of hyaluronan by capillary viscosity. In Hyaluronan in Drug Delivery- 4th International Workshop, ed. D. Willoughby. London: Royal Society of Medicine, 1996, 97–107.

[57] Fujii K., Kawata M., Kobayashi Y., Okamoto A., Nishinari K. Effects of the addition of hyaluronate segments with different chain lengths on the viscoelasticity of hyaluronic acid solutions. Biopolymers, 1996; 38(5), 583– 591.

[58] Pasquali-Ronchetti I., Quaglino D., Mori G., Bacchelli B., Ghosh P. Hyaluronan-phospholipid interactions. J. Struct. Biol., 1997; 120(1), 1–10.

[59] Mo Y., Takaya T., Nishinari K., Kubota K., Okamoto A. Effects of sodium chloride, guanidine hydrochloride, and sucrose on the viscoelastic properties of sodium hyaluronate solutions. Biopolymers, 1999; 50(1), 23–34.

[60] Ghosh P., Hutadilok N., Adam N., Lentini A. Interactions of hyaluronan (hyaluronic-acid) with phospholipids as determined by gel permeation chromatography, multi-angle laser-light-scattering photometry and H-NMR spectroscopy. Int. J. Biol. Macromol., 1994; 16(5), 237–244.

[61] Liao Y.H., Jones S.A., Forbes B., Martin G.P., Brown M.B. Hyaluronan: Pharmaceutical Characterization and Drug Delivery. Drug Delivery, 2005; 12(6), 327–342.

[62] Stern R., Jedrzejas M. J. Hyaluronidases: Their Genomics, Structures, and Mechanisms of Action. Chem. Rev., 2006; 106, 818−839.

[63] Kreil G. Hyaluronidases-a group of neglected enzymes. Protein Sci., 1995; 4(9), 1666-1669.

[64] Necas J., Bartosikova L., Brauner P., Kolar J. Hyaluronic acid (hyaluronan): a review. Veterinarni Medicina, 2008; 53(8), 397–411.

[65] Chabreček P., Šoltés B., Kállay Z., Novák I. Gel permeation chromatographic characterization of sodium hyaluronate and its fractions prepared by ultrasonic degradation. Chromatographia, 1990; 30(3-4), 201-204.

[66] Chabreček P., Šoltés L., Orvisky E. Comparative depolymerization of sodium hyaluronate by ultrasonic and enzymatic treatments *J.* Appl. Polym. Sci., 1991; 48, 233-241.

[67] Reháková M., Bakoš D., Soldán M., Vizárová K. Depolymerization reactions of hyaluronic acid in solution. Int. J. Biol. Macromol., 1994; 16(3), 121-124.

[68] Šoltés L., Mislovičová D., Sèbille B. Insight into the distribution of molecular weights and higher-order structure of hyaluronans and some β-(1→3)-glucans by size exclusion chromatography. Biomed. Chromatogr., 1996; 10(2), 53-59.

[69] Vercruysse K.P., Lauwers A.R., Demeester J.M. Absolute and empirical determination of the enzymatic activity and kinetic investigation of the action of hyaluronidase on hyaluronan using viscosimetry. Biochem. J., 1995; 306, 153-160.

[70] Kubo K., Nakamura T., Takagaki K., Yoshida Y., Endo M. Depolymerization of hyaluronan by sonication. Glycoconjugate J., 1993; 10(6), 435-439.

[71] Ghosh S., Kobal I., Zanette D., Reeds W.F. Conformational contraction and hydrolysis of hyaluronate in sodium hydroxide solutions. Macromolecules, 1993; 26(17), 4685-4693.

[72] Reed C.E., Reed W.F. Light scattering power of randomly cut random coils with application to the determination of depolymerization rates. J. Chem. Phys., 1989; 91(11), 7193-7199.

[73] Lowry K.M, Beavers E.M. Thermal stability of sodium hyaluronate in aqueous solution. Journal of Biomedical Materials Research, 1994; 28(10), 1239–1244.

[74] Bothner H., Waaler T. Limiting viscosity number and weight average molecular weight of hyaluronate samples produced by heat degradation. Int. Jou Biol. Macromolecules, 1988; 10(5), 287-291.

[75] Stern R. Hyaluronan catabolism: a new metabolic pathway. Eur. J. Cell Biol., 2004; 83(7), 317-325.

[76] Kuo J.W., Prestwich G.D. Hyaluronc acid. Materials of Biological Origin – Materials Analysis and Implant Uses, Comprehensive Biomaterials, 2010.

[77] Banerji S., Wright A.J., Noble M., Mahoney D.J., Campbell I.D., Day A.J., Jackson D.G. Structures of the CD44–hyaluronan complex provide insight into a fundamental carbohydrate-protein interaction. Nat Struct Mol Biol., 2007; 14, 234-239.

[78] Reichenbach S., Blank S.,. Rutjes A.W.S, Shang A., King E.A., Dieppe P.A., Jüni P., Trelle S. Hylan versus hyaluronic acid for osteoarthritis of the knee: A systematic review and meta-analysis. Arthritis & Rheumatism, 2007; 57(8), 1410–1418.

[79] Bergman K., Elvingson C., Hilborn J., Svensk G., Bowden T. Hyaluronic acid derivatives prepared in aqueous media by triazine-activated amidation. Biomacromolecules, 2007; 8(7), 2190–2195.

[80] Pelletier S., Hubert P., Lapicque F., Payan E., Dellacherie E. Amphiphilic derivatives of sodium alginate and hyaluronate: synthesis and physico-chemical properties of aqueous dilute solutions. Carbohydrate Polymers, 2000; 43(4), 343–349.

[81] Maleki A., Kjøniksen A., Nyström B. Effect of pH on the behavior of hyaluronic acid in dilute and semidilute aqueous solutions. Macromolecular Symposia, 2008; 274(1), 131–140.

[82] Prestwich G.D., Kuo J.W. Chemically-modified HA for therapy and regenerative medicine. Curr. Pharm. Biotechnol., 2008; 9(4), 242-245.

[83] Burdick J.A., Prestwich G.D. Hyaluronic Acid Hydrogels for Biomedical Applications. Adv. Mater., 2011; 23(12), H41-H56.

[84] Oh E.J., Park K., Kim K.S., Kim J., Yang J., Kong J., Lee M.Y., Hoffman A.S., Hahn S.K. Target specific and long- acting delivery of protein, peptide, and nucleotide therapeutics using hyaluronic acid derivatives. Journal of Controlled Release, 2010; 141(1), 2–12.

[85] Bulpitt P., Aeschlimann D. New strategy for chemical modification of hyaluronic acid: preparation of functionalized derivatives and their use in the formation of novel biocompatible hydrogels. Journal of Biomedical Materials Research, 1999; 47(2), 152–169.

[86] Schneider A., Picart C., Senger B., Schaaf P., Voegel J., Frisch B. Layer-by-layer films from hyaluronan and amine-modified hyaluronan. Langmuir, 2007; 23(5), 2655–2662.

[87] Kuo J.W., Swann D.A., Prestwich G.D. Chemical modification of hyaluronic acid by carbodiimides. Bioconjugate Chemistry, 1991; 2(4), 232–241.

[88] Pouyani T., Prestwich G.D. Functionalized derivatives of hyaluronic acid oligosaccharides: drug carriers and novel biomaterials. Bioconjugate Chem., 1994; 5(4), 339-347.

[89] Shu X.Z., Liu Y., Luo Y., Roberts M.C., Prestwich G.D. Disulfide cross-linked hyaluronan hydrogels. Biomacromolecules, 2002; 3(6), 1304-1311.

[90] Magnani A., Rappuoli R., Lamponi S., Barbucci R. Novel polysaccharide hydrogels: characterization and properties. Polymers for Advanced Technologies, 2000; 11(8–12), 488–495.

[91] Della Valle F. Crosslinked carboxy polysaccharides. 1994, EP0341745 B1.

[92] Bellini D., Topai A. Amides of hyaluronic acid and the derivatives thereof and a process for their preparation, 2000; WO2000001733 A1.

[93] Iannace S., Ambrosio L., Nicolais L., Rastrelli A. Pastorello A. Thermomechanical Properties of Hyaluronic Acid Derived Products. J. Mater. Sci. Mater. Med., 1992; 3(1), 59–64.

[94] Maleson T., Lindqvist B.L. Gels of crosslinked hyaluronic acid for use as a vitreous humor substitute, 1986; WO1986000079 A1.

[95] Oh E.J., Kang S., Kim B., Jiang G., Cho I.H., Hahn S.K. Control of the molecular degradation of hyaluronic acid hydrogels for tissue augmentation. Jou. Biomed. Mater. Res. Part A, 2008; 86(3), 685-693.

[96] Pravata L., Braud C., Boustta M., El Ghzaoui A., Tømmeraas K., Guillaumie F., Schwach-Abdellaoui K., Vert M. New amphiphilic lactic acid oligomer–hyaluronan

conju-gates: synthesis and physicochemical characterization. Biomacromolecules, 2008; 9(1), 340–348.

[97] Glass J.R., Dickerson K.T., Stecker K., Polarek J.W. Characterization of a hyaluronic acid-Arg-Gly-Asp peptide cell attachment matrix. Biomaterials, 1996; 17(11), 1101–1108.

[98] Jia X., Colombo G., Padera R., Langer R., Kohane D.S. Prolongation of sciatic nerve blockade by in situ cross-linked hyaluronic acid. Biomaterials, 2004; 25(19), 4797–4804.

[99] Bellini D., Topai A. Amides of hyaluronic acid and the derivatives thereof and a process for their preparation, 1999; EP1095064.

[100] Platt V.M., Szoka F.C. Anticancer therapeutics: targeting macromolecules and nanocarriers to hyaluronan or CD44, a hyaluronan receptor. Molecular Phar-maceutics, 2008; 5(4), 474–486.

[101] Mamalis N. OVDs: viscosurgical, viscoelastic, and viscoadaptive. What does this mean?. J Cataract Refract Surg, 2002; 28(9),1497–1498.

[102] Arshinoff S.A., Wong E. Understanding, retaining, and removing dispersive and pseudodispersive ophthalmic viscosurgical devices. J Cataract Refract Surg, 2003; 29(12), 2318–2323.

[103] Burkhard Dick H., Krummenauer F., Augustin A.J., Pakula T., Pfeiffer N. Healon5 viscoadaptive formulation: comparison to Healon and Healon GV. J Cataract Refract Surg, 2001; 27(2), 320-326.

[104] Maltese A., Borzacchiello A., Mayol L., Bucolo C., Maugeri F., Nicolais L., Ambrosio L. Novel polysaccharides based viscoelastic formulations for ophthalmic surgery: rheological characterization. Biomaterials, 2006; 27(29), 5134-5142.

[105] Titze I.R. The human instrument. Sci.Am., 2008; 298(1), 94-101.

[106] Titze I.R. Principles of Voice Production. Prentice Hall, 1994; xxiv, 354.

[107] Anthea M., Hopkins J., McLaughlin C.W., Johnson S., Warner M.Q., LaHart D., Wright J.D. Human Biology and Health. Englewood Cliffs, 1993.

[108] Butler J.E., Hammond T.H., Gray S.D. Gender-related differences of hyaluronic acid distribution in the human vocal fold. Laryngoscope, 2001; 111(5), 907–911.

[109] Chan R.W., Gray S.D., Titze I.R. The importance of hyaluronic acid in vocal fold biomechanics. Otolaryngol Head Neck Surg, 2001; 124(6), 607–614.

[110] Titze I.R. The physics of small-amplitude oscillation of the vocal folds. Jou Acoust Soc Am, 1988; 83, 1536-1552.

[111] Titze I.R. Transcript of the 10th Symposium, Care of the Professional Voice, 1982; 52.

[112] Hertegård S., Dahlqvist Å., Laurent C., Borzacchiello A., Ambrosio L. Viscoelastic properties of rabbit vocal folds after augmentation. Otolaryngology Head Neck Surgery, 2003; 128(3), 401-406.

[113] Dahlqvist Å., Gärskog O., Laurent C., Hertegård S., Ambrosio L., Borzacchiello A. Viscoelasticity of rabbit vocal folds after injection augmentation, Laryngoscope, 2004; 114(1), 138-142.

[114] Borzacchiello A., Mayol L., Ambrosio L., Gärskog O., Dahlqvist Å. Rheological Characterization of Vocal Folds after Injection Augmentation in a Preliminary Animal Study. J. of Bioactive and Compatible Polymers, 2004; 19(4), 331-341.

[115] Barbucci R., Rappuoli R., Borzacchiello A., Ambrosio L. Synthesis, chemical and rheological characterisation of new hyaluronic based hydrogels, Journal of Biomaterials Science Polymer Edition, 2000; 11(4), 383-399.

[116] Migliore A., Giovannangeli F., Bizzi E., Massafra U., Alimonti A., Laganà B., Diamanti Picchianti A., Germano V., Granata M., Piscitelli P. Viscosupplementation in the management of ankle osteoarthritis: a review. Arch Orthop Trauma Surg, 2011; 131(1), 139–147.

[117] Balazs E.A., Denlinger J.L. Viscosupplementation: A new concept in the treatment of osteoarthritis. J Rheumatol, 1993; 39, 3–9.

[118] Laurent T.C., Fraser J.R., Laurent U.B.G., Engstrom-Laurent A. Hyaluronan in inflammatory joint disease. Acta Orthop Scand, 1995; 66(226), 116–120.

[119] Kirwan J.R., Rankin E. Intra-articular therapy in osteoarthritis. Baillieres Clin Rheumatol, 1997; 11(4), 769–794.

[120] Fajardo M., P.E. Disease-Modifying Therapies for Osteoarthritis Drugs & Aging, 2005; 22, 2, 141-161.

[121] Bellamy N., Campbell J., Robinson V., Gee T.L., Bourne R., Wells G.A. Viscosupplementation for the treatment of osteoarthritis of the knee. The Cochrane Library, 2009.

[122] Wright K.E., Maurer S.G., Di Cesare P.E. Viscosupplementation for osteoarthritis. Am J Orthop, 2000; 29(2), 80–88.

[123] Ghosh P., Guidolin D. Potential mechanism of action of intraarticular therapy in osteoarthiritis: are the effects molecular weight dependent?. Semin Arthritis Rheum, 2002; 32(1), 10–37.

[124] Adams M.E., Lussier A.J., Peyron J.G. A risk-benefit assessment of injections of hyaluronan and its derivatives in the treatment of osteoarthritis of the knee. Drug Saf, 2000; 23(2), 115-130.

[125] Martens P.B. Bilateral symmetric inflammatory reaction to hylan G-F 20 injection. Arthritis Rheum, 2001; 44(4), 978-979.

[126] Allen E., Krohn K. Adverse reaction to Hylan GF-20. J Rheumatol, 2000; 27(6), 1572.

[127] Bernardeau C., Bucki B., Lioté F. Acute arthritis after intraarticular hyaluronate injection: onset of effusions without crystal. Am Rheum Dis, 2001; 60(5), 518-520.

[128] Pleimann J.H., Davis W.H., Cohen B.E., Anderson R.B. Viscosupplementation for the arthritic ankle. Foot Ankle Clin, 2002; 7(3), 489–494.

[129] Wang C.W., Gao L.H., Jin X.Y., Chen P.B., Zhang G.M. Clinical study of sodium hyaluronate in supplementary treatment of comminuted fracture of ankle. Chinese Journal of Reparative and Reconstructive Surgery, 2002; 16(1), 21–22.

[130] Gaston M.S., Tiemessen C.H., Philips J.E. Intra-articular hip viscosupplementation with synthetic hyaluronic acid for osteoarthritis: efficacy, safety and relation to pre-injection radiographs. Arch Orthop Trauma Surg, 2007; 127(10), 899–903.

[131] Migliore A., Tormenta S., Martin L.S.M., Valente C., Massafra U., Granata M., Alimonti A. Open pilot study of ultrasound-guided intra-articular injection of hylan G-F20 (Synvisc) in the treatment of symptomatic hip osteoarthritis. Clin Rheumatol, 2005; 24(3), 285–289.

[132] Tikiz C., Ünlü Z., Şener A., Efe M., Tüzün Ç. Comparison of efficacy of lower and higher molecular weight viscosupplementation in the treatment of hip osteoarthritis. Clin Rheumatol, 2005; 24(3), 244–250.

[133] Migliore A., Martin L.S.M., Alimonti A., Valente C., Tormenta S. Efficacy and safety of viscosupplementation by ultrasound-guided intra-articular injection in osteoarthritis of the hip. Osteoarthritis Cartilage, 2003; 11, 305–306.

[134] Migliore A., Tormenta S., Massafra U., Bizzi E., Iannessi F., Alimonti A., Granata M. Intra-articular administration of hylan G-F 20 in patients with symptomatic hip osteoarthritis: tolerability and eVectiveness in a large cohort study in clinical practice. Curr Med Res Opin, 2008; 24(5), 1309–1316.

[135] Migliore A., Tormenta S., Massafra U., Carloni E., Padalino C., Iannessi F., Alimonti A., Martin L.S.M., Granata M. Repeated ultrasound-guided intra-articular injections of 40 mg of Hyalgan may be useful in symptomatic relief of hip osteoarthritis. Osteoarthritis Cartilage, 2005; 13, 1126–1127.

[136] Migliore A., Tormenta S., Martin L.S.M., Iannessi F., Massafra U., Carloni E., Monno D., Alimonti A., Granata M. The symptomatic effects of intra-articular administration of hylan G-F 20 on osteoarthritis of the hip: clinical data of 6 months follow-up. Clin.Rheumatol, 2006; 25(3), 389–393.

[137] Migliore A., Tormenta S., Massafra U., Martin L.S.M., Carloni E., Padalino C., Alimonti A., Granata M. 18-month observational study on efficacy of intraarticular hyaluronic acid (Hylan G-F 20) injections under ultrasound guidance in hip osteoarthritis. Reumatismo, 2006; 58(1), 39–49.

[138] Labbe M., Ridgeland E., Savoie F.H. The short-term efficacy of hyaluronic acid injections for the treatment of degenerative arthrosis of the shoulder. Arthroscopy, 2003; 19, S13–S18.

[139] Marshall,K.W. Intra-articular hyaluronan therapy. Foot Ankle Clin, 2003; 8, 221–232.

[140] Clarke S., Lock V., Duddy J., Sharif M., Newman J.H., Kirwan J.R. Intra-articular hylan G-F 20 in the management of patellofemoral osteoarthritis of the knee (POAK). The Knee, 2005; 12(1), 57–62.

[141] Roux C., Fontas E., Breuil V., Brocq O., Albert C., Euller-Ziegler L. Injection of intra-articular sodium hyaluronidate (sinovial) into the carpometacarpal joint of the thumb (CMC1) in osteoarthritis. A prospective evaluation of effcacy. Joint Bone Spine, 2007; 74(4), 368–372.

[142] Allison D.D, Grande-Allen K.J. Review. Hyaluronan: a powerful tissue engineering tool. Tissue Engineering, 2006; 12(8), 2131-2140.

[143] Delmage J.M., Powars D.R., Jaynes P.K., Allerton S.E. The selective suppression of immunogenicity by hyaluronic acid. Ann. Clin. Lab. Sci., 1986; 16(4), 303-310.

[144] Richter A.W., Ryde E.M., Zetterstrom E.O. Non-immunogenicity of a purified sodium hyaluronate preparation in man. Int. Arch. Allergy Appl. Immunol., 1979; 59(1), 45-48.

[145] Tomihata K., Ikada Y. Crosslinking of hyaluronic acid with water-soluble carbodiimide. J. Biomed. Mater. Res., 1997; 37(2), 243-251.

[146] Vercruysse K.P., Marecak D.M., Marecek J.F., Prestwich G.D. Synthesis and in vitro degradation of new polyvalent hydrazide cross-linked hydrogels of hyaluronic acid. Bioconjug. Chem., 1997; 8(5), 686-694.

[147] Laurent T.C., Hellsing K., Gelotte B. Cross-linked gels of hyaluronic acid. Acta Chem. Scand., 1964; 18, 274-275.

[148] Liu Y., Shu X.Z., Prestwich G.D. Biocompatibility and stability of disulfide-crosslinked hyaluronan films. Biomaterials, 2005; 26(23), 4737-4746.

[149] Bayer Leach J., Bivens K.A., Patrick C.W.J., Schmidt C.E. Photocrosslinked hyaluronic acid hydrogels: natural, biodegradable tissue engineering scaffolds. Biotechnol.Bioeng., 2003; 82(5), 578-589.

[150] Hemmrich K., Van de Sijpe K., Rhodes N.P., Hunt J.A., Di Bartolo C., Pallua N, Blondeel P., von Heimburg D. Autologous In Vivo Adipose Tissue Engineering in Hyaluronan-Based Gels—A Pilot. Study Journal of Surgical Research, 2008; 144(1), 82–88.

[151] Yoo H.S., Lee E.A., Yoon J.J, Park T.G. Hyaluronic acid modified biodegradable scaffolds for cartilage tissue engineering. Biomaterials, 2005; 26(14), 1925–1933.

[152] Leach J.B,, Schmidt C.E. Characterization of protein release from photocrosslinkable hyaluronic acid-polyethylene glycol hydrogel tissue engineering scaffolds. Biomaterials, 2005; 26(2), 125–135.

[153] Weigel P.H., Fuller G.M., LeBoeuf R.D. A model for the role of hyaluronic acid and fibrin in the early events during the inflammatory response and wound healing. Journal of Theoretical Biology, 1986; 119(2), 219–234.

[154] Ma L., Gao C., Mao Z., Zhou J., Shen J., Hu X., Han C. Collagen/chitosan porous scaffolds with improved biostability for skin tissue engineering. Biomaterials, 2003; 24(26), 4833–4841.

[155] Zacchi V., Soranzo C., Cortivo R., Radice M., Brun P., Abatangelo G. In vitro engineering of human skin-like tissue. Jou Biom Mat Res, 1998; 40(2), 187-194.

[156] Von Heimburg D., Zachariah S., Low A., Pallua N. Influence of different biodegradable carriers on the in vivo behavior of human adipose precursor cells. Plast Reconstr Surg, 2001; 108(1), 411–420.

[157] Halbleib M., Skurk T., de Luca C., von Heimburg D., Hauner H. Tissue engineering of white adipose tissue using hyaluronic acid-based scaffolds. I: in vitro differentiation of human adipocyte precursor cells on scaffolds. Biomaterials, 2003; 24(18), 3125–3132.

[158] Hemmrich K., von Heimburg D., Rendchen R., Di Bartolo C., Milella E., Pallua N. Implantation of preadipocyte-loaded hyaluronic acidbased scaffolds into nude mice to evaluate potential for soft tissue engineering. Biomaterials, 2005; 26(34), 7025–7037.

[159] Borzacchiello A., Gloria A:, Mayol L., Dickinson S., Miot S., Martin I., Ambrosio L. Natural/synthetic porous scaffold designs and properties for fibro-cartilaginous tissue engineering. Journal of Bioactive and Compatible Polymers, 2011; 26(5) 437–451.

[160] Gloria A., Borzacchiello A., Causa F., Ambrosio L. Rheological characterization of hyaluronic acid derivatives as injectable materials toward nucleus pulposus regeneration. Journal Of Biomaterials Applications, 2012; 26(6), 745-759.

[161] Campoccia D., Doherty P., Radice M., Brun P., Abatangelo G., Williams D.F.,. Semisynthetic resorbable materials from hyaluronan esterification. Biomaterials, 1998; 19(23), 2101-2127.

[162] Pavesio A., Abatangelo G., Borrione A., Brocchetta D., Hollander A.P., Kon E., Torasso F., Zanasi S., Marcacci M. Hyaluronan-based scaffolds (Hyalograft C) in the treatment of knee cartilage defects: preliminary clinical findings. Novartis Found. Symp., 2003; 249, 203-217.

[163] Baumann,L. Dermal fillers. J Cosmet Dermatol., 2004; 3(4), 249-250.

[164] Santoro S., Russo L., Argenzio V., Borzacchiello A. Rheological properties of cross-linked hyaluronic acid dermal fillers. J Appl Biomater Biomech., 2011; 9(2), 127-136.

[165] Drobnik,J. Hyaluronan in drug delivery. Advanced Drug Delivery Reviews, 1991; 7(2), 295–308.

[166] Esposito E., Menegatti E., Cortesi R. Hyaluronan based microspheres as tools for drug delivery: a comparative study. Int J Pharm, 2005; 288(1), 35–49.

[167] Järvinen K., Järvinen T., Urtti A. Ocular absorption following topical delivery. Adv Drug Dev Rev, 1995; 16(1), 3–19.

[168] Langer K., Mutschler E., Lambrecht G., Mayer D., Troschau G., Kreuter J. Methylmethacrylate sulfopropylmethacrylate copolymer nanoparticles for drug delivery – Part III. Evaluation as drug delivery system for ophthalmic applications. Int J Pharm, 1997; 157(2), 219–231.

[169] Moreira C.A., Moreira A.T., Armstrong D.K., Jelliffe R.W., Woodford C.C., Liggett P.E., Trousdale M.D. In vitro and in vivo studies with sodium hyaluronate as a carrier for intraocular gentamicin. Acta Ophthalmol, 1991; 69(1), 50–56.

[170] Moreira C.A., Armstrong D.K., Jelliffe R.W., Moreira A.T., Woodford C.C., Liggett P.E., Trousdale M.D. Sodium hyaluronate as a carrier for intravitreal gentamicin an experimental study. Acta Ophthalmol, 1991; 69(1), 45–49.

[171] Herrero-Vanrell R., Fernandez-Carballido A., Frutos G., Cadorniga R. Enhancement of the mydriatic response to tropicamide by bioadhesive polymers. J Ocul Pharmacol Ther, 2000; 16(5), 419–428.

[172] Morimoto K., Yamaguchi H., Iwakura Y., Morisaka K., Ohashi Y., Nakai Y. Effects of viscous hyaluronate-sodium solutions on the nasal absorption of vasopressin and an analogue. Pharmacol Res, 1991; 8(4), 471–474.

[173] Drobnik J. Hyaluronan in drug delivery. Advanced Drug Delivery Reviews, 1991; 7(2), 295–308.

[174] Luo Y., Prestwich G.D. Synthesis and selective cytotoxicity of a hyaluronic acid-antitumor bioconjugate. Bioconjug Chem, 1999; 10(5), 755–763.

[175] Peer D., Florentin A., Margalit R. Hyaluronan is a key component in cryoprotection and formulation of targeted unilamellar liposomes. Biochim Biophys Acta-Biomembranes, 2003; 1612(1), 76–82.

[176] Eliaz R.E., Szoka F.C. Liposome-encapsulated doxorubicin targeted to CD44: a strategy to kill CD44-overexpressing tumor cells. Cancer Res, 2001; 61, 2592–2601.

[177] Peer D., Margalit R. Physicochemical evaluation of a stability-driven approach to drug entrapment in regular and in surface-modified liposomes. Arch Biochem Biophy, 2000; 383(2), 185–190.

[178] Brown M.B., Jones S.A. Hyaluronic acid: a unique topical vehicle for the localized delivery of drugs to the skin. JEADV, 2005; 19(3), 308–318.

[179] Segura T., Chung P.H., Shea L.D. DNA delivery from hyaluronic acid-collagen hydrogels via a substrate-mediated approach. Biomaterials, 2005; 26(13), 1575–1584.

[180] Hoare T.D., Kohane D.S. Hydrogels in drug delivery: progress and challenges. Polymer, 2008; 49(8), 1993-2007.

[181] Hamman J.H. Chitosan based polyelectrolyte complexes as potential carrier materials in drug delivery systems. Mar. Drugs, 2010; 8, 1305-1322.

[182] Lee H., Ahn C., Park T.G. Poly[lactic-co-(glycolic acid)]-grafted hyaluronic acid copolymer micelle nanoparticles for target-specific delivery of Doxorubicin. Macromol. Biosci., 2009; 9(4), 336–342.

[183] Mayol L., Biondi M., Quaglia F., Fusco S., Borzacchiello A., Ambrosio L., La Rotonda M.I. Injectable thermally responsive mucoadhesive gel for sustained protein delivery. Biomacromolecules, 2011; 12(1), 28–33.

[184] Mayol L., Quaglia F., Borzacchiello A., Ambrosio L., La Rotonda M.I. A novel poloxamers/hyaluronic acid in situ forming hydrogel for drug delivery: rheological, mucoadhesive and in vitro release properties. European Journal of Pharmaceutics and Biopharmaceutics, 2008; 70(1), 199-206.

[185] Coradini D., Zorzet S., Rossin R., Scarlata I., Pellizzaro C., Turrin C., Bello M., Cantoni S., Speranza A., Sava G., Mazzi U., Perbellini A. Inhibition of hepatocellular carcinomas *in vitro* and hepatic metastases *in vivo* in mice by the histone deacetylase inhibitor HA-But. Clin. Cancer Res., 2004; 10, 4822–4830.

[186] Lee H., Mok H., Lee S., Oh Y.K., Park T.G. Target-specific intracellular delivery of siRNA using degradable hyaluronic acid nanogels. J Controlled Release, 2007; 119(2), 245-252.

[187] Auzenne E., Ghosh S.C., Khodadadian M., Rivera B., Farquhar D., Price R.E., Ravoori M., Kundra V., Freedman R.S., Klostergaard J. Hyaluronic acid-paclitaxel: antitumor efficacy against CD44(+) human ovarian carcinoma xenografts. Neoplasia, 2007; 9(6), 479–486.

[188] Eliaz R.E., Szoka F.C.J. Liposome-encapsulated Doxorubicin Targeted to CD44: a strategy to kill CD44-overexpressing tumor cells. Cancer Res., 2001; 61, 2592–2601.

[189] Eliaz R.E., Nir S:, Marty C., Szoka F.C.J. Determination and modeling of kinetics of cancer cell killing by doxorubicin and doxorubicin encapsulated in targeted liposomes. Cancer Res., 2004; 64, 711–718.

[190] Kim J.H., Kim Y.S., Kim S., Park J.H., Kim K., Choi K., Chung H., Jeong S.Y., Park R.W., Kim I.S., Kwon I.C. Hydrophobically modified glycol chitosan nanoparticles as carriers for paclitaxel. J. Controlled Release, 2006; 111(1-2), 228-234.

[191] Park K., Kim J.H., Nam Y.S., Lee S., Nam H.Y., Kim K., Park J.H., Kim I.S., Choi K., Kim S.Y., Kwon I.C. Effect of polymer molecular weight on the tumor targeting characteristics of self-assembled glycol chitosan nanoparticles. J. Controlled Release, 2007, 122(3), 305-314.

[192] Min K.H., Park K., Kim Y.S., Bae S.M., Lee S., Jo H.G., Park R.W., Kim I.S., Jeong S.Y., Kim K., Kwon I.C. Hydrophobically modified glycol chitosan nanoparticles-encapsulated camptothecin enhance the drug stability and tumor targeting in cancer therapy. J. Controlled Release, 2008; 127(3), 208-218.

[193] Maeda H., Wu J., Sawa T., Matsumura Y., Hori K. Tumor vascular permeability and the EPR effect in macromolecular therapeutics: a review. J Controlled Release, 2000; 65(1-2), 271-284.

[194] Hobbs S.K., Monsky W.L., Yuan F., Roberts W.G., Griffith L., Torchilin V.P., Jain R.K. Regulation of transport pathways in tumor vessels: Role of tumor type and microenvironment. Proc. Natl. Acad. Sci. U. S. A., 1998; 95(8), 4607–4612.

[195] Duncan R. Polymer conjugates as anticancer nanomedicines. Nat. Rev. Cancer, 2006; 6, 688–701.

[196] Yun Y.H., Goetz D.J., Yellen P., Chen W. Hyaluronan microspheres for sustained gene delivery and site specific targeting. Biomaterials, 2004; 25(1), 147–157.

-PART 1-

HYALURONIC ACID-COATED BIODEGRADABLE NANOPARTICLES AS NEW DRUG CARRIERS FOR TUMOR TARGETING

CHAPTER 2

Hyaluronic Acid-Coated Biodegradable Nanoparticles: Preparation, Characterization and Preliminary Assesment as New Drug Carriers For Tumor Targeting

ABSTRACT

Nanoparticles (NPs) can passively accumulate into tumors, taking advantage of enhanced permeation and retention (EPR) effect. However, NPs *in vivo* efficacy can be hampered by lack of cell internalization and/or by the fact that the loaded drugs may be released before NPs uptake. Hyaluronic acid (HA) is attractive for tumor-targeted delivery since it can specifically bind to the cancer cells overexpressing CD44 receptor. For these reasons HA based NPs can be efficiently internalized by cells by means of both a passive and an active mechanism.

In this context, the aim of this work was to formulate HA-coated biodegradable NPs for the intracellular targeting of chemotherapeutic(s). In particular, NPs made of poloxamers and polylactic-coglycolic acid (PLGA) blends were coated with HA by a single emulsion technique. NPs were characterized for their size, morphology and zeta potential.

2.1 INTRODUCTION

In the last years NPs have attracted great interest in the field of cancer therapy [1-3] thanks to their ability to encapsulate a quantity of poorly water-soluble anticancer drugs and release them in a sustained manner at target site; in this way from a side they can enhance the intracellular concentration of drugs in cancer cells and from other side they

allow to avoid toxicity in normal cells, overcoming the lack of specificity of conventional chemotherapeutic therapy [4-7] (figure 2.1).

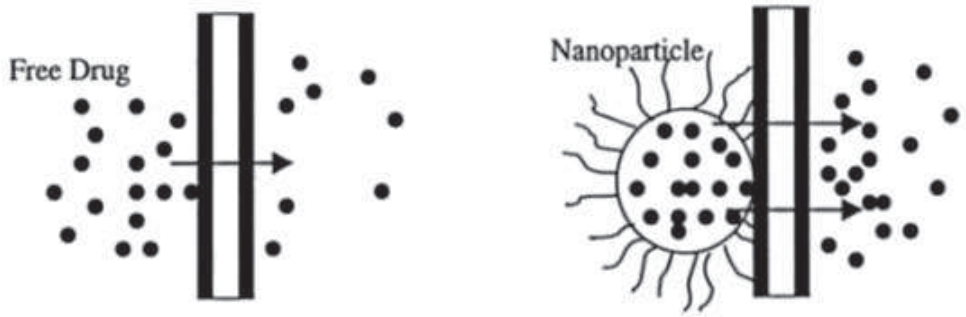

Figure 2.1: Schematic representation of drug absorption through biological membrane in the case of free drug and in the case of nanoparticles

Kumaresh S. Soppimath, Tejraj M. Aminabhavi, Anandro R. kulkarni, Walter E. Rudzinski. "Biodegradable polymeric nanoparticles as drug delivery devices". Journal of Controlled Release 2001. Vol. 70: 1-20.

Furthermore, NPs can accumulate into tumor cells and tissues by taking advantage of passive and/or active targeting [8-11]. The passive tumor targeting phenomenon of NPs is known as the enhanced permeability and retention (EPR) effect, that is the property by which NPs tend to accumulate in tumor tissue much more than they do in normal tissues (figure 2.2).

The general explanation that is given for this phenomenon is that, in order for tumor cells to grow quickly, they must stimulate the production of blood vessels. The newly formed tumor vessels are usually abnormal in form and architecture (leaky, non-organized and hyperpermeable). So nanoparticles can passively accumulate at target sites and a preferential extravasation of circulating nanoparticles occurs [12-19].

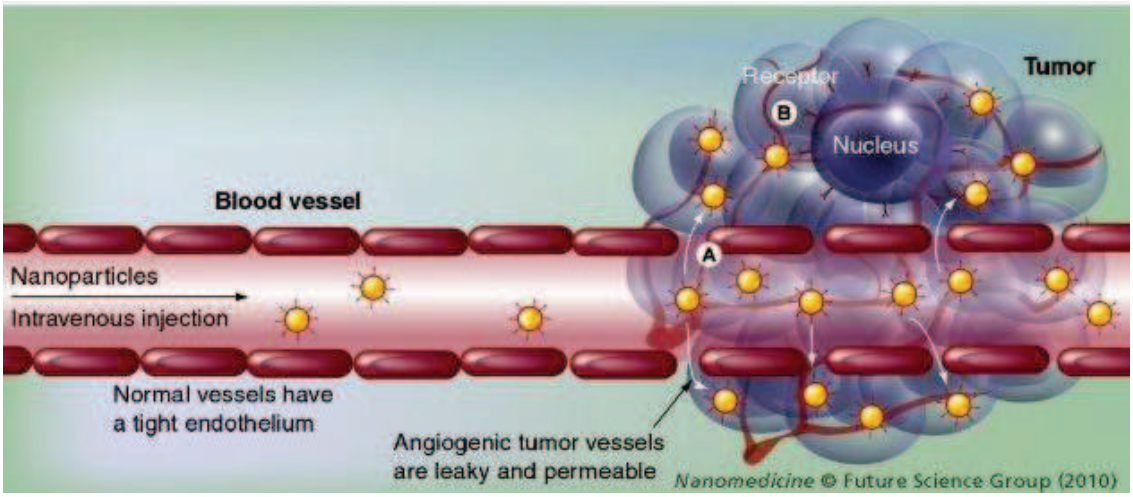

Figure 2.2: Passive targeting strategy of NPs, enhanced permeability and retention (EPR) effect

Nanomedicine, Future science group (2010)

However, this passive targeting strategy of NPs is limited by the possible lack of cell internalization and/or by the release of the loaded drugs before NPs uptake [20]. To overcome these limitations in recent years the research has been devoted to the preparation of NPs functionalized with antibodies [21-23], nucleic acids [24-25], proteins [26-29], and various ligands [30-32]. Functionalized NPs can recognize and bind in a specific way to the tumor cells, and they can be internalized by means of receptor-mediated endocytosis [33-35].

Of the different ligands studied, antibody fragments have been extensively used for NPs funzionalization. However, the use of antibodies for therapeutic purposes suffers from their sometimes potent immunogenicity and as a consequence the binding affinity for the target is often deteriorated [36].

HA is a naturally occurring polysaccharide composed of repeating disaccharides of D-glucuronic acid and N-acetyl-D-glucosamine and mainly present in the extra-cellular matrix of the mammalian connective tissues [37-41]. It is an important structural element in the skin and is present in high concentration in the synovial joint fluids, vitreous humor of the eyes, hyaline cartilage, disc nucleus and umbilical cord [42-46]. HA plays a major role in several functions in vivo such as lubrification of arthritis joints, viscoelastic properties of soft tissues and it is involved in important cell functions such as cell motility, cell matrix adhesion and cell organization [47-51]. Thanks to its excellent biocompatibility, biodegradability, unique physical, chemical and biological

properties and to the ease of chemical functionalisation, HA has generated increasing interest among researchers and it is already used in several biomedical applications such as regenerative medicine [52] and drug delivery [53-57].

In particular HA is an attractive material for tumor-targeted delivery since it can specifically bind to the cancer cells overexpressing CD44 receptor [58-61]. In this way NPs enter the tumor through the leaky microvascolature of tumors, HA binds to CD44 cell receptors and conseguently there is a co-internalization of HA and drug leading to an increased intracellular drug release (figure 2.3).

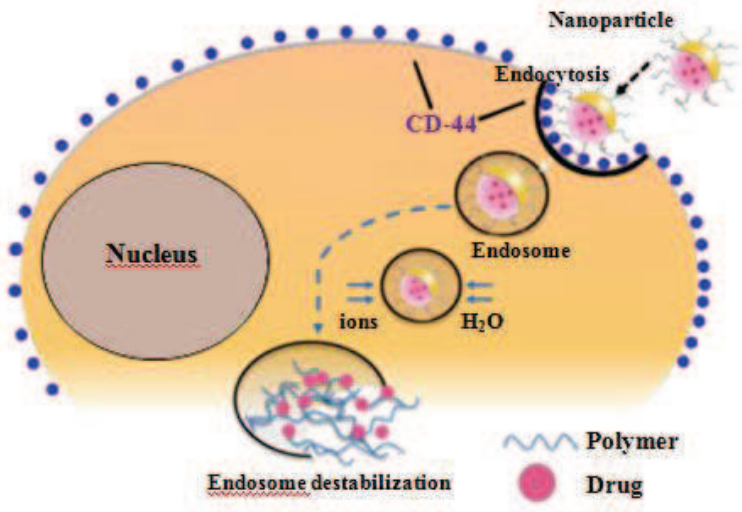

Figure 2.3: Active targeting strategy of NPs

Several HA-based drug carriers have been studied for tumor targeting. Since HA has multiple functional groups available for chemical conjugation, several HA-drug conjugates have been developed as macromolecular prodrugs in which the conjugated drugs become active upon release from the backbone of HA [62-65].

Otherwise, HA has been chemically anchored onto various nanoparticles containing drugs [66-72]. For example PLGA-grafted HA copolymers were synthesized and utilized as target specific micelle carriers for Doxorubicin. For grafting hydrophobic PLGA chains onto the backbone of hydrophilic HA, HA was solubilized in an anhydrous DMSO by nano-complexing with dimethoxy-PEG. The carboxylic groups of HA were chemically grafted with PLGA, producing HA-g-PLGA copolymers. Resultant HA-g-PLGA self-assembled in aqueous solution to form multi-cored micellar

aggregates and Doxorubicin was encapsulated during the self-assembly [73] (figure 2.4).

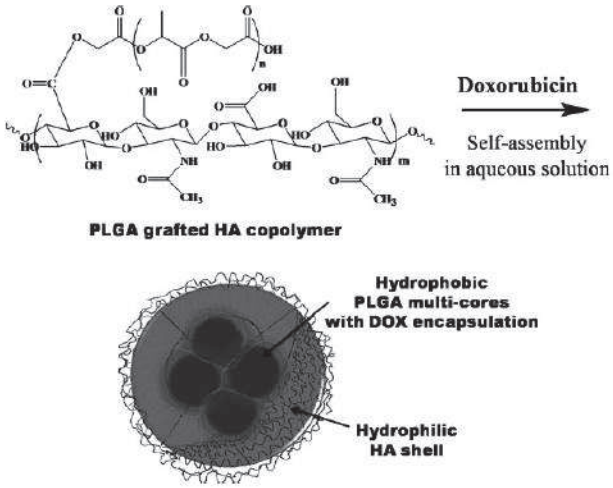

Figure 2.4: HA-g-PLGA self-assembled in aqueous solution to form multi-cored micellar aggregates and Doxorubin was encapsulated during the self-assembly.

Hyukjin Lee, Cheol-Hee Ahn, Tae Gwan ParkPoly[lactic-co-(glycolic acid)]-Grafted Hyaluronic Acid Copolymer Micelle Nanoparticles for Target-Specific Delivery of DoxorubicinMacromol. Biosci. 2009, 9, 336–342

These HA modified macromolecular prodrugs and nano-sized drug carriers exhibited enhanced tumor targeting ability and therapeutic efficacy, compared to free anticancer agents. It has been reported that the pharmacokinetics of drug conjugates and nanoparticles are determined by their physicochemical properties such as surface chemistry, size, surface charge, and molecular weight [74-75].

However HA modified macromolecular prodrugs and nano-sized drug carriers were obtained by means of a chemical reaction.

In this context, the aim of this work was to formulate HA-coated biodegradable NPs for the intracellular targeting of chemotherapeutic(s).

PLGA is the mainly polymer used in drug delivery for its peculiar properties of biocompatibility and biodegradability. However NPs of PLGA had no targeting groups for specific tumor cells and also a phenomenon of aggregation often occurs. In order to overcome this problem, the idea was to create a HA shell around the biodegradable core of NP in order to improve the PLGA NPs dimensional stability taking advantage

of the negative charge of HA that implies a electrostatic repulsion between the NPs. Furthermore HA shell was binded to the biodegradable core by means of a physical binding using an anphiphilic polymer that acts as a bridge between the hydrophobic PLGA and the hydrophilic HA (figure 2.5). In this way it was possible to obtain a stable drug carrier in a simple way avoiding the problems related to a chemical reaction.

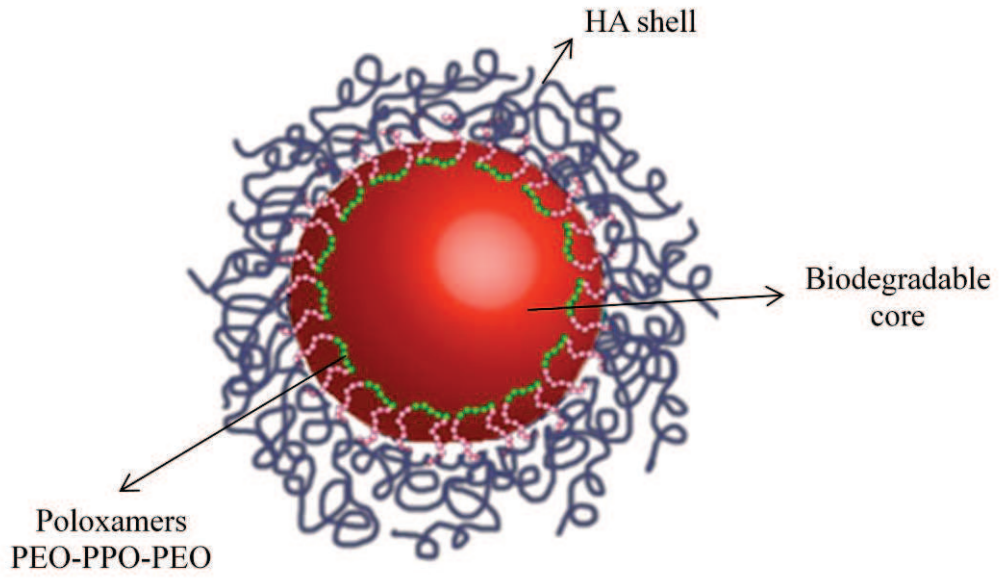

Figure 2.5: Schematic representation of the nanoparticles characterized by HA shell, biodegradable core and poloxamers that act as bridge between PLGA particles and HA

In particular NPs made of poloxamers and PLGA blends were coated with HA by a single emulsion technique. NPs were characterized for their size, morphology and zeta potential.

2.2 MATERIALS AND METHODS

2.2.1 *Materials*

Hyaluronic acid (HA) with a weight-average molecular weight (MW) of 850,000 Da was provided by Novozymes Biopharma (Denmark). Poly(lactic-co-glycolic acid)

(PLGA) (RG504H, MW 12,000 Da) was purchased from Boherniger Ingelheim (Germany).

Poloxamers (PEOa-PPOb-PEOa), a group of amphiphilic triblock polymers, designed with variable numbers of oxyethylene (a) and oxypropylene (b) units, were employed. In particular in this study, poloxamer F127 (a=100 and b=65) and F68 (a=76 and b=29), obtained from Lutrol (Basf, Germany), were used.

Phosphate buffer saline (PBS) tablets without calcium and magnesium were obtained from MP Biomedicals Inc. (France).

2.2.2 *Nanoparticles preparation*

NPs were prepared by a single emulsion technique (oil in water). In order to obtain NPs suitable for biomedical applications, formulations with different amount of HA, poloxamers, and PLGA were prepared.

In table 2.1 all the formulations prepared were reported:

-NPs characterized by PLGA and poloxamers, indicated with PP, at different polymers concentrations (2, 4, 6% w/v) (PP2, PP4, PP6);

- NPs characterized by PLGA, poloxamers, HA, indicated with PP HA, with a constant amount of HA (30 mg) and at different polymers concentrations in the organic phase (2, 4, 6% w/v), (PP2-HA30, PP4-HA30, PP6-HA30);

- NPs characterized by PLGA, poloxamers, HA at the same concentration of polymers in the organic phase (2% w/v) and different amounts of HA (6, 30, 60 mg) (PP2-HA6, PP2-HA30, PP2-HA60);

- NPs characterized by PLGA, poloxamers, HA at different concentrations of poloxamers (0, 0.5, 1% w/v) in the water phase.

Briefly, solutions of PLGA and poloxamers (F127 and F68 1:1 w/w) in acetone, at different polymer concentrations and keeping constant PLGA-poloxamers weight ratio, were prepared. The organic phase was emulsified by vortexing for 5 min with the aqueous phase containing different HA and poloxamers amounts. The resulting emulsion was sonicated for 4 min at 4°C using a Branson Ultrasonic Cleaners (Model 3510) and the solvent was evaporated at 35°C for 35 minutes by using a device called a rotary evaporator (Laborota 4010 digital, HEIDOLPH).

A solution of sucrose, that acts as a cryoprotectant, prepared by mixing 600 mg of sucrose in 9 ml of bidistilled water was added to the NPs suspension.

Nanoparticles were finally separated from supernatant by centrifugation at 13000 rpm for 60 minutes and lyophilized (Heto PowerDry PL6000 Freeze Dryer, Thermo Electron Corp., USA; -50 °C, 0.73 hPa) for 24 h.

Formulations	Oil phase					Water phase			
	PLGA (mg)	F68 (mg)	F127 (mg)	C_3H_6O (ml)	Polymer concentration in the organic phase, % (w/v)	HA (mg)	F68 (µl)	F127 (µl)	DDW (ml)
PP2	10	5	5	1	2	-	-	-	6
PP4	20	10	10	1	4	-	-	-	6
PP6	30	15	15	1	6	-	-	-	6
PP2-HA 6	10	5	5	1	2	6	300 (0.5% w/v)	300 (0.5% w/v)	2.4
PP2-HA 30	10	5	5	1	2	30	300 (0.5% w/v)	300 (0.5% w/v)	2.4
PP4-HA 30	20	10	10	1	4	30	300 (0.5% w/v)	300 (0.5% w/v)	2.4
PP6-HA 30	30	15	15	1	6	30	300 (0.5% w/v)	300 (0.5% w/v)	2.4
PP2-HA 60	10	5	5	1	2	60	300 (0.5% w/v)	300 (0.5% w/v)	2.4
PP2-HA 30 (no poloxamers water phase)	10	5	5	1	2	30	-	-	3
PP2-HA 30 (1% poloxamers water phase)	10	5	5	1	2	30	300 (1% w/v)	300 (1% w/v)	2.4

Table 2.1: Formulations with different amount of HA, poloxamers, and PLGA

2.2.3 *Nanoparticles characterization: morphology, mean size, size distribution and ζ potential*

Nanoparticles morphology was investigated through a transmission electron microscopy (TEM, FEI Tecnai G12 Spirit Twin) with emission source LaB6 (120 kV, spotsize 1) using 400 mesh carbon-coated copper grids at RT. The carbon-coated copper grid was immersed in ultradiluted NP suspension and, after the drying phase, the grid was placed on a rod holder for the TEM characterization. Three grids per NP suspension were prepared and a minimum of four micrographs per grid were acquired.

Nanoparticles mean size, size distribution and ζ potential were determined by laser light scattering (LS, ZetaSizer Nano ZS, Malvern Instruments, Malvern, UK) on a ultra-diluted suspensions in water (12 runs each sample).

NP size, size distribution and ζ potential were also determined after 25 days to assess device stability in the time. Stability tests were performed in order to verify a possible nanoparticles aggregation. Results were averaged on at least five measurements.

2.3 RESULTS AND DISCUSSION

2.3.1 *Morphological characterization*

The morphology of the nanoparticles was studied in distilled water at room temperature by transmission electron microscopy (TEM).

Selected TEM micrographs of nanoparticles at a PLGA concentration of 2% w/v indicated with P2 (figure 2.6), nanoparticles prepared with PLGA and poloxamers F68 and F127 at a polymer concentration of 2% w/v indicated with PP2 (figure 2.7) and nanoparticles prepared with PLGA, poloxamers F68 and F127 at a polymer concentration in the organic phase of 2% w/v and different amount of HA (6 mg, 30 mg, 60 mg) indicated with PP2HA6, PP2HA30, PP2HA60 (figure 2.8) were reported.

From the figures it can be noticed that all the nanoparticles show a spherical shape.

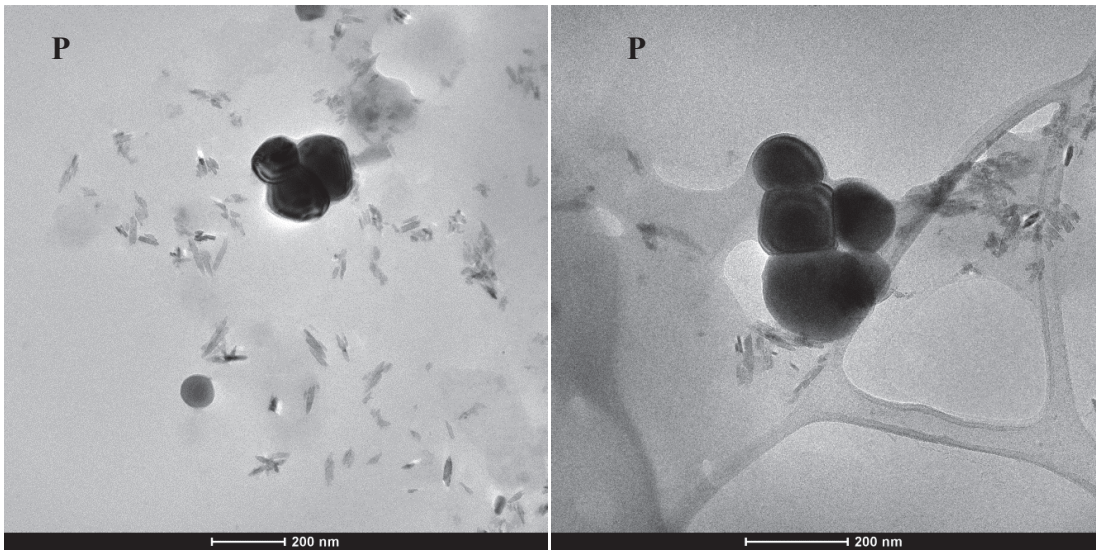

Figure 2.6: Selected TEM micrographs of nanoparticles of PLGA at a concentration of 2%

In the case of nanoparticles of bare PLGA it is clear that an aggregation phenomenon occurred (figure 2.6).

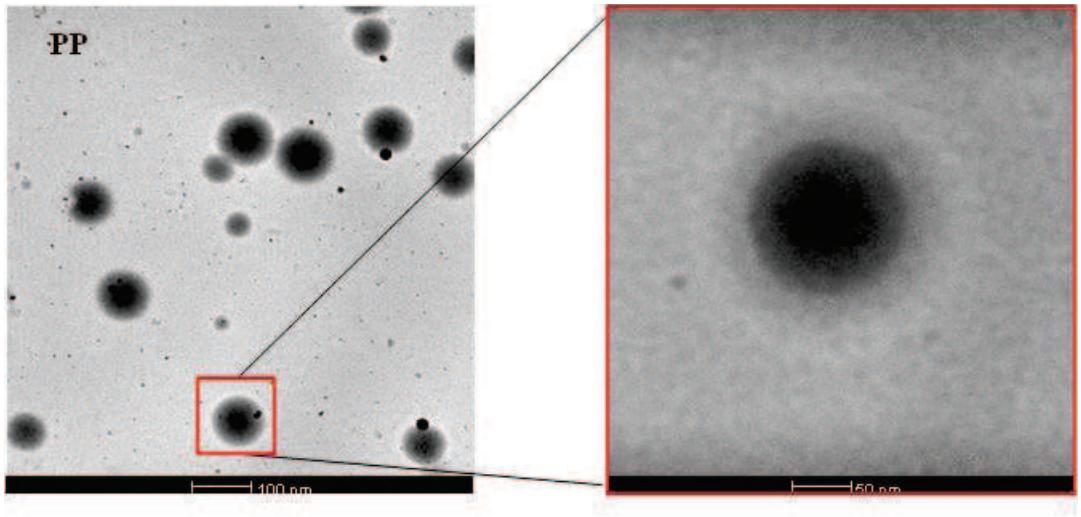

Figure 2.7: Selected TEM micrographs of nanoparticles of PLGA and poloxamers F68 and F127 at a polymer concentration of 2%

By adding the poloxamers, nanoparticles relatively polydisperse and with a good dimensional stability were obtained (figure 2.7).

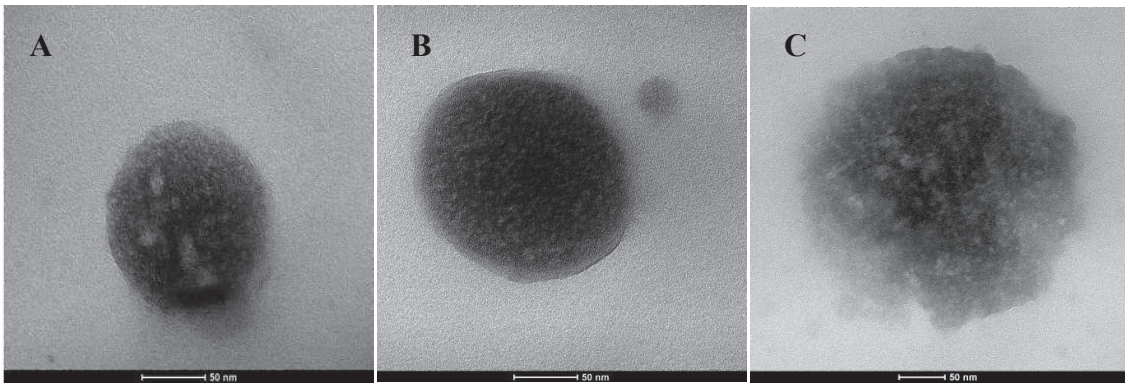

Figure 2.8: Selected TEM micrographs of nanoparticles prepared with PLGA, poloxamers F68 and F127 at a polymer concentration of 2% and different amount of HA, 6 mg (A), 30 mg (B), 60 mg (C).

TEM images of HA based NPs show that also in this case nanoparticles with a spherical shape were obtained but it can be noticed a sort of pockets, probably due to the interaction of HA with the polymers. Indeed, HA and poloxamers constitute a sort of tangled skein which coats the particle (figure 2.8).

2.3.2 *Mean size and size distribution*

The processing variables such as polymer concentration in organic phase, HA amount and poloxamers concentration influences the mean size and the size distribution. Hence the method was optimized to produce nanoparticles of small size and narrow size distribution.

In table 2.2 the results in terms of size of bare PLGA NPs and NPs prepared with PLGA and poloxamers at different polymer concentrations (2 %, 4 %, 6 % w/v) were reported. The results demonstrate that the diameter of NPs slowly increases by increasing the PLGA concentration from 2 to 6 % w/v. Higher concentration of polymer produced a more viscous solution that caused a reduction in the rate of diffusion of polymer solution in the water phase. It is well accepted that the size of nanoparticles is directly dependent on the rate of diffusion of organic solvent to the outer aqueous environment. The faster the diffusion rate is, the smaller the particles would result [76-77].

Furthermore comparing the particles size of bare PLGA NPs and of NPs prepared with PLGA and poloxamers, it can be noticed that the size of bare PLGA NPs is bigger than

the particles with PLGA and poloxamers. This result suggests that in the case of bare PLGA NPs there is an immediate aggregation and the presence of poloxamers influences positively the stability of NPs.

Formulation	Particle mean diameter (0), [*nm*]	Particle mean diameter (10 days), [*nm*]
P	166.6 ± 0.4	260.4 ± 0.8
PP 2%	110.2 ± 0.4	147.8 ± 0.4
PP 4%	113.5 ± 1.8	147.8 ± 0.4
PP 6%	129.8 ± 0.8	185.5 ± 1.3

Table 2.2: Results in terms of size and dimensional stability of bare PLGA NPs and NPs prepared with PLGA and poloxamers at different polymer concentrations (2 %, 4 %, 6 % w/v)

Formulation	Particle mean diameter (0), [*nm*]	Particle mean diameter (10 days), [*nm*]
PP2–HA30	290.5 ±11.9	287.9 ± 4.1
PP4–HA30	301.0 ± 7.9	360.2 ± 7.8
PP6–HA30	308.4 ± 14.9	332.1 ± 7.3

Table 2.3: Results in terms of size and dimensional stability of NPs prepared with PLGA, poloxamers and HA at different polymer concentrations (2 %, 4 %, 6 % w/v) and keeping constant HA amount (30 mg)

In table 2.3 the effect of the adding of HA on NPs size was reported. In particular we show the dimensional results of NPs prepared with PLGA, poloxamers and HA at different polymer concentrations in the organic phase (2 %, 4 %, 6 % w/v) keeping

constant HA amount (30 mg). The adding of HA in the formulations determined an increase of NPs size as it can be expected.

In table 2.4 the effect of poloxamers concentration in the water phase on nanoparticles size, keeping constant PLGA and HA concentrations was shown. In particular the size of nanoparticles prepared with a polymer concentration in the organic phase of 2% w/v, an HA amount of 30 mg and different concentrations (0, 0.5% w/v, 1% w/v) of poloxamers (F68 and F127) solutions was reported. From the results it can be noticed that by varying the poloxamers concentration the better result in terms of NPs size was obtained in the case particles prepared with a poloxamer concentration of 0.5% w/v.

Formulation	F 68, w/v	F 127, w/v	Particle mean diameter (0), [*nm*]	Particle mean diameter (25 days), [*nm*]
PP2–HA30	-	-	330.2±20.6	369.7±21.4
PP2–HA30	0.5%	0.5%	290.5±11.9	287.9±4.1
PP2–HA30	1%	1%	349.2±36.5	312.6±27.8

Table 2.4: Effect of poloxamers concentration on nanoparticles size and dimensional stability, keeping constant PLGA and HA concentration

Furthermore the effect of HA amount on nanoparticles size, keeping constant PLGA and poloxamers concentrations was reported. In particular the diameter of particles prepared at PLGA and poloxamers concentrations in water phase of 2% w/v and 0.5% w/v respectively, and different amount of HA (6 mg, 30 mg, 60 mg) was shown in table 2.5.

The amount of HA is a crucial parameter in the design of the formulations because the quantitative of HA must be such that from a side a shell is formed around all the biodegradable core and on the other hand it must be not too big to lead to a phenomenon of NPs aggregation.

From the results it can be concluded that by varying the HA amount from 6 mg to 30 mg and 60 mg the best formulation in terms of size is that of the NPs prepared at a HA amount of 6mg. By increasing the HA amount the nanoparticles size increases signifcatively and it is possible that an aggregation phenomenon was occurred.

Formulation	Particle mean diameter (0), [*nm*]	Particle mean diameter (25 days), [*nm*]
PP2–HA6	169.8 ± 4.2	186.1 ± 1.2
PP2–HA30	290.5 ± 11.9	287.9 ± 4.1
PP2–HA60	234.5 ± 4.1	231.4 ± 7.0

Table 2.5: Effect of HA amount on nanoparticles size and dimensional stability, keeping constant PLGA and poloxamers concentrations

This hypothesis is confirmed from the results related to the polydispersity index (PdI) reported in figure 2.9. Infact by increasing the HA amount from 6 mg, to 30 mg up to 60 mg, there is an increase of PdI from 0.3, that indicates a narrow size distribution, for PP2-HA 6, to 0.5 for PP2-HA 30, to 0.7, that is indicative of a wide size distribution, in the case of PP2-HA 60.

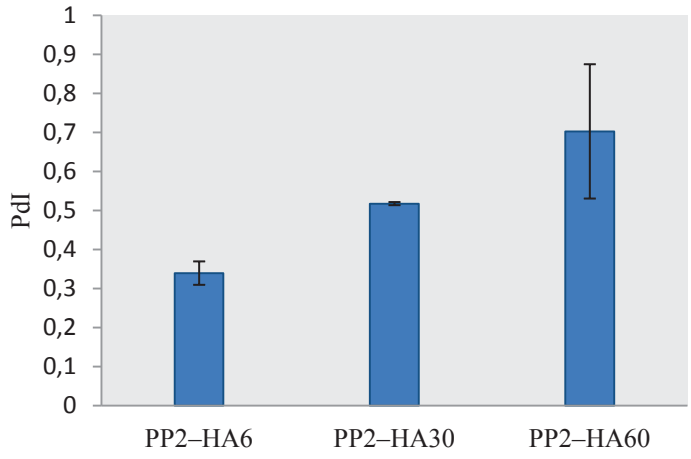

Figure 2.9: Polydispersity Index (PdI) of particles prepared at different HA amount (PP2-HA6, PP2-HA30, PP2-HA60)

2.3.3 *Dimensional stability*

In the clinical administration of NPs, a phenomenon of particle aggregation may occur, affecting the drug release profile and probably implying vessel occlusion. For these reasons, the steric stability of nanoparticles is an important aspect to be considered.

In table 2.2 the dimensional stability in the time of bare PLGA NPs and NPs prepared with PLGA and poloxamers at different polymer concentrations (2 %, 4 %, 6 % w/v) was reported. In particular the NPs diameter at time zero and after 10 days of NPs preparation was shown.

Stability tests demonstrated that in the case of bare PLGA NPs there is an increase of NPs size of about 56 % in the time; so it can be concluded that after 10 days in the case of bare PLGA particles an aggregation phenomena occurred, while PLGA-Poloxamers particles size does not change significantly in the time. Therefore the presence of poloxamers influences positively dimensional stability of the particles.

The dimensional stability of NPs prepared with PLGA, poloxamers and HA at different polymer concentrations (2 %, 4 %, 6 % w/v) keeping constant HA amount (30 mg) was shown in table 2.3. The results demonstrated that the formulations prepared with HA show a good stability in the time in all cases.

In table 2.4 the effect of poloxamers concentration in the water phase on dimensional stability of the nanoparticles, keeping constant PLGA and HA concentrations was shown. In particular the size of nanoparticles prepared with a polymer concentration in the organic phase of 2% w/v, an HA amount of 30 mg and different concentrations (0, 0.5% w/v, 1% w/v) of poloxamers (F68 and F127) solutions was reported. From the results it can be noticed that by varying the poloxamers concentration the better result in terms of dimensional stability of the NPs was obtained in the case of particles prepared with a poloxamer concentration of 0.5% w/v.

Furthermore the effect of HA amount on diamensional stability of the NPs, keeping constant PLGA and poloxamers concentrations was reported in table 2.5.

In particular the diameter of particles prepared at polymer in organic phase and poloxamers in water phase concentrations of 2% w/v and 0.5% w/v respectively, and different amount of HA (6 mg, 30 mg, 60 mg) at time zero and after 25 days was shown.

From the results it can be concluded that all the formulations prepared at different amount of HA show a good dimensional stability in the time.

In figure 2.10 the evaluation of the diameter in the time of the NPs prepared at a polymer concentration in the organic phase of 2% w/v, with an HA amount of 6mg and a poloxamers concentration of 0.5% w/v in water phase was reported. As it can be noticed the variation in the NPs size is not significative and the formulation prepared with HA show a very good stability probably due to the negative charge on the surface of the NPs that determines an electrostatic repulsion between the NPs. So this is the best formulation in terms of both size and dimensional stability.

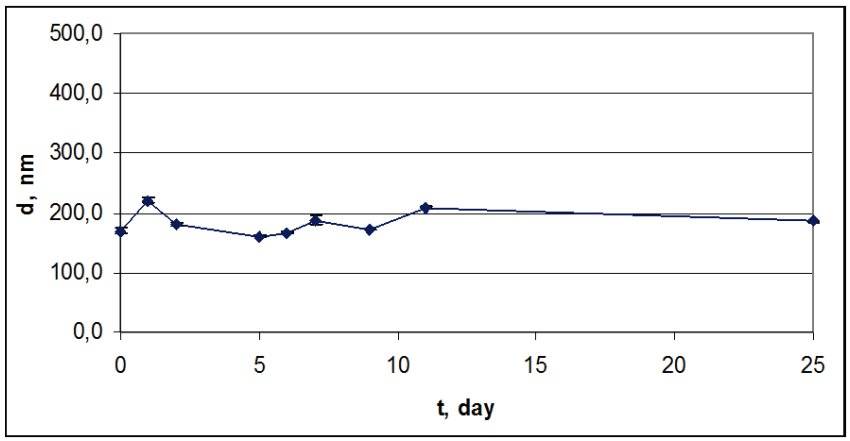

Figure 2.10: Dimensional stability in the time of nanoparticles PP2 HA 6

2.3.4 *Zeta potential*

In table 2.6 the results in terms of zeta potential of bare PLGA NPs and NPs prepared with PLGA and poloxamers at different polymer concentrations (2 %, 4 %, 6 % w/v) were reported. The zeta potential of bare PLGA NPs is around –27 mV; the presence of poloxamers and the variation of polymer concentrations does not effect on zeta potential.

The zeta potential of NPs prepared with PLGA, poloxamers and HA at different polymer concentrations in the organic phase (2 %, 4 %, 6 %, w/v) keeping constant HA amount (30 mg) was reported in table 2.7. The results show that the presence of HA in the formulations determines a decrease in the ζ potential; in particular the zeta potential passes from -27 mV in the case of particles without HA to -40 mV in the case of particles prepared with HA. The explanation of this phenomenon is related to the

negative charge of HA. This result can be an indication of the fact that HA was effectively settled around the biodegradable core of the particle forming a shell.

Formulation	Zeta potential (0), [*mV*]	Zeta potential (10 days), [*mV*]
P	-27.7 ± 2.0	-30.2 ± 2.1
PP 2%	-23.1 ± 2.3	-19.4 ± 2.2
PP 4%	-29.9 ± 0.6	-17.9 ± 3.5
PP 6%	-26.7 ± 1.9	-26.1 ± 0.7

Table 2.6: Results in terms of zeta potential of bare PLGA NPs and NPs prepared with PLGA and poloxamers at different polymer concentrations (2 %, 4 %, 6 % w/v)

Formulation	Zeta potential (0), [*mV*]	Zeta potential (10 days), [*mV*]
PP2–HA30	-40.3 ± 2.9	-34.2 ± 8.1
PP4–HA30	-37.6 ± 0.9	-31.9 ± 5.8
PP6–HA30	-39.2 ± 3.1	-32.2 ± 2.5

Table 2.7: Results in terms of zeta potential of NPs prepared with PLGA, poloxamers and HA at different polymer concentrations (2 %, 4 %, 6 % w/v) and keeping constant HA amount (30 mg)

In table 2.8 the effect of poloxamers concentration in water phase on nanoparticles zeta potential, was shown. In particular the zeta potential of nanoparticles prepared keeping

constant polymer concentration in the organic phase at 2% w/v, and HA amount at 30 mg and at different concentrations (0, 0.5% w/v, 1% w/v) of poloxamers (F68 and F127) solutions was reported.

From the results it can be noticed that even if the HA amount, that determines the negative charge of the NPs surface, is the same in all tested formulations, the NPs zeta potential changes from about -27 mV and -28 mV in the case of particles prepared at a poloxamers concentration of 0% and 1% w/v respectively to -40 mV in the case of particles prepared at a poloxamers concentration of 0.5% w/v.

In the absence of poloxamers in the organic phase, particles show the same zeta potential of NPs prepared with bare PLGA, suggesting that probably without poloxamers in the organic phase, HA is not able to form a shell around the biodegradable core. When the poloxamers concentration is 0.5% w/v, the zeta potential decreases significantly probably due to the presence of HA around the particles. In the case of the result obtained by analyzing the zeta potential of NPs prepared with a poloxamers concentration of 1% w/v, it is possible that the poloxamers concentration is so high that a part of poloxamers takes place around HA shell, shielding the particle.

From this results it can be concluded that in order to obtain nanoparticles characterized by a biodegradable core, a HA shell and poloxamers as bridge between hydrophobic core and hydrophilic shell, the optimum poloxamers concentration is 0.5% w/v.

Formulation	**F 68, w/v**	**F 127, w/v**	**Zeta potential (0), [*mV*]**	**Zeta potential (25 days), [*mV*]**
PP2–HA30	-	-	-28.4±2.2	-27±3.1
PP2–HA30	0.5%	0.5%	-40.3±2.9	-34.2±8.1
PP2–HA30	1%	1%	-27.8±2.0	-35.1±3.4

Table 2.8: Effect of poloxamers concentration on nanoparticles zeta potential, keeping constant PLGA and HA concentration

Furthermore the effect of HA amount on nanoparticles zeta potential, keeping constant PLGA and poloxamers concentrations was reported. In particular the zeta potential of particles prepared with a polymer concentration in the organic phase of 2% w/v, poloxamers concentrations of 0.5% w/v in the water phase, and different amount of HA (6 mg, 30 mg, 60 mg) was shown in table 2.9.

From the results it can be concluded that in the case of particles prepared with 6 mg and 30 mg of HA the zeta potential is about -40 mV; in the case instead of particles prepared with 60 mg of HA an increase of zeta potential from -40 mV to -22 mV was shown. A possible explanation of this phenomenon can be that in the case of particles at HA amount of 60 mg an aggregation between the nanoparticle occurred, resulting in a less exposed surface and therefore in an increase of the mean zeta potential.

Formulation	Zeta potential (0), [*mV*]	Zeta potential (25 days), [*mV*]
PP2–HA6	-37.3 ± 3.5	-29.4 ± 3.8
PP2–HA30	-40.3 ± 2.9	-34.2 ± 8.1
PP2–HA60	-22.2 ± 2.7	-24.6 ± 4.6

Table 2.9: Effect of HA amount on nanoparticles zeta potential, keeping constant PLGA and poloxamers concentrations

2.3.5 *Zeta potential stability*

Zeta potential stability tests in the time were performed on bare PLGA NPs and NPs prepared with PLGA and poloxamers at different polymer concentrations (2 %, 4 %, 6 % w/v) (table 2.6). In particular the NPs zeta potential at time zero and after 10 days of NPs preparation was shown. As it can be noticed from table 2.6 the zeta potential does not change in a significative manner in the time for all the formulations reported.

The zeta potential stability of NPs prepared with PLGA, poloxamers and HA at different polymer concentrations in the organic phase (2 %, 4 %, 6 %, w/v), keeping constant HA amount (30 mg) was reported in table 2.7. The results demonstrate that

the presence of HA in the formulations determines a decrease in the ζ potential than the particles of bare PLGA and there is a good zeta potential stability in the time. Furthemore there is a slightly increase of zeta potential after 10 days from -40.3 ± 2.9mV to -34.2 ± 8.1mV in the case of PP2 HA30, from -37.6± 0.9 mV to -31.9±5.8 mV in the case of PP4 HA30 and from -39.2±3.1 mV to -32.2±2.5 mV in the case of PP6 HA30, probably due to the HA degradation in the time.

In table 2.8 the effect of poloxamers concentration in the water phase on zeta potential stability was reported. In particular the zeta potential at time zero and after 25 days for the NPs prepared at the same polymer concentration (2% w/v) in the organic phase and the same amount of HA in the water phase (30 mg) and different F68 and F127 concentration in the water phase (0, 0.5%, 1% w/v) was shown.

As reported before without the presence of poloxamers in the external phase, the particles show the same potential of NPs of bare PLGA, indicating probably that HA was not binded to the biodegradable core.

As regards particles prepared at a poloxamers concentration of 0.5% w/v the zeta potential passes from -40.3±2.9mV to -34.2±8.1 mV after 25 days. The zeta potential decreases because of the presence of HA and in the time probably increases for HA degradation.

When poloxamers concentration is 1% w/v in the water phase the zeta potential passes from -27.8±2.0 mV to -35.1±3.4 mV after 25 days. In this case probably at time zero the poloxamers concentration is so high that poloxamers shield HA shell around the particle; in the time the interaction between HA shell and PEO segments of poloxamers can be weakened because of the stronger interaction between the hydrophilic groups of poloxamers and the water.

The effect of HA amount on zeta potential stability of the nanoparticles was shown in table 2.9. In particular the zeta potential of particles prepared with a polymer concentration in the organic phase of 2% w/v, poloxamers concentrations of 0.5% w/v in water phase, and different amount of HA (6 mg, 30 mg, 60 mg) was reported.

From the results it can be noticed that after 25 days all the formulations show an increase of zeta potential probably due to the HA degradation in the time.

2.4 CONCLUSIONS

HA coated biodegradable NPs for tumor targeting were developed. The nanoparticles shown a spherical shape and a size ranging from 170 to 300 nm. In the case of bare PLGA particles immediate aggregation phenomena occured; HA addition allowed to obtain stable NPs size for more than 10 days. It's important to underline that HA amount must be optimized to match possible tropism towards CD44 receptor and NP aggregation.

REFERENCES

[1] Cho K., Wang X., Nie S., Chen Z., Shin D.M., Therapeutic Nanoparticles for Drug Delivery in Cancer. Clin Cancer Res, 2008; 14, 1310-1316.

[2] Ross J.S., Schenkein D.P., Pietrusko R., Rolfe M., Linette G., Stec J., Stagliano N.E., Ginsburg G.S., Symmans W.F., Pusztai L., Hortobagyi G.N. Targeted therapies for cancer. Am J Clin Pathol, 2004; 122, 598- 609.

[3] Brigger I., Dubernet C., Couvreur P. Nanoparticles in cancer therapy and diagnosis. Advanced Drug Delivery Reviews, 2002; 54(5), 631-51.

[4] Cho H.J., Yoon H.Y., Koo H., Ko S.H., Shim J.S., Lee J.H., Kim K., Kwon I.C., Kim D.D. Self-assembled nanoparticles based on hyaluronic acid-ceramide (HA-CE) and Pluronic® for tumor-targeted delivery of docetaxel. Biomaterials, 2011; 32(29), 7181-90.

[5] He Q., Gao Y., Zhang L., Zhang Z., Gao F., Ji X., Li Y., Shi J. A pH-responsive mesoporous silica nanoparticles-based multi-drug delivery system for overcoming multi-drug resistance. Biomaterials, 2011; 32(30), 7711-20.

[6] Vergara D, Bellomo C., Zhang X., Vergaro V., Tinelli A., Lorusso V., Rinaldi R., Lvov Y.M., Leporatti S. Maffia M. Lapatinib/Paclitaxel polyelectrolyte nanocapsules for overcoming multidrug resistance in ovarian cancer. Nanomedicine, 2012; 8(6), 891-899.

[7] Malam Y., Loizidou M., Seifalian A.M. Liposomes and nanoparticles: nanosized vehicles for drug delivery in cancer. Trends in Pharmacological Sciences, 2009; 30(11), 592-599.

[8] Bae K.H., Chung H.J. Park T.G. Nanomaterials for cancer therapy and imaging. Mol. Cells, 2011; 31(4), 295-302.

[9] Gao Y., Chen L., Gu W., Xi Y., Lin L., Li Y. Targeted Nanoassembly Loaded with Docetaxel Improves Intracellular Drug Delivery and Efficacy in Murine Breast Cancer Model. Mol. Pharmacol., 2008; 5(6), 1044-1054.

[10] Tang N., Du G., Wang N., Liu C., Hang H., Liang W. Improving penetration in tumors with nanoassemblies of phospholipids and doxorubicin. J. Natl Cancer Inst., 2007; 99(13), 1004-1015.

[11] Wang J., Mongayt D., Torchilin V.P. Polymeric micelles for delivery of poorly soluble drugs: Preparation and anticancer activity in vitro of paclitaxel incorporated into mixed micelles based on poly(ethylene glycol)-lipid conjugate and positively charged lipids. J Drug Targeting, 2005; 13(1), 73-80.

[12] Wang A.W., Langer R., Farokhzad O.C. Nanoparticle Delivery of Cancer Drugs. Annu. Rev. Med., 2012; 63, 185-198.

[13] Davis M.E., Chen Z., Shin D.M. Nanoparticle therapeutics: an emerging treatment modality for cancer. Nature Reviews-drug discovery, 2008; 7, 771-782.

[14] Cho K., Wang X., Nie S., Chen Z., Shin D.M. Therapeutic Nanoparticles for Drug Delivery in Cancer. Clin Cancer Res, 2008; 14, 1310-1316.

[15] Davis M.E., Chen Z., Shin D.M. Nanoparticle therapeutics: an emerging treatment modality for cancer. Nature Reviews-drug discovery, 2008; 7, 771-782.

[16] Ferrari M. Cancer nanotechnology: opportunities and challenges. Nature Rev. Cancer, 2005; 5, 161-171.

[17] Peer D., Karp J.M., Hong S., Farokhzad O.C., Margalit R., Langer R. Nanocarriers as an emerging platform for cancer therapy. Nature Nanotechnology, 2007; 2, 751-760.

[18] Duncan R. Polymer conjugates as anticancer nanomedicines. Nat. Rev. Cancer, 2006; 6, 688–701.

[19] Duncan R. The dawning era of polymer therapeutics. Nat. Rev. Drug Discovery, 2003; 2, 347-360.

[20] Choi K.Y., Chung H., Min K.H., Yoon H.Y., Kim K., ParkJ .H., Kwon I.C., Jeong S.Y. Self-assembled hyaluronic acid nanoparticles for active tumor targeting. Biomaterials, 2010; 31(1), 106–114.

[21] Lukyanov A.N., Elbayoumi T.A., Chakilam A.R., Torchilin V.P. Tumor-targeted liposomes: doxorubicin-loaded long-circulating liposomes modified with anticancer antibody. J Control Release, 2004; 100(1), 135–44.

[22] Park J.W., Kirpotin D.B., Hong K., Shalaby R., Shao Y., Nielsen U.B., Marks J.D., Papahadjopoulos D., Benz C.C. Tumor targeting using anti-her2 immunoliposomes. J Control Release, 2001; 74(1- 3), 95–113.

[23] Sapra P., Allen T.M. Internalizing antibodies are necessary for improved therapeutic efficacy of antibody-targeted liposomal drugs. Cancer Res, 2002; 62(24), 7190–7194.

[24] Farokhzad O.C., Cheng J., Teply B.A., Sherifi I., Jon S., Kantoff P.W., Richie J.P., Langer R. Targeted nanoparticle-aptamer bioconjugates for cancer chemotherapy in vivo. Proc Natl Acad Sci U S A, 2006; 103(16), 6315–6320.

[25] Farokhzad O.C., Jon S., Khademhosseini A., Tran T.N., Lavan D.A., Langer R. Nanoparticle- aptamer bioconjugates: a new approach for targeting prostate cancer cells. Cancer Res, 2004; 64(21), 7668–7672.

[26] Bies C., Lehr C.M., Woodley,J.F. Lectin-mediated drug targeting: history and applications. Adv Drug Deliv Rev, 2004; 56(4), 425–435.

[27] Minko T. Drug targeting to the colon with lectins and neoglycoconjugates. Adv Drug Deliv Rev, 2004; 56(4), 491–509.

[28] Qian Z.M., Li H., Sun H., Ho K. Targeted drug delivery via the transferrin receptor mediated endocytosis pathway. Pharmacol Rev, 2002; 54(4), 561–587.

[29] Sahoo S.K., Labhasetwar V. Enhanced antiproliferative activity of transferring conjugated paclitaxel-loaded nanoparticles is mediated via sustained intracellular drug retention. Mol Pharm, 2005; 2(5), 373–383.

[30] Lee R.J., Low P.S. Delivery of liposomes into cultured KB cells via folate receptor mediated endocytosis. J Biol Chem, 1994; 269(5), 3198–3204.

[31] Lu Y., Low P.S.. Folate-mediated delivery of macromolecular anticancer therapeutic agents. Adv Drug Deliv Rev, 2002; 54(5), 675–693.

[32] Eliaz R.E., Szoka F.C.J. Liposome-encapsulated doxorubicin targeted to CD44: a strategy to kill CD44-overexpressing tumor cells. CancerRes, 2001; 61(6), 2592–2601.

[33] Peer D., Karp J.M., Hong S., Farokhzad O.C., Margalit R., Langer R. Nanocarriers as an emerging platform for cancer therapy. Nature Nanotechnology, 2007; 2(12), 751-760.

[34] Torchilin V.P. Multifunctional nanocarriers. Adv Drug Deliv Rev, 2006; 58(14), 1532–1555.

[35] Byrne J.D., Betancourt T., Brannon-Peppas L. Active targeting schemes for nanoparticle systems in cancer therapeutics. Adv Drug Deliv Rev, 2008; 60(15), 1615–1626.

[36] Stacy K.M. Therapeutics MAbs: saving lives and making billions. The Scientist, 2005; 19(3), 17–19.

[37] Gatej I., Popa M., Rinaudo M. Role of the pH on Hyaluronan Behavior in Aqueous Solution. Biomacromolecules, 2005; 6(1), 61-67.

[38] Lapčík L.J., Lapčík L., De Smedt S., Demeester J., Chabrecek P. Hyaluronan: Preparation, Structure, Properties, and Applications. Chemical rewiew, 1998; 98(8), 2663-2684.

[39] Ambrosio L., Borzacchiello A., Netti P.A., Nicolais L. Rheological properties of hyaluronic acid based solutions. Polymeric Materials Science and Engineering, 1999; 79, 244-245.

[40] Ambrosio L., Borzacchiello A., Netti P.A., Nicolais L. Rheological study on Hyaluronic acid and its derivatives solutions. J. of Macromolecular Science-Pure and Applied Chemistry, 1999; A36(7-8), 991-1000.

[41] Barbucci R., Rappuoli R., Borzacchiello A., Ambrosio L. Synthesis, chemical and rheological characterisation of new hyaluronic based hydrogels, Journal of Biomaterials Science Polymer Edition, 2000; 11(4), 383-399.

[42] Monheit G.D., Coleman K.M. Hyaluronic acid fillers. Dermatologic Therapy, 2006; 19(3), 141–150.

[43] Borzacchiello A., Netti P.A., Ambrosio L., Nicolais L. Hyaluronic acid derivatives mimic the rheological properties of vitreous body. New Frontiers in Medical Sciences: Redefining Hyaluronan, 2000; 195-202.

[44] Borzacchiello A., Ambrosio L. Network formation of low molecular weight hyaluronic acid derivatives. Journal of Biomaterials Science Polymer Edition, 2001; 12(3), 307-316.

[45] Barbucci R., Lamponi S., Borzacchiello A., Ambrosio L., Fini M., Torricelli P., Giardino R. Hyaluronic acid hydrogel in the treatment of osteoarthritis. Biomaterials, 2002; 23(23), 4503-4513.

[46] Xuejun Xin, Borzacchiello A., Netti P.A., Ambrosio L., Nicolais L. Hyaluronic Acid Based Semi Interpenetrating Materials. J. Biomater. Sci. Polymer Edn, 2004; 15(9), 1223-1236.

[47] Mori M., Yamaguchi M., Sumitomo S., Takai Y. Hyaluronic-based biomaterials in tissue engineering. Acta Histochem. Cytochem, 2004; 37(1), 1-5.

[48] Borzacchiello A., Mayol L., Gaerskog O., Dahlqvist A., Ambrosio L. Evaluation of injection augmentation treatment of hyaluronic acid based materials on rabbit vocal folds viscoelasticity. Journal of Materials Science: Materials in Medicine, 2005; 16(6), 553-557.

[49] Borzacchiello A., Mayol L., Ramires P.A., Di Bartolo C., Pastorello A., Ambrosio L., Milella E. Structural and rheological characterization of hyaluronic acid-based scaffolds for adipose tissue engineering. Biomaterials, 2007; 28, 4399–4408.

[50] Fusco S., Borzacchiello A., Miccio L., Pesce G., Rusciano G., Sasso A., Netti P.A. High frequency viscoelastic behaviour of low molecular weight hyaluronic acid water solutions. Biorheology, 2007; 44(5-6), 403-418.

[51] Borzacchiello A., Mayol L., Schiavinato A., Ambrosio L. Effect of hyaluronic acid amide derivative on equine synovial fluid viscoelasticity. Journal of biomedical materials research, 2010; 92A(3), 1162-1170.

[52] Mironov V., Kasyanov V., Zheng Shu X., Eisenberg C., Eisenberg L., Gonda S., Trusk T., Markwald R.R., Prestwich G.D. Fabrication of tubular tissue constructs by centrifugal casting of cells suspended in an in situ crosslinkable hyaluronan-gelatin hydrogel. Biomaterials, 2005; 26(36), 7628–7635.

[53] Auzenne E., Ghosh S.C., Khodadadian M., Rivera B., Farquhar D., Price R.E., Ravoori M., Kundra V., Freedman R.S., Klostergaard J. Hyaluronic acid-paclitaxel: antitumor efficacy against CD44(+) human ovarian carcinoma xenografts. Neoplasia, 2007; 9(6), 479–486.

[54] Peer D., Margalit R. Loading mitomycin C inside long circulating hyaluronan targeted nano-liposomes increases its antitumor activity in three mice tumor models. Int J Cancer, 2004; 108(5), 780–789.

[55] Luo Y., Bernshaw N.J., Lu Z.R., Kopecek J., Prestwich G.D. Targeted delivery of doxorubicin by HPMA copolymer-hyaluronan bioconjugates. Pharm Res, 2002; 19(4), 396–402.

[56] Luo Y., Prestwich G.D. Synthesis and selective cytotoxicity of a hyaluronic acid-antitumor bioconjugate. Bioconjug Chem, 1999; 10(5), 755–763.

[57] Lee H., Lee K., Park T.G. Hyaluronic acid-paclitaxel conjugate micelles: synthesis, characterization, and antitumor activity. Bioconjug Chem, 2008; 19(6), 1319–1325.

[58] Toole B.P. Hyaluronan: from extracellular glue to pericellular cue. Nat. Rev. Cancer, 2004; 4, 528–539.

[59] Jaracz S., Chen J., Kuznetsova L.V., Ojima I. Recent advances in tumor-targeting anticancer drug conjugates. Bioorg. Med. Chem., 2005; 13(17), 5043–5054.

[60] Gotte M., Yip G.W. Heparanase, hyaluronan, and cd44 in cancers: a breast carcinoma perspective. Cancer Res., 2006; 66, 10233–10237.

[61] Choi K.Y., Min K.H., Na J.H., Choi K., Ki ,K. Park J.H., Kwon, I.C., Jeong S.Y. Self-assembled hyaluronic acid nanoparticles as a potential drug carrier for cancer therapy: synthesis, characterization, and in vivo biodistribution. J. Mater. Chem., 2009; 19, 4102–4107.

[62] Pouyani T., Prestwich G.D. Functionalized derivatives of hyaluronic acid oligosaccharides: drug carriers and novel biomaterials. Bioconjugate Chem., 2007; 5(4), 339-347.

[63] Coradini D., Zorzet S., Rossin R., Scarlata I., Pellizzaro C., Turrin C., Bello M., Cantoni S., Speranza A., Sava G., Mazzi U., Perbellini A. Inhibition of hepatocellular carcinomas in vitro and hepatic metastases in vivo in mice by the histone deacetylase inhibitor HA-But. Clin. Cancer Res., 10, 2004; 4822–4830.

[64] Lee H., Mok H., Lee S., Oh Y.K., Park T.G. Target-specific intracellular delivery of siRNA using degradable hyaluronic acid nanogels. J Controlled Release, 2007; 119(2), 245-252.

[65] Auzenne E., Ghosh S.C., Khodadadian M., Rivera B., Farquhar D., Price R.E., Ravoori M., Kundra V., Freedman R.S., Klostergaard J. Hyaluronic acid-paclitaxel: antitumor efficacy against CD44(+) human ovarian carcinoma xenografts. Neoplasia, 2007; 9(6), 479–486.

[66] Eliaz R.E., Szoka F.C.J. Liposome-encapsulated Doxorubicin Targeted to CD44: a strategy to kill CD44-overexpressing tumor cells. Cancer Res., 2001; 61, 2592–2601.

[67] Eliaz R.E., Nir S:, Marty C., Szoka F.C.J. Determination and modeling of kinetics of cancer cell killing by doxorubicin and doxorubicin encapsulated in targeted liposomes. Cancer Res., 64, 2004; 711–718.

[68] Peer D., Margalit R. Loading mitomycin C inside long circulating hyaluronan targeted nano-liposomes increases its antitumor activity in three mice tumor models. Int J Cancer, 2004; 108(5), 780–789.

[69] Yadav A.K., Agarwal A., Rai G., Mishra P., Jain S., Mishra A.K., Agrawal H., Agrawal G.P. Development and characterization of hyaluronic acid decorated PLGA nanoparticles for delivery of 5-fluorouracil. Drug Delivery, 2010; 17(8), 561–572.

[70] Yadav A.K., Mishra P., Mishra A.K., Mishra P., Jain S., Agrawal G.P. Development and characterization of hyaluronic acid–anchored PLGA nanoparticulate carriers of doxorubicin. Nanomedicine: Nanotechnology, Biology, and Medicine, 2007; 3(4), 246–257.

[71] Choi K.Y., Min K.H., Yoon H.Y:, Kim K., Park J.H., Kwon I.C:, Choi K., Jeong S.Y. PEGylation of hyaluronic acid nanoparticles improves tumor targetability in vivo. Biomaterials, 2011; 32(7), 1880-1889.

[72] Cho H., Yoon I., Yoon H.Y., Koo H., Jin Y., Ko S., Shim J., Kim K., Kwon I.C., Kim D. Polyethylene glycol-conjugated hyaluronic acid-ceramide self-assembled nanoparticles for targeted delivery of doxorubicin. Biomaterials, 2012; 33(4), 1190-1200.

[73] Lee H., Ahn C., Park T.G. Poly[lactic-co-(glycolic acid)]-grafted hyaluronic acid copolymer micelle nanoparticles for target-specific delivery of Doxorubicin. Macromol. Biosci., 2009; 9(4), 336–342.

[74] Nishiyama N. Nanomedicine: nanocarriers shape up for long life. Nat. Nanotechnol., 2007; 2(4), 203–204.

[75] Ferrari M. Nanogeometry: Beyond drug delivery. Nat. Nanotechnol., 2008; 3, 131–132.

[76] Dong Y., Feng S.S. Methoxy poly (ethylene glycol)-poly (lactide) (MPEG-PLA) nanoparticles for controlled delivery of anticancer drugs. Biomaterials, 2004; 25(14), 2843-2849.

[77] Paul M., Laatiris A., Fessi H., Dufeu B., Durand B., Deniau M., Astier A. Pentamidine-loaded poly (D,L-lactide) nanoparticles: adsorption and drug release. Drug Dev Res, 1998; 43(2), 98-104.

CHAPTER 3

Irinotecan encapsulation and release from stable Hyaluronic Acid-Coated Biodegradable Nanoparticles

ABSTRACT

The preparation and characterization of a novel HA coated nanoparticulate system for tumor targeting were reported in the previous chapter. In this chapter the performance of these HA based nanoparticles (NPs) for the controlled release of a chemiotherapeutic drug, Irinotecan, mainly used for the colonrectal cancer therapy, Irinotecan, was evaluated. Thanks to the amphiphilic nature of these nanostructured systems characterized by a hydrophobic core and a hydrophilic shell, the NPs were able to successful encapsulate Irinotecan with a entrapment efficiency of 61.2 %. In vitro drug release was also evaluated. The results demonstrated that NPs were able to sustain a controlled release up to 24 days.

3.1 INTRODUCTION

The administration of drugs through the implantation or injection of drug delivery systems allows to obtain advantages over conventional drug therapies, facing limitations such as drug insolubility and instability in physiological environment and unspecific targeting [1-4].

In particular the entire quantity of drug necessary for a certain period is administered at once, and is released in a controlled manner, maintaining from a side drug concentration within therapeutic window and from another hand avoiding side effects [5-7].

In this context the design of advanced drug delivery systems and the development of carriers with properties suitable for the particular disease and treatment has become crucial [8-11].

In the previous chapter the preparation and the characterization of hyaluronic acid (HA)-coated nanoparticles were reported. In particular nanoparticles characterized by a biodegradable core of polylactic-coglycolic acid (PLGA), a shell of HA and anphiphilic polymers, known as Poloxamers or Pluronics, that act as a bridge between the hydrophobic PLGA and the hydrophilic HA were considered.

Thanks to the presence of hydrophobic domains of PLGA, the particles can be stable sites for the encapsulation of poorly-water soluble drugs. On the other side HA is a natural and biocompatible material that does not trigger adverse reactions when it is injected in vivo [12-14] and moreover it gives to the particle a hydrophilic character that allows long circulating times in body fluids [15-16].

Furthermore since HA can specifically bind to the cancer cells overexpressing at their surface CD44, an HA binding receptor [17-19], the particles can be efficiently internalized by the cells by means of both a passive (enhanced permeability and retention, EPR effect) and an active targeting [20-22].

Considering the afore mentioned features, these nanoparticles can be considered interesting systems as carriers of active agents.

In order to assess their performance as drug carriers it is necessary to known the loaded amount of drug and its release kinetic from the particle.

In particular in this chapter the encapsulation and the release of a chemoterapeutic agent, Irinotecan, was assessed.

3.2 MATERIALS AND METHODS

3.2.1 *Materials*

Hyaluronic acid (HA) with a weight-average molecular weight (MW) of 850,000 Da was provided by Novozymes Biopharma (Denmark). Poly(lactic-co-glycolic acid)

(PLGA) (RG504H, MW 12,000 Da) was purchased from Boherniger Ingelheim (Germany).

Poloxamers (PEOa-PPOb-PEOa), a group of amphiphilic triblock polymers, designed with variable numbers of oxyethylene (a) and oxypropylene (b) units, were employed. In particular in this study, poloxamer F127 (a=100 and b=65) and F68 (a=76 and b=29), obtained from Lutrol (Basf, Germany), were used.

Irinotecan, acetone and dimethyl sulfoxide (DMSO) were obtained from Sigma Aldrich (USA). Sucrose were purchased from Riedel de Haen (Germany).

Phosphate buffer saline (PBS) tablets without calcium and magnesium were obtained from MP Biomedicals Inc. (France).

3.2.2 *Drug-loaded Nanoparticles preparation*

Irinotecan loaded nanoparticles with and without HA were prepared by a single emulsion technique. In particular Irinotecan (2.5 mg) were added in the oil phase, prepared with 50 mg of PLGA, 25mg of F68, 25 mg of F127 and 5 ml of acetone. The water phase was characterized by 30 mg of HA dissolved in 12 ml of distilled water, 1.5 ml of F68 solution (at 0.5% w/v) and 1.5 ml of F127 solution (at 0.5% w/v). The same formulation was prepared without HA in the water phase and without poloxamers in the organic phase. In particular Irinotecan (2.5 mg) was added in the oil phase, prepared with 100 mg of PLGA in 5 ml of acetone and emulsified with the water phase characterized by 12 ml of distilled water, 1.5 ml of F68 solution (at 0.5% w/v) and 1.5 ml of F127 solution (at 0.5% w/v). The formulation prepared with and without HA were indicated as PPH and P respectively.

The organic phase was emulsified by vortexing for 5 min with the aqueous phase. The resulting emulsion was sonicated for 4 min at 4°C using a Branson Ultrasonic Cleaners (Model 3510) and the solvent was evaporated at room temperature for overnight.

A solution of sucrose, prepared by mixing 600 mg of sucrose in 25 ml of bidistilled water, was added to the NPs suspension. Nanoparticles were finally separated from supernatant by centrifugation at 13000 rpm for 60 minutes and lyophilized (Heto PowerDry PL6000 Freeze Dryer, Thermo Electron Corp., USA; -50 °C, 0.73 hPa) for 24 h.

3.2.3 *Mean size, dimensional stability and zeta potential*

Nanoparticles mean size and ζ potential were determined by laser light scattering (LS, ZetaSizer Nano ZS, Malvern Instruments, Malvern, UK) on a ultra-diluted suspensions in water (12 runs each sample).
NP size were determined at time zero and after 25 days to assess devices stability in the time. Stability tests were performed in order to verify a possible nanoparticles aggregation. Results were averaged on at least five measurements.

3.2.4 *Drug entrapment efficiency*

Drug entrapment efficiency was calculated by dissolving freeze-dried NPs (1 mg) in 1 ml of DMSO. The resulting solution was sonicated (FALC, Italy) for 1 h in a water bath at 59 kHz, 100% power.
Irinotecan content was quantified by measuring absorbance (UV-1800, UV-VIS spectrophotometer, Shimadzu, Japan) at 370 nm. The linearity of the spectrophotometer response was verified on Irinotecan solutions in DMSO (0.04–10 μg/ml concentration range; $r^2 > 0.99$). Entrapped Irinotecan percentage was calculated as

$$\text{Loading efficiency} = \frac{100 * \text{Drug entrapped}}{\text{Drug total}}$$

Results were averaged on three batches.

3.2.5 *In vitro release kinetic of Irinotecan*

For release experiments, NPs were suspended in 10 ml of release medium (PBS at pH 7.4) and incubated at 37 °C in an orbital incubator (SI50, Stuart R, UK) operating at 100 rpm.
At scheduled time intervals, 1 ml aliquots were withdrawn and replaced with the same volume of fresh media. The aliquots were ultracentrifugated and the supernatant was analyzed through spectrophotometric analysis (λ = 364.5 nm) to assess the content of

Irinotecan. The instrument response was linear over the concentration range 0.1–50 μg/ml ($r^2 > 0.99$). The experiments were run in triplicate.

The release data were fitted to the following semiempirical equations, adapted from methods reported in literature and describing drug release from HA-based systems as the result of a Fickian diffusional and a degradation mechanisms [23].

The diffusion contribution is expressed by:

$$F_{diff} = F_{diff,\infty} \cdot \left(1 - e^{(-k_{diff} \cdot t)}\right) \quad (3.1)$$

where $F_{diff,\infty}$ is the burst fraction at time infinity and k_{diff} is the first order rate constant associated with the 'burst' release.

The rate constant k_{diff} is equal to DACs/WLF_{diff} h1 where *D* and *C*s are the diffusion coefficient and solubility of the drug, respectively, *A* is the surface area of drug available for dissolution and $h1$ is the apparent aqueous diffusion boundary layer thickness. Thus k_{diff} is expected to increase with increased drug solubility and surface area.

The second release phase (F_{deg}), describing release of drug trapped in the polymer ($1-F_{diff,\infty}$) is considered dependent on polymer erosion and may be described by bulk degradation kinetics:

$$F_{deg} = \left(1 - F_{diff,\infty}\right) \cdot \frac{\left(e^{(kt-ktmax)}\right)}{\left(1+e^{(kt-ktmax)}\right)} \quad (3.2)$$

where t_{max} and *k* are the time to the maximum rate and the rate constant respectively of the polymer degradation release phase.

The overall released fraction is given by the sum of diffusional and degradation contributions, i.e.:

$$F = F_{diff} + F_{deg} = F_{diff,\infty} \cdot \left(1 - e^{(-k_{diff} \cdot t)}\right) + \left(1 - F_{diff,\infty}\right) \cdot \frac{\left(e^{(kt-ktmax)}\right)}{\left(1+e^{(kt-ktmax)}\right)} \quad (3.3)$$

3.3 RESULTS and DISCUSSION

3.3.1 *Mean size and dimensional stability*

Size plays an important role in determining the drug release behavior of the irinotecan loaded nanoparticles. It was demonstrated that particles with smaller dimension tends to accumulate in the tumor tissues due to the facilitated extravasation [24] and a better internalization occurs [25]. Furthermore smaller particles are easier to be intravenously injected and their sterilization may be simply done by filtration [26-27].

In table 3.1 the results in terms of size of blank (PPH) and Irinotecan-loaded NPs (PPH+Irin) were reported. As it can be noticed the presence of drug implies an increase of NPs diameter from 169.8 ± 4.2 nm to 263 ± 3 nm. Although this result is unexpected, it can be explained considering that probably despite NPs were centrifugated in order to eliminate not-encapsulated drug, a small fraction of drug remains on the NPs surface promoting interactions between NPs. As confirmed by dimensional stability results, these interactions are sufficiently weak, infact after 25 days the NPs size decreases from 263 ± 3 nm to 201 ± 1 nm.

Formulation	Particle mean diameter (0), [*nm*]	Particle mean diameter (25 days), [*nm*]
PPH	169.8 ± 4.2	186.1 ± 1.2
PPH+Irin	263 ± 3	201 ± 1

Table 3.1: Size of blank (PPH) and Irinotecan-loaded NPs (PPH+Irin) measured at time zero and after 25 days.

3.3.2 *Zeta potential*

NPs surface charge is another important factor to be considered in the design of particles for drug delivery application. In table 3.2 the zeta potential of blank and Irinotecan-loaded NPs was reported. The results demonstrated that the presence of irinotecan does not affect the surface charge of NPs.

Formulation	Zeta potential, [*mV*]
PPH	-37.3 ± 3.5
PPH+Irin	-35.78 ± 6

Table 3.2: Zeta potential of blank (PPH) and Irinotecan-loaded NPs (PPH+Irin)

3.3.3 *Drug entrapment efficiency*

The results related to the drug encapsulation efficiency are summarized in table 3.3. The drug content was found to be 58.8 % (w/w) in the case of particle prepared with bare PLGA and 61.2 % (w/w) in the case of particle prepared with a polymer concentration in the organic phase of 2% (w/v), a poloxamers concentration in the water phase of 0.5% (w/v) and HA amount of 30 mg.

Formulation	Encapsulation efficiency EE %
P	58.8
PPH	61.2

Table 3.3: Percentage of drug encapsulation efficiency of particle prepared with bare PLGA (P) and with the adding of poloxamers and HA in the formulation (PPH).

The results demonstrated that the presence of HA does not affect significantly the drug entrapment efficiency.

3.3.4 *In vitro release kinetic of Irinotecan*

Experimental and simulated in vitro fractional release profiles of Irinotecan from nanoparticles P and PPH in phosphate buffer were reported in figures 3.1 and 3.1.

The results demonstrated that nanoparticles P and PPH were able to sustain the Irinotecan release for at least 24 days. From figures 3.1 and 3.2 it can be noticed that after 24 h a burst effect occurred. In particular after 24 h a released Irinotecan fractions were 0.336 and 0.261 from nanoparticles P and PPH respectively. Furthermore the experimental data were fitted by a mathematical model reported in the methods section. The applied model allowed to discriminate the degradation and diffusion contributions to Irinotecan release from NPs. In table 3.4 the models parameters obtained by fitting experimental release data to equation 3.3 were reported.

The results shown that the Irinotecan release from NPs is due to the combination of diffusional and degradation mechanisms. The release profiles shown that the initial release is controlled by diffusion; the degradation mechanism, instead governs a secondary slower release.

	NPs P	**NPs PPH**
$F_{diff,\infty}$	0.150± 0.009	0.127± 0.02
k_{diff}, h^{-1}	0.063± 0.001	0.040± 0.0005
k, h^{-1}	0.007± 0.0002	0.008± 0.0004
t_{max}, h	166.5± 10	191.5± 13

Table 3.4: Model parameters as calculated by fitting experimental release data to Eq. 3.3.

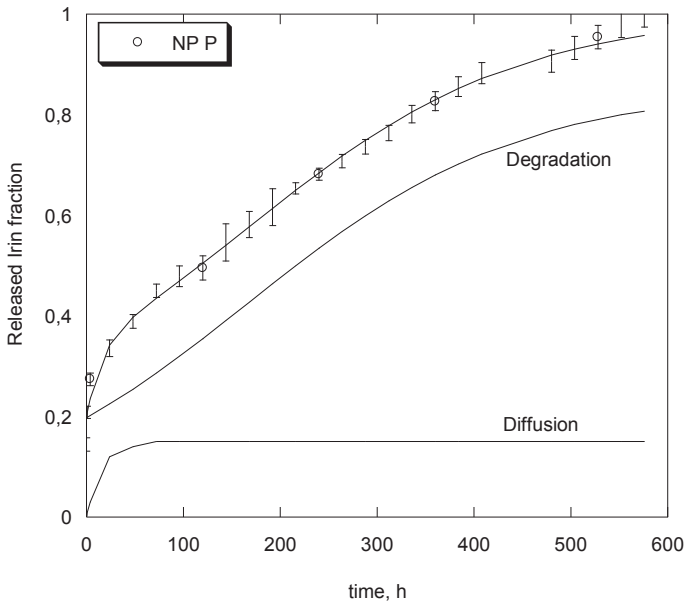

Figure 3.1: In vitro Irinotecan release profiles from nanoparticles P. Solid lines represent model simulations. Fitting was performed by Eq. 3.3

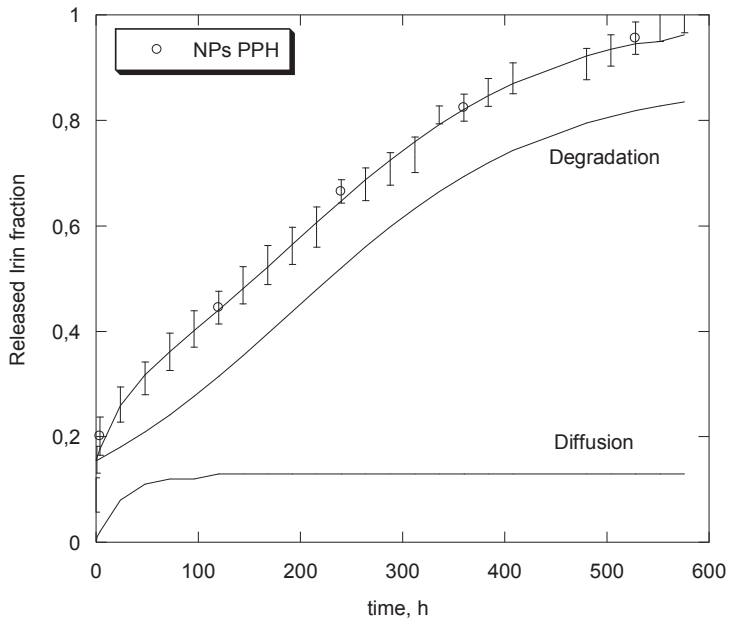

Figure 3.2: In vitro Irinotecan release from nanoparticles PPH. Solid lines represent model simulations. Fitting was performed by Eq. 3.3

3.4 CONCLUSIONS

In this chapter the drug encapsulation efficiency and in vitro drug release for a novel nanoparticulate system, using Irinotecan as drug model, were evaluated. The amphiphilic nature of these nanostructured devices, characterized by a inner hydrophobic core and a hydrophilic shell, allowed to obtain a drug encapsulation efficiency of 61.2% and in vitro sustained Irinotecan release up to 24 days.

REFERENCES

[1] Allen T.M., Cullis P.R. Drug Delivery Systems: Entering the Mainstream. Science, 2004; 303 (5665), 1818-1822.

[2] Allen T.M. Ligand-Targeted Therapeutics in Anticancer Therapy. Nature Reviews Cancer, 2002; 2, 750-763.

[3] Soppimath K.S., Aminabhavi T.M, Kulkarni A.R., Rudzinski W.E. Biodegradable polymeric nanoparticles as drug delivery devices. J. Controlled Release, 2001; 70(1-2), 1-20.

[4] Moghimi S.M., Hunter A.C., Murray J.C. Long-Circulating and Target-Specific Nanoparticles: Theory to Practice. Pharmacol Rev, 2001; 53, 283-318.

[5] Brigger I., Dubernet C., Couvreur P. Nanoparticles in cancer therapy and diagnosis Adv. Drug Delivery Rev, 2002; 54(5), 631-651.

[6] Peer D., Karp J.M., Hong S., Farokhzad O.C., Margalit R., Langer R. Nature Nanotechnology, 2007; 2, 751-60.

[7] Moghimi S.M., Hunter A.C., Murray J.C. Nanomedicine: current status and future prospects. The FASEB Journal, 2005; 19(3), 311-330.

[8] Ferrari M. Cancer nanotechnology: opportunities and challenges. Nature Reviews Cancer, 2005; 5, 161-171.

[9] Kostarelos K. Rational design and engineering of delivery systems for therapeutics: biomedical exercises in colloid and surface science. Advances in Colloid and Interface Science, 2003; 106(1-3), 147-168.

[10] Kostarelos K. Rational design and engineering of delivery systems for therapeutics: biomedical exercises in colloid and surface science. Advances in Colloid and Interface Science, 2003; 106(1-3), 147-168.

[11] Hubbell J.A. Enhancing drug function. Science, 2003; 300 (5619), 595-596.

[12] Bergman K., Elvingson C., Hilborn J., Svensk G., Bowden, T. Hyaluronic acid derivatives prepared in aqueous media by triazine-activated amidation. Biomacromolecules, 2007; 8(7), 2190–2195.

[13] Prestwich G.D., Kuo J.W. Chemically-modified HA for therapy and regenerative medicine. Curr Pharm Biotechnol, 2008; 9(4), 242-245.

[14] Burdick, J.A., Prestwich, G.D. Hyaluronic Acid Hydrogels for Biomedical Applications. Adv Mater, 2011; 23(12), H41-H56.

[15] Moghimi S.M., Szebeni J. Stealth liposomes and long circulating nanoparticles: critical issues in pharmacokinetics, opsonization and protein-binding properties. Progress in Lipid Research, 2003; 42(6), 463-478.

[16] Kogan G., Šoltés L., Stern R., Gemeiner P. Hyaluronic acid: a natural biopolymer with a broad range of biomedical and industrial applications. Biotechnol Lett, 2007; 29, 17-25.

[17] Aruffo A., Stamenkovic I., Melnick M., Underhill C.B., Seed, B. CD44 is the principal cell surface receptor for hyaluronate. *Cell*, 1990; 61(7), 1303–1313.

[18] Banerji S., Wright A.J., Noble M., Mahoney D.J., Campbell I.D., Day A.J., Jackson D.G. Structures of the Cd44-hyaluronan complex provide insight into a fundamental carbohydrate-protein interaction. Nat Struct Mol Biol, 2007; 14(3), 234-239.

[19] Entwistle J., Hall C.L., Turley E.A. HA receptors: regulators of signaling to the cytoskeleton. J Cell Biochem, 1996; 61(4), 569 –577.

[20] Maeda H., Wu J., Sawa T., Hori K. Tumor vascular permeability and the EPR effect in macromolecular therapeutics. Jou Controlled Release, 2000; 65(1-2), 271-284.

[21] Brigger I., Dubernet C:, Couvreur P. Nanoparticles in cancer therapy and diagnosis. Advanced Drug Delivery Reviews, 2002; 54(5), 631-51.

[22] Hashizume H., Baluk P., Morikawa S., McLean J.W., Thurston G., Roberge S., Jain R.K., McDonald D.M. Openings between defective endothelial cells explain tumor vessel leakiness. Am. J. Pathol., 2000; 156(4), 1363-1380.

[23] Corrigan O.I., Li X. Quantifying drug release from PLGA nanoparticulates. European Journal of Pharmaceutical Sciences, 2009; 37(3-4), 477–485.

[24] Yuan F., Leuning M., Huang S.K., Berk D.A., Papahadjopoulos D., Jain R.K. Microvascular permeability and interstitial penetration of sterically stabilized (stealth) liposomes in human tumor xenograft. Cancer Res, 1994; 54, 3352–6.

[25] Desai M.P., Labhasetwar V., Walter E., Levy R.J., Amidon G.L. The mechanism of uptake of biodegradable microparticles in CaCO-2 cells is size dependant. Pharm Res, 1997; 14(11), 1568–73.

[26] Kwon G.S., Kataoka K. Block copolymer micelles as long-circulating drug vehicles. Adv Drug Deliv Rev, 1995; 16(2-3), 295–309.

[27] Konan Y.N., Gurney R., Allémann E. Preparation and characterization of sterile and freeze-dried sub-200nm nanoparticles. Int J Pharm, 2002; 233(1-2), 239–52.

-PART 2-

AMPHIPHILIC HYALURONIC ACID DERIVATIVES TOWARDS THE DESIGN OF MICELLES FOR THE SUSTAINED DELIVERY OF HYDROPHOBIC DRUGS AND FOR THE VISCOSUPPLEMENTATION

CHAPTER 4

Preparation And Characterization Of Novel Self-Associative Nanostructured Soft Carriers Based On Amphiphilic Hyaluronic Acid Derivatives

ABSTRACT

The idea of this study was to combine Hyaluronic acid (HA) viscosupplementation and a local/controlled delivery of a hydrophobic anti-inflammatory drug.
In particular the ability of an octenyl succinic anhydride (OSA) modified HA (OSA-HA), to act as a viscosupplementation agent and as a drug delivery system wanted to be investigated.
To do this a characterization of these systems was necessary. For this reason morphological, dimensional, calorimetric and rheological studies of this novel HA derivatives were conducted. From morphological analysis it resulted that micelles are spherical objects with diameters around 100 nm. Differential scanning calorimetric (DSC) analysis revealed that the ability of HA to sequester water seems to be enhanced by the introduction of lipophilic functions within HA molecules, resulting in a further decrease of the fraction of free water able to freeze compared to the unmodified HA. Moreover, OSA-HA solutions appeared to be an appropriate tool to be used in viscosupplentation therapy owing to their suitable viscoelastic features.

4.1 INTRODUCTION

Amphiphilic copolymers, once in an aqueous solutions, can self-assemble into micelles owing to a high solubility difference between the hydrophilic and the hydrophobic

segments [1, 2, 3].These systems can be used as drug delivery carriers due to their potential high drug-loading capacity and possibility to load a variety of drugs with diverse features into the hydrophobic core of the micelles to treat several diseases [4, 5]. Hyaluronic acid (HA) is a natural mucoadhesive polysaccharide, a main constituent of the extracellular matrix of connective tissues, which displays biodegradability and biocompatibility properties. It is composed of alternating D-glucuronic acid (GlcA) and N-acetyl-D-glucosamine (GlcNAc) repeating units linked together *via* β-(1,4) and β-(1,3) glycosidic junctions [6]. HA is a major ligand of the adhesion receptor CD44, which is also expressed at the surface of chondrocytes [7]. In solution, HA displays an extraordinary capability to retain water, and behaves as an expanded random coil occupying a large hydrodynamic volume. This causes neighboring molecules to overlap, thus forming the transient network structure with a marked viscoelasticity [8]. These compelling features make HA a ductile and versatile biopolymer used for several applications in the biomedical field. For instance, HA is commonly used in topical ophthalmology for the dry eye treatment and as a viscoelastic device in ophthalmologic surgery owing to the ability to form highly viscous solutions even at low concentrations [9, 10, 11, 12]. Moreover, intra-articular injection of HA (viscosupplementation) is one of the most used therapies for the treatment of knee osteoarthritis, its goal being to restore the elastic and viscous properties of the synovial fluid (SF) [13, 14]. Pathologic alterations occurring in joint diseases, indeed, lead to a decrease in SF of HA molecular weight and concentration, and consequently a decline in SF viscoelastic properties [15]. The beneficial improvements in SF viscoelastic properties, and joint functions, derive from both the intrinsic viscoelastic properties of HA and its potential stimulatory effect on the synthesis of high molecular weight HA by synoviocytes [16]. Currently, several viscosupplemention products based on HA are commercially available and an important research effort has been devoted to chemically modify HA, through coupling or crosslinking reactions, preserving its biocompatibility. Indeed, native HA, once *in vivo*, undergoes a rapid degradation due to its sensitivity to hyaluronidase and high hydrophilicity. To avoid these drawbacks, among the possible chemical modification, various pendant chains have been grafted onto HA to increase its residence time and viscoelastic features [14]. Many chemical modifications involving HA carboxyl and/or hydroxyl groups to obtain a proper HA molecule for different applications were

investigated [17]. In particular as regards to the modification of HA carboxyl groups, an alkylated derivatives of HA was obtained using alkyl aldehydes in water/ethanol mixtures in the presence of sodium cyanoborohydride [18]. Furthermore alkyl bromides in dimethyl sulfoxide (DMSO) was used for the preparation of an amphiphilic water soluble derivatives of HA [19]. Methyl ester HA derivatives was also obtained using alkyl silyl diazomethanes in methanol/diethyl ether mixtures [20].

Other more recent modifications of HA molecule involve hydroxyl groups; in particular HA hydroxyl groups were modified with acylchlorides in N, N dimethylformamide (DMF) in the presence of pyridine [21] or with alkyloxymethyloxiranes in a water/DMSO mixture [22] or also with aryl-or alkyl-vinyl sulfones in water/acetone mixtures in the presence of sodium hydroxide [23] (table 4.1).

HA group involved	Group used to modified HA	Solvent	Reference
-COOH	alkyl aldehydes	water/ethanol mixtures	[18]
	alkyl bromides	DMSO	[19]
	alkyl silyl diazomethanes	methanol/diethyl ether mixtures	[20]
-OH	acylchlorides	N, N dimethylformamide	[21]
	alkyloxymethyloxiranes	water/DMSO mixture	[22]
	aryl-or alkyl-vinyl sulfones	water/acetone mixtures	[23]

Table 4.1: HA modifications involving carboxyl and hydroxyl groups

However the current methods used to modify the HA molecule are characterized by some drawbacks. First the modifications involving HA carboxyl groups could modify the distribution of negative charges along the molecule, affecting important biological and pharmacological properties of native HA [24]. Secondly organic solvents or organic solvent/water mixtures were used in the reactions and this implies environmental issues, limits the upscalability of the preparation methods and often requires converting HA into its tetraalkylammonium salt or preparing reactive HA intermediates that makes more complex the preparation methods and often results in HA degradation.

Moreover, to stimulate the production of healthy HA and facilitate the homeostasis in the joint region, oral administration of anti-inflammatory drugs is often necessary in combination, or as an alternative to HA viscosupplementation. However, the prolonged

use of such drugs can cause important systemic adverse effects and, therefore, intra-articular injections of anti-inflammatory drug/s are often practiced [25]. However, conventional dosage forms do not provide a prolonged release of the drug, thus leading to the necessity of frequent injections, which can cause inflammations and lower patient compliance. To avoid these drawbacks, a local/sustained delivery of anti-inflammatory drug would be desirable.

In this frame, the idea of this study was to design and characterize a delivery system and, at the same time, able to restore the viscoelastic features of pathologic SF.

To this aim, an amphiphilic HA derivative able to selfassemble into micelles and possessing suitable viscoelastic features to act as a viscosupplementation agent was designed.

A new amphiphilic HA derivative and, in particular, an octenyl succinic anhydride (OSA) modified HA was synthesized through a simple reaction in an aqueous medium, which involves exclusively HA hydroxyl groups [26]. The resulting derivatives present great potential since, first of all, no organic solvents are used in the reaction, thus avoiding environmental issues and allowing the upscalability of the preparation method; secondly, the reaction does not involve HA carboxyl groups which can neutralize negative charges along the polymer backbone. Actually, it is important to maintain the charge distribution that can confer an electrostatically-induced stability in the perspective of using the self-assembling properties of these derivatives towards the design of micelles for the delivery of poorly soluble drugs.

In this chapter preliminary studies based on a morphological, dimensional, calorimetric and rheological characterization of this novel HA derivatives were conducted.

4.2 MATERIALS AND METHODS

4.2.1 *Materials*

Hyaluronic acid (HA) with a weight-average molecular weight (MWw) of 850,000 Da (HA850) was provided by Novozymes Biopharma (Denmark). Octenyl succinic anhydride (OSA; MW: 210.27 Da, purity P97%, mixture of *cis* and *trans*) salts was obtained from Sigma-Aldrich (USA). Distilled water from Milli-Q (Millipore, USA) was used. OSA-HA derivatives, with a percentage of substitution of 6%, were provided

by Novozymes. They were synthetized as previously reported [26], and briefly summarized in the following *Methods* section.

4.2.2 *Preparation of hyaluronic acid derivative*

OSA-modified derivative at 6% degree of substitution was prepared by dissolving HA850 overnight at room temperature in de-ionized water. NaHCO3 was added to the solution and mixed at room temperature (RT) for 1h. Afterwards, the pH of the HA solution was adjusted to 8.5 with NaOH (0.5 M). OSA was added dropwise to the alkaline HA solution under vigorous stirring. The reaction medium was mixed at RT and the resulting crude product was dialysed against milli-Q water (7.5 L) using molecular porous membrane tubing (Spectra/Por®4, MWCO 12,000–14,000 Da; Spectrum Laboratories, Rancho Dominguez, California, United States) at 4 °C. The purified OSA–HA was finally freeze-dried. OSA-HA solutions were prepared by dissolving OSA-HA powder in bidistilled water or phosphate buffer saline (PBS; 120 mM NaCl, 2.7 mM KCl, 10 mM phosphate salts; pH 7.4) in the 0.1÷5% w/v concentration range.

4.2.3 Differential Scanning Calorimetry (DSC)

Thermoanalytical tests were carried out on solutions of HA and OSA-HA to study how the chemical modification could influence the interactions between the polysaccharide chains and water. The heat involved in the solid-to-liquid phase transition of water within HA solutions was determined by a differential scanning calorimeter (DSC; DSC Q20, TA Instruments, U.S.A.), calibrated with a pure indium standard. The samples were prepared in flasks by simple stirring overnight at room temperature, until transparent and homogeneous solutions were obtained. The samples were placed in hermetically sealed aluminum pans, equilibrated at –30°C and heated to 20°C at 2°C/min. Measurements were carried out under an inert nitrogen atmosphere, purged at a flow rate of 50.0 mL/min. The heat evolved by the fusion of water (W/g) within the solutions was calculated from the recorded DSC thermograms by integrating the endothermic melting peaks and normalized with respect to the actual content of water.

4.2.4 Morphology and size distribution of OSA-HA micelles

The morphology of OSA-HA micelles were investigated by transmission electron microscopy (TEM, FEI Tecnai G12 Spirit Twin) with emission source LaB6 (120 kV, spotsize 1) using 400 mesh carbon-coated copper grids at RT. The OSA-HA solutions at 1 mg/ml, in water and PBS, were prepared. The carbon-coated copper grid was immersed in OSA-HA solution and, after the drying phase, the grid was placed on a rod holder for the TEM characterization. Three grids per OSA-HA solution were prepared and a minimum of four micrographs per grid were acquired.
Micelle mean size and size distribution were determined by laser light scattering (LS, ZetaSizer Nano ZS, Malvern Instruments, Malvern, UK) on a ultra-diluted suspensions in water (12 runs each sample).

4.2.5 Rheological properties

Small amplitude oscillatory shear tests were performed to evaluate the time-dependent response of these materials and their linear viscoelastic properties (G', G''). The frequency was in the range from 0.01 to 10 Hz. The measurements were carried out through a strain controlled rotational rheometer (Gemini Bohlin Instruments, UK), using a parallel plate geometry (PP30 cell). The tests were carried out at the controlled temperatures of 25 and 37°C using a thermostatic bath.
In a dynamic test the material is subjected to a sinusoidal shear strain:

$$\gamma = \gamma_0 \sin(\omega t) \qquad (4.1)$$

where γ_0 is the shear strain amplitude, ω is the oscillation frequency (which can be also expressed as 2 f, where f is the frequency in Hz) and *t* the time. The mechanical response, expressed as shear stress τ of viscoelastic materials, is intermediate between an ideal pure elastic solid (obeying to the Hooke's law) and an ideal pure viscous fluid (obeying to the Newton's law) and, therefore, it is out of phase with respect to the imposed deformation as expressed by:

$$\tau = G'(\omega) \cdot \gamma_0 \sin(\omega t) + G''(\omega) \cdot \gamma_0 \cos(\omega t) \quad (4.2)$$

where $G'(\omega)$ is the storage or elastic modulus and $G''(\omega)$ is the loss or viscous modulus. G' gives information about the elasticity or the energy stored in the material during deformation, whereas G" describes the viscous component or the energy dissipated as heat. Since viscoelastic properties strongly depend upon the time-scale of observation, it will be reported the dependence of G' and G" upon the frequency, the so called mechanical spectrum.

In order to identify the linear viscoelastic response range of the materials, preliminary strain sweep tests were performed on the samples, at the oscillation frequency of 1 Hz. The tests were repeated at least three times on each sample.

4.3 RESULTS and DISCUSSION

An amphiphilic HA derivative based on the reaction between HA and OSA in mildly alkaline aqueous media was previously developed through a novel and easily upscalable modification method [26] (figure 4.1). The obtained polymer can be regarded as a fishbone-like macromolecule consisting of a linear backbone carrying randomly distributed hydrophobic octenyl succinate (OS) side groups with a 6% degree of substitution (DS).

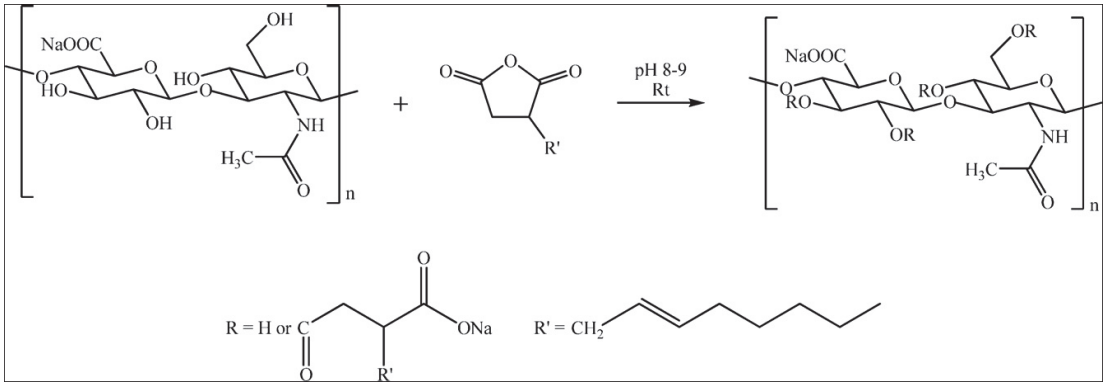

Figure 4.1: Scheme of chemical modification of HA with OSA.

4.3.1 *Differential Scanning Calorimetry (DSC)*

Figure 4.2 shows DSC thermograms of water, HA and OSA-HA (DS = 6 %) solutions. As shown in the figure, in all cases a single melting peak, caused by the fusion of free water was observed. Melting temperature (T_m) was here defined as the temperature at which the DSC curve shifts towards the endothermic direction. In particular, T_m obtained with HA and OSA-HA solutions were found to be lower than that of pure water. The heat of fusion was 335.9, 320.2 and 302.8 J/g for water, HA and OSA-HA, respectively, as reported in Table 4.2.

	ΔH_m **, (J/g)**	T_m **, (°C)**
Water	335.9 ± 2.7	0.21 ± 0.28
HA (DS = 0)	320.2 ± 5.9	-5.88 ± 1.07
OSA-HA (DS = 6%)	302.8 ± 9.2	-7.39 ± 1.05

Table 4.2: Melting enthalpies and temperatures of water, HA and OSA-HA

The decrease of T_m in the case of HA and OSA-HA solutions was associated to the occurrence of intermolecular interactions between HA and water. Likewise, the reduction of peak areas in the presence of HA, and hence of the melting enthalpies, could also be ascribed to the interactions of HA chains with water. It is well known that a certain number of water molecules are restrained in the junction zone where the polysaccharide chains interact among each other to form a gel network structure, thus reducing the amount of free water available for freezing [27]. In our case, both T_m and melting enthalpy of OSA-HA were found to be lower compared to unsubstituted HA. This result can indicate that the ability of HA to sequester water seems to be enhanced due the introduction of lipophilic functions within HA molecules, thus resulting in a further decrease of the fraction of free water able to freeze compared to the unmodified HA.

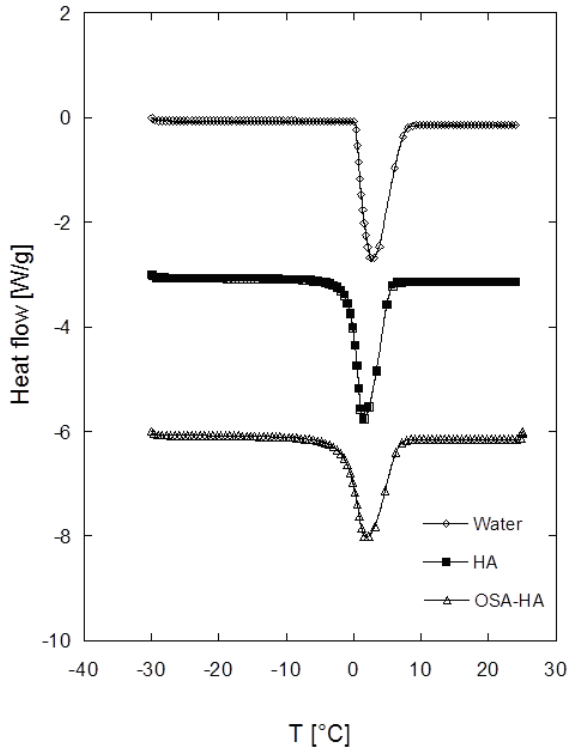

Figure 4.2: Representative endotherms for pure water, unsubstituted HA, OSA-HA (DS = 4.6%). Exotherm is oriented upwards.

4.3.2 *Morphology and size distribution of OSA-HA micelles*

In figures 4.3A and 4.3B selected TEM images of OSA-HA micelles at 1 mg/ml, in water and PBS respectively, are shown. As it can be seen, micelles are spherical objects with diameters around 100 nm in both water and PBS. Figure 4.4 presents LS measurements of OSA-HA micelles. This analysis evidenced the presence of a somewhat polydisperse population of objects with a mean diameter of about 400 nm. The discrepancy between the results of these techniques could be due to micelle aggregation. It is, indeed, likely to occur a dispersion of spherical hydrophobic domains, formed by the pendant OS groups, surrounded by a hydrophilic matrix of unmodified HA chains that interact each other through intra- and intermolecular hydrogen bonds. This hypothesis of micelle aggregation is also suggested by the difference in the molecular weight of HA chains and OS side groups. As a consequence, through TEM analysis it is possible to directly obtain a single micelle picture which appears spherical with a diameter in the order of 100 nm. In a LS experiments, instead, the Brownian

motion of micelles in suspension causes the scattering of a laser light at different intensities which are correlated to particle size trough the Stokes-Einstein relationship. In this latter case, the laser light can be scattered by a single micelle or by a group of aggregated micelles, as previously described, thus giving higher apparent mean diameter values of the micelles. A schematic representation of the possible organization of the OSA-HA micellar system is depicted in figure 4.5. Analogous results were obtained for the low molecular weight OSA-HA derivative, as previously reported [28].

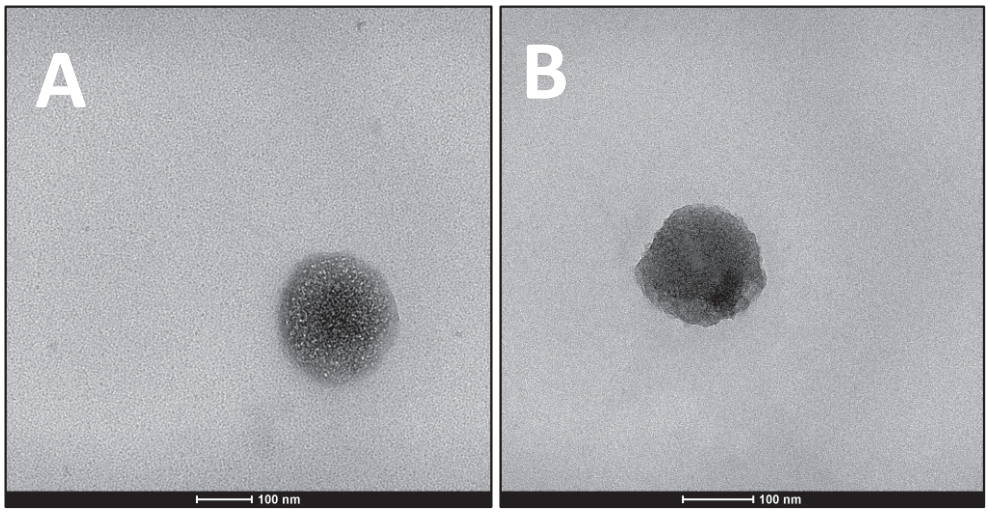

Figure 4.3: Selected TEM images of OSA-HA micelles at 1 mg/ml in water (A) and PBS (B).

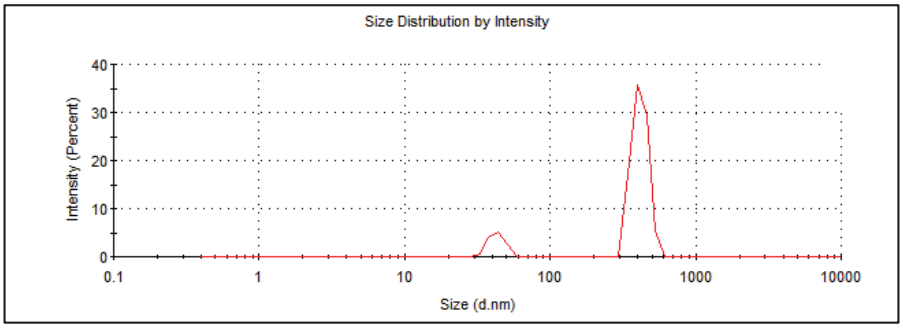

Figure 4.4: PCS results of OSA-HA micelles

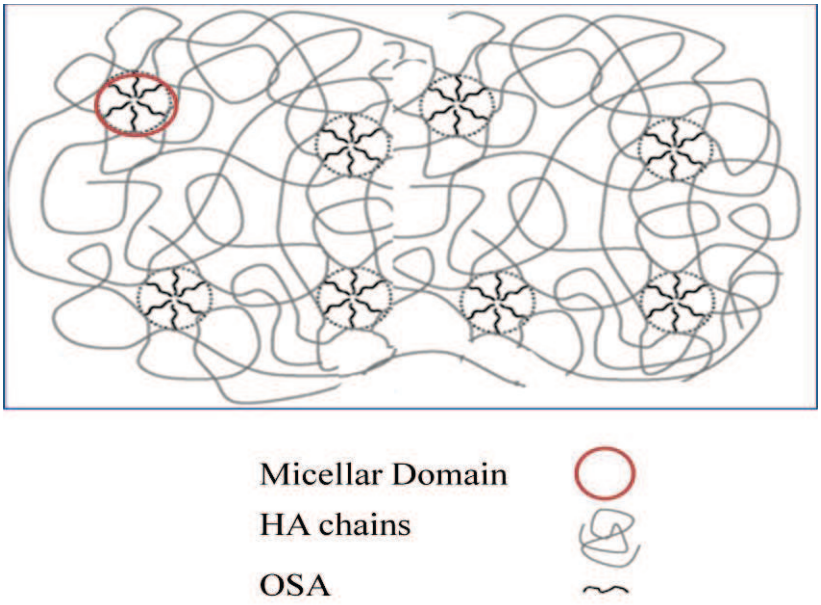

Figure 4.5: Graphical representation of the hypnotized structure of OSA-HA micelles

4.3.3 *Rheological properties*

In the perspective of using the novel OSA derivatives as viscosupplementation products, the rheological features assume a crucial role since they must properly restore the biomechanical functions of the normal SF. To this aim, the rheological properties of unmodified and modified HA solutions were studied to evaluate the effect of the chemical modification, concentration and ionic strength of the dissolving medium.

In figure 4.6 the elastic and the viscous moduli curves as a function of the oscillation frequency (mechanical spectra) of HA and OSA-HA solutions at 50 mg/ml in PBS and distilled water are reported. Both HA and OSA-HA solutions behave as entangled solutions; indeed they are namely viscous at low frequency (G'' > G') and prevalently elastic at high frequencies (G' > G''); the limit between the two regions is represented by the crossover frequency. These observations can be explained by consideration of the following. At low frequencies, the molecular chains can release stress by disentanglement and molecular rearrangement during the period of oscillation, and hence, the solution shows viscous behavior (G'' > G'). At high frequencies, however, molecular chains cannot disentangle during this short period of oscillation, and

therefore, they behave as a temporarily cross-linked network, and the elastic behavior (G' > G'') is prevalent. Furthermore, from a quantitative point of view, both the viscoelastic parameters of OSA-HA solutions are lower than the corresponding values of the unmodified HA solutions. In particular, at 1 Hz, G' ad G'' values, at 50 mg/ml in water, decreases from 369 to 111 Pa and from 417 to 181 Pa respectively, and the cross over frequency increases from ~ 1 Hz to ~ 4 Hz.

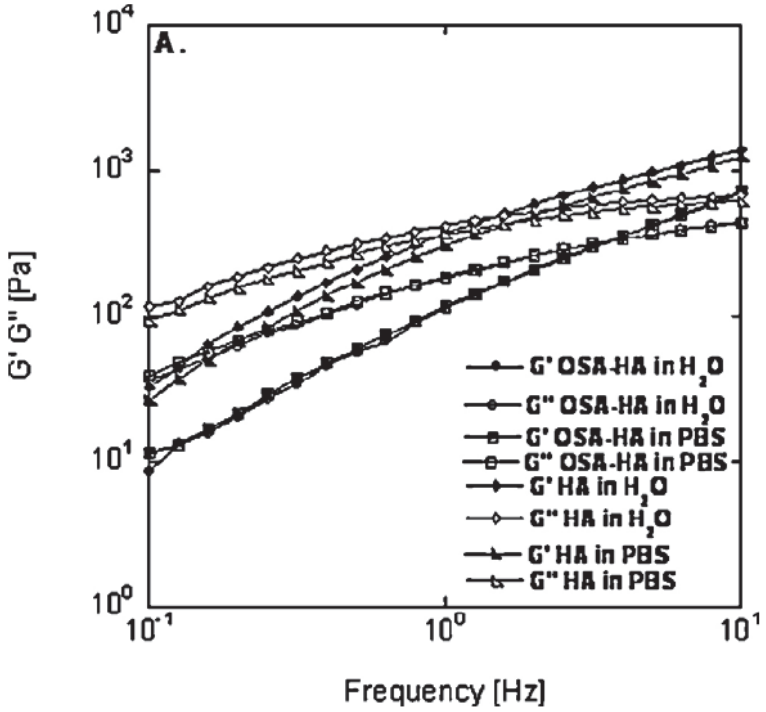

Figure 4.6: Mechanical spectra of HA and OSA-HA solutions at 50mg/ml in water and PBS.

This result can be explained taking into account that the chemical modification leads to a shrinkage of the macromolecular coils which, in turn, reduce the probability of intermolecular interactions with a consequent weakening of the polymeric network which become prevalently elastic at higher frequency. Moreover, these results highlighted that ionic strength does not affect the rheological properties of HA and OSA/HA solutions. Indeed, the mechanical spectra in PBS and water were found to be identical.

Figures 4.7 A, B, C report the mechanical spectra of OSA-HA solutions at 10 mg/ml, 25 mg/ml and 50 mg/ml and in Table 4.3 the viscoelastic parameters of OSA-HA solutions at f = 2Hz are shown. It can be noticed that the increase of OSA-HA concentration leads

to an increase of both the elastic and the viscous moduli. In particular, the values of both viscoelastic parameters increase of one order of magnitude passing by 10 mg/ml to 25 mg/ml and of two orders of magnitude passing by 25 mg/ml to 50 mg/ml. This result can indicate that the increase of OSA-HA concentration leads to an enhanced organization. The OSA-HA solutions exhibit a rheological behavior similar to the human synovial fluid, that is viscous at low frequencies and prevalently elastic at high frequencies and characterized by the presence of crossover frequency [29].

Furthermore the our amphiphilic HA derivatives show higher values of both viscous and elastic moduli than those of healthy human synovial fluid; in particular in the case of the OSA-HA solutions at a concentration of 50 mg/ml, G' and G'' reach the values of 249 and 234 Pa, respectively.

The rheological features of OSA-HA solutions are particularly attractive for viscosupplementation applications aimed at restoration of the viscoelasticity of diseased SF. Several products are currently used in viscosupplementation which differ in HA source, molecular weight, concentration and chemical modification thus resulting in a wide array of rheological behaviors from both qualitative and quantitative standpoints.

For example, at a frequency of 2 Hz, HYALGAN® is characterized by G' and G'' of respectively 0.1 and 0.8 Pa, HYADD4, a derivative of HA, presents an elastic modulus of 40 Pa and a viscous modulus of 10 Pa, and SYNVISC HYLAN G-F20®, made of cross-linked HA, shows the elastic and viscous moduli values of about 98 Pa and 20 Pa respectively, [30-31, 13]. It can be noticed that OSA-HA solutions, at a concentration of 50 mg/ml, show values of G' higher than those of viscosupplementation products currently used in clinical practice. The prevalent elastic character of an HA-based viscosupplementation products is not a problem being desirable in osteoarthritis applications. This is not only because of its capability to reduce the mechanical energy applied on the cartilage, but also because HA derivatives, with high elasticity, show analgesic ability. It has been reported that substances with enhanced elastic characteristics reduce the effect of nociceptive stimulus on medial articular nerve activity and decrease the sensory response to passive movements of inflamed knee joints. Hypothetically, this positive effect is due to their capacity to absorb a significant part of the mechanical energy of the stimulus, thus reducing the transmission to the mechano-transduction apparatus where pain signal originates.

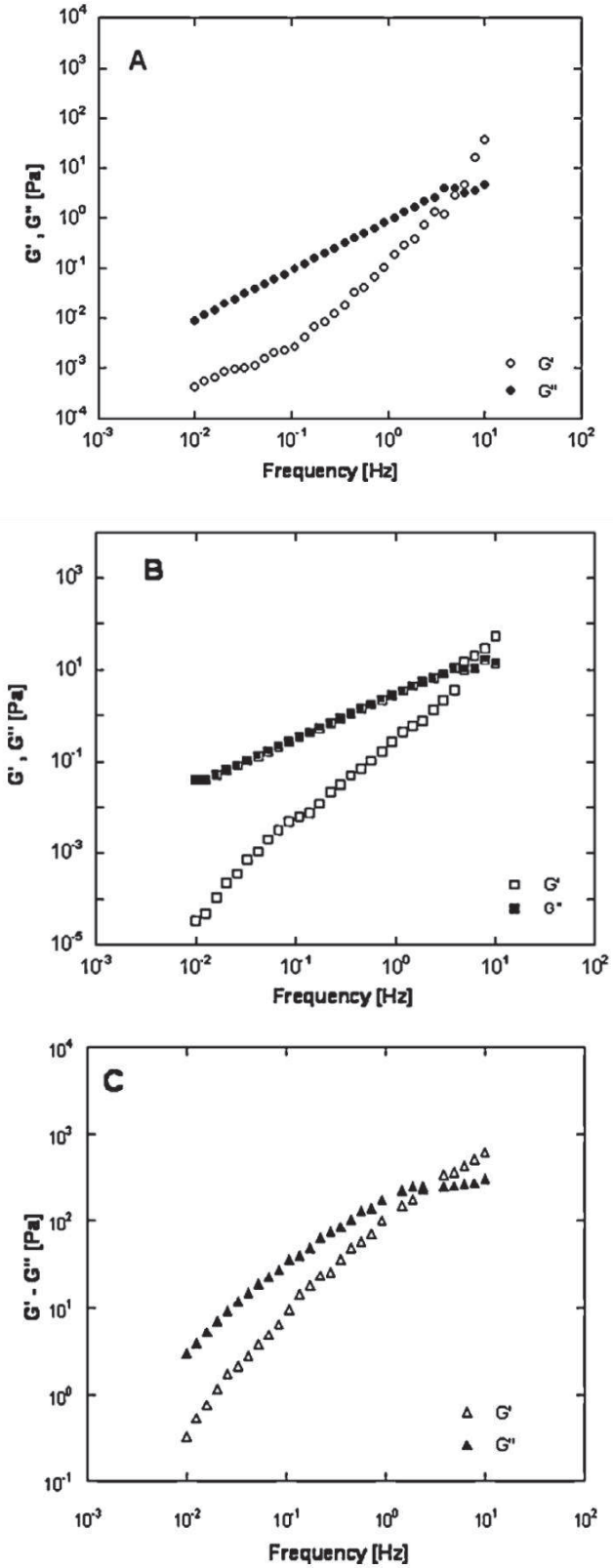

Figure 4.7: Mechanical spectra of OSA-HA solutions at 10 mg/ml (A), 25 mg/ml (B) and 50 mg/ml (C).

$[HA_{osa}]$, (*mg/ml*)	G', (*Pa*)	G'', (*Pa*)
10	0.72	2.14
25	1.34	6.57
50	249	234

Table 4.3: Viscoelastic parameters of OSA-HA solutions at f = 2 Hz

4.4 *Conclusions*

In this study the morphological, calorimetric and rheological study of a novel amphiphilic high molecular weight HA derivative and, in particular, an octenyl succinic anhydride (OSA) modified HA (OSA-HA) was reported.

From morphological analysis it resulted that micelles are spherical objects with diameters around 100 nm.

Differential scanning calorimetric (DSC) analysis revealed that the ability of HA to sequester water seems to be enhanced by the introduction of lipophilic functions within HA molecules, resulting in a further decrease of the fraction of free water able to freeze compared to the unmodified HA.

Finally, OSA-HA, thanks to its suitable viscoelastic features, is potentially useful in restoring SF rheological properties during a viscosupplementation therapy.

REFERENCES

[1] van Hest J.C., Delnoye D.A., Baars M.W., van Genderen M.H., Meijer E.W. Polystyrene-dendrimer amphiphilic block copolymers with a generation-dependent aggregation. Science, 1995; 268, 1592-1595.

[2] Cho B.K., Jain A., Nieberle J., Mahajan S., Wiesner U., Gruner S.M., Turk S., Rader H.J. Synthesis and self-assembly of amphiphilic dendrimers based on aliphatic polyether-type dendritic cores. Macromolecules, 2004; 37, 4227-4234.

[3] Pravata L., Braud C., Boustta M., El G.A., Tommeraas K., Guillaumie F., Schwach-Abdellaoui K., Vert M. New amphiphilic lactic acid oligomer-hyaluronan conjugates: synthesis and physicochemical characterization. Biomacromolecules, 2008; 9, 340-348.

[4] Harada A., Kataoka K. Supramolecular assemblies of block copolymers in aqueous media as nanocontainers relevant to biological applications. Progress in Polymer Science, 2006; 31, 949-982.

[5] Li G., Liu J., Pang Y., Wang R., Mao L., Yan D., Zhu X., Sun J. Polymeric micelles with water-insoluble drug as hydrophobic moiety for drug delivery. Biomacromolecules, 2011; 12, 2016-2026.

[6] Almond A. Hyaluronan. Cell Mol. Life Sci., 2007; 64, 1591-1596.

[7] Savani R.C., Cao G., Pooler P.M., Zaman A., Zhou Z., DeLisser H.M. Differential involvement of the hyaluronan (HA) receptors CD44 and receptor for HA-mediated motility in endothelial cell function and angiogenesis. J. Biol. Chem., 2001; 276, 36770-36778.

[8] Fusco S., Borzacchiello A., Miccio L., Pesce G., Rusciano G., Sasso A., Netti P.A. High frequency viscoelastic behaviour of low molecular weight hyaluronic acid water solutions. Biorheology, 2007; 44, 403-418.

[9]Maltese A., Borzacchiello A., Mayol L., Bucolo C., Maugeri F., Nicolais L., Ambrosio L. Novel polysaccharides-based viscoelastic formulations for ophthalmic surgery: rheological characterization. Biomaterials, 2006; 27, 5134-5142.

[10] Borzacchiello A., Mayol L., Ramires P.A., Pastorello A., Di B.C., Ambrosio L., Milella E. Structural and rheological characterization of hyaluronic acid-based scaffolds for adipose tissue engineering. Biomaterials, 2007; 28, 4399-4408.

[11] Mayol L., Quaglia F., Borzacchiello A., Ambrosio L., La Rotonda M.I. A novel poloxamers/hyaluronic acid in situ forming hydrogel for drug delivery: rheological, mucoadhesive and in vitro release properties. Eur. J. Pharm. Biopharm., 2008; 70, 199-206.

[12] Mayol L., Biondi M., Quaglia F., Fusco S., Borzacchiello A., Ambrosio L., La Rotonda M.I. Injectable thermally responsive mucoadhesive gel for sustained protein delivery. Biomacromolecules, 2011; 12, 28-33.

[13] Borzacchiello A., Mayol L., Schiavinato A., Ambrosio L. Effect of hyaluronic acid amide derivative on equine synovial fluid viscoelasticity. J. Biomed. Mater. Res. A, 2010b; 92, 1162-1170.

[14] Fakhari A., Berkland C. Applications and emerging trends of hyaluronic acid in tissue engineering, as a dermal filler and in osteoarthritis treatment. Acta Biomater., 2013b; 9, 7081-7092.

[15] Gomez J.E., Thurston G.B. Comparisons of the oscillatory shear viscoelasticity and composition of pathological synovial fluids. Biorheology, 1993; 30, 409-427.

[16] Ghosh P., Guidolin D. Potential mechanism of action of intra-articular hyaluronan therapy in osteoarthritis: Are the effects molecular weight dependent? Seminars in Arthritis and Rheumatism, 2002; 32, 10-37.

[17] Vasi A.M., Popa M.I., Butnaru M., Dodi G., Verestiuc L. Chemical functionalization of hyaluronic acid for drug delivery applications. Materials Science and Engineering C, 2014; 38,177–185.

[18] Creuzet C., Kadi S., Rinaudo M., Auzely-Velty R., New associative systems based on alkylated hyaluronic acid, synthesis and aqueous solution properties, Polymer, 2006; 47, 2706–2713.

[19] Pelletier S., Hubert P., Lapicque F., Payan E., Dellacherie E. Amphiphilic derivatives of sodium alginate and hyaluronate: synthesis and physicochemical properties of aqueous dilute solutions, Carbohydr. Polym., 2000; 43, 343–349.

[20] Kumar V., Longin F., Schwach-Abdellaoui K., Gross R.A.. Methyl esters of hyaluronic acid, World Intellectual Property Organization, 2008; Pat. WO 2008/091915 A1.

[21] Kawaguchi Y., Matsukawa K., Gama Y., Ishigami Y. New polysaccharide surfactants from hyaluronate, Chem. Express, 1991; 6, 647–650.

[22] Mlochova P., Hajkova V., Steiner B., Bystricky S., Koos M., Medova M., Velebny V. Preparation and characterization of biodegradable alkyl ether derivatives of hyalorunonan, Carbohydr. Polym., 2007; 69, 344–352.

[23] Eenschooten S.C., Christensen M.W. Aryl/Alkyl vinyl sulfone hyaluronic acid derivatives, World Intellectual Property Organization, 2007; Pat WO 2007/098770A1.

[24]Benesova K., Pekar M., Lapcik L., Kucerik J. Stability evaluation of *n*-alkyl hyaluronic acid derivatives by DSC and TG measurement. J. Therm. Anal. Calorim., 2006; 83, 341-348.

[25] Gerwin N., Hops C., Lucke A. Intraarticular drug delivery in osteoarthritis. Adv. Drug Deliv. Rev., 2006; 58, 226-242.

[26] Eenschooten C., Guillaumie F., Kontogeorgis G.M., Stenby E.H., Schwach-Abdellaoui K. Preparation and structural characterisation of novel and versatile amphiphilic octenyl succinic anhydride-modified hyaluronic acid derivatives. Carbohydrate Polymers, 2010; 79, 597-605.

[27] Hatakeyama T., Quinn F.X., Hatakeyama H. Changes in freezing bound water in water-gellan systems with structure formation. Carbohydrate Polymers, 1996; 30, 155-160.

[28] Eenschooten C., Vaccaro A., Delie F., Guillaumie F., Tommeraas K., Kontogeorgis G.M., Schwach-Abdellaoui K., Borkovec M., Gurny R. Novel self-associative and multiphasic nanostructured soft carriers based on amphiphilic hyaluronic acid derivatives. Carbohydrate Polymers, 2012; 79, 597-605.

[29] Balazs E.A. Viscosupplementation for treatment of osteoarthritis: from initial discovery to current status and results. Surg. Technol. Int., 2004; 12, 278-289.

[30] Altman R.D., Moskowitz R. Intraarticular sodium hyaluronate (Hyalgan) in the treatment of patients with osteoarthritis of the knee: a randomized clinical trial. Hyalgan Study Group. J. Rheumatol., 1998; 25, 2203-2212.

[31] Petrella R.J., DiSilvestro M.D., Hildebrand C. Effects of hyaluronate sodium on pain and physical functioning in osteoarthritis of the knee: a randomized, double-blind, placebo-controlled clinical trial. Arch. Intern. Med., 2002; 162, 292-298.

CHAPTER 5

Hydrophobic Drug Release From Micelles Based On Amphiphilic Hyaluronic Acid Derivatives

ABSTRACT

In the previous chapter the preparation and morphological, dimensional, calorimetric and rheological characterization of novel self associative nanostructured soft carriers based on an amphiphilic hyaluronic acid derivative were reported and it was demonstrated that these systems appeared interesting tools to be used in viscosupplentation therapy owing to their suitable viscoelastic features. In this chapter the ability of these systems to self-assemble into micelles, load a hydrophobic drug, release the active molecule in situ with controlled kinetics and to act as a solubility enhancer was studied.

5.1 INTRODUCTION

Hyaluronic acid (HA) is a naturally occurring polysaccharide, mainly present in the extracellular matrix of connective tissues [1].
It is composed of alternating D-glucuronic acid and N-acetyl-D-glucosamine repeating units linked together *via* β-(1,4) and β-(1,3) glycosidic junctions [2-6].
Thanks to its versatile properties, such as biocompatibility, nonimmunogenicity, biodegradability and viscoelasticity, it has been used for several biomedical applications. With the development of different strategies for the modification of its structure, HA has become an important building blocks for the production of new biomaterials to be used in regenerative medicine and drug delivery [7-10].

Although HA is an excellent biomaterial, because of its hydrophilic nature, native HA is unsuitable for the encapsulation of hydrophobic drugs.

In order to overcame this problem, the strategy used was to modify HA molecules with hydrophobic groups, obtaining a more favourable starting material for the production of stable nanostructures and the durable encapsulation of hydrophobic drugs.

However the current methods used for the preparation of amphiphilic HA present some drawbacks. The first one is the use of organic solvent in the modification reaction that implies environmental issues, limits the upscalability of the preparation methods and moreover often requires converting HA into its tetraalkylammonium salt or preparing reactive HA intermediates that makes more complex the preparation methods and often results in HA degradation [11].

On the other hand the HA modifications involve carboxyl groups resulting in an alteration of the distribution of negative charges along the polymer backbone at physiological pH and probably affecting fundamental biological and pharmacological HA properties.

Therefore the aim of this work was to design a delivery system based on an amphiphilic HA derivative able to self-assemble into micelles, load a hydrophobic drug and release the active molecule in situ with controlled kinetics. The new syntetized amphiphilic HA derivative is an octenyl succinic anhydride (OSA) modified HA, obtained through a simple reaction in an aqueous medium, and which involves exclusively HA hydroxyl groups [12].

Theses derivatives present great potential since, firstly no organic solvents are used in the reaction, thus avoiding environmental issues and allowing the upscalability of the preparation method; secondly, the reaction does not involve HA carboxyl groups which can neutralize negative charges along the polymer backbone. Actually, it is important to maintain the charge distribution that can confer an electrostatically-induced stability in the perspective of using the self-assembling properties of these derivatives toward the design of micelles for the drug delivery of poorly soluble drugs.

In particular the idea of this work was to study to the release of a commonly used hydrophobic anti-inflammatory drug to treat joint pathologies, known as triamcinolone acetonide (TA).

In the treatment of osteoarthrite, in order to stimulate the production of healthy HA and facilitate the homeostasis in the joint region, oral administration of anti-inflammatory drugs is often necessary in combination, or as an alternative to HA viscosupplementation [13-17]. However, the prolonged use of such drugs can cause important systemic adverse effects and, therefore, intra-articular injections of anti-inflammatory drug/s are often practiced [18]. However, conventional dosage forms do not provide a prolonged release of the drug, thus leading to the necessity of frequent injections, which can cause inflammations and lower patient compliance. To avoid these drawbacks, a local/sustained delivery of anti-inflammatory drug would be desirable.

For these reasons the idea was to design a delivery system able to prolong the release of an anti-inflammatory drug into the joint cavity and, at the same time, able to restore the viscoelastic features of pathologic synovial fluid, acting as a viscosupplementation agent.

In the previous chapter morphological, dimensional, calorimetric and rheological studies of these systems were reported and it was demonstrated that OSA-HA solutions appeared to be an appropriate tool to be used in viscosupplentation therapy owing to their suitable viscoelastic features.

In this chapter the ability of this novel amphiphilic HA derivative to selfassemble into micelles and to act as a solubility enhancer and as a modulator of release kinetics of TA was investigated.

5.2 MATERIALS AND METHODS

5.2.1 *Materials*

Hyaluronic acid (HA) with a weight-average molecular weight (MWw) of 850,000 Da (HA850) was provided by Novozymes Biopharma (Denmark). Octenyl succinic anhydride (OSA; MW: 210.27 Da, purity P97%, mixture of *cis* and *trans*) salts and HPLC-grade solvents were obtained from Sigma-Aldrich (USA). Distilled water from Milli-Q (Millipore, USA) was used, and triamcinolone acenotide (TA) was obtained from Farmalabor (Italy). OSA-HA derivatives, with a percentage of substitution of 6%, were provided by Novozymes. They were synthetized as reported in the previous chapter.

5.2.2 *Preparation of solutions*

The solutions for the dissolution tests and drug release kinetics were prepared by adding OSA-HA, at 1, 2.5 and 5 mg/ml, to a suspension of TA in bidistilled water (100 µg/ml). A suspension of TA in bidistilled water at the same concentration (100 µg/ml) was used as control. In all the solutions the excess of TA was present and visible at the bottom of the vials.

5.2.3 *Dissolution tests*

Dissolution tests were performed by using the solutions prepared. At scheduled time intervals (2, 4, 6, 24, 48 hrs), the solutions were centrifuged (1200 rpm for 15 min) in order to eliminate the unloaded drug and supernatant analyzed by means of reversed-phase high-performance liquid chromatography (RP-HPLC) (figure 5.1).

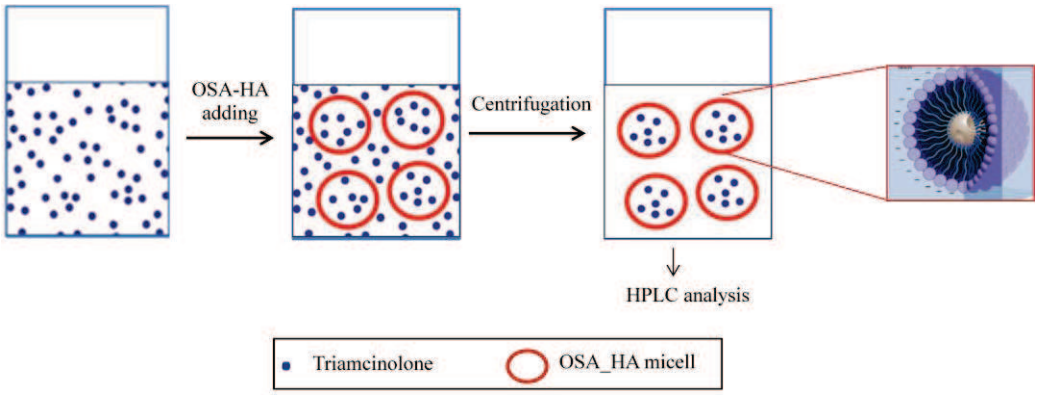

Figure 5.1: Schematic representation of OSA-HA micelles formation and triamcinolone encapsulation

The chromatograph was equipped with a HPLC LC-10AD pump (Shimadzu, Milano, Italy), a 7725i injection valve (Rheodyne), a SPV-10A UV-vis detector (Shimadzu) set at the wavelength of 254 nm and a C-R6A integrator (Shimadzu). RP-HPLC experiments were carried out using a Luna C18 (150 × 4.6 mm) column (Phenomenex, Klwid, USA). The mobile phase was a mixture of water and acetonitrile (50:50 v/v). The flow rate was set at 1 mL/min, and the stop time was 10 min. The results were averaged on three independent batches. The experiments were run in triplicate.

5.2.4 *Release kinetics*

As for the *in vitro* release kinetics of TA from OSA-HA-based gels, they were evaluated by immersing dialysis membranes (Spectra/Por Biotech Cellular ester, molecular cut off: 12 kDa) loaded with 5 ml of gels in 80 ml of PBS at 37 °C. At scheduled time intervals, the release medium was withdrawn, replaced with the same volume of fresh medium, and analyzed by reversed-phase high-performance liquid chromatography (RP-HPLC).

The release data were fitted to the following semiempirical equations, adapted from methods reported in literature and describing drug release from HA-based systems as the result of a dissolutive and a Fickian diffusional mechanisms [19-20].

The dissolutive contribution is expressed by:

$$F_{diss} = F_{diss,\infty} \cdot k_{diss} \cdot t^{0.5} \tag{5.1}$$

where F_{diss} and $F_{diss,_\infty}$ are the drug fractions released by dissolution at time t and after an infinite time, respectively, k_{diss} is the kinetic dissolution parameter. The diffusional contribution to drug release is given by:

$$F_{diff} = \left(1 - F_{diss,\infty}\right) \cdot \left(1 - exp\left(-k_{diff} \cdot t\right)\right) \tag{5.2}$$

Here F_{diff} is the drug fractions released due to diffusion at time t and k_{diff} is the kinetic diffusional parameter. The overall released fraction is given by the sum of diffusional and dissolution contributions, i.e.:

$$F = F_{diss} + F_{diff} = \left(F_{diss,\infty} \cdot k_{diss} \cdot t^{0.5}\right) + \left(\left(1 - F_{diss,\infty}\right) \cdot \left(1 - exp\left(-k_{diff} \cdot t\right)\right)\right) \tag{5.3}$$

5.3 RESULTS and DISCUSSION

5.3.1 *Dissolution tests*

In figure 5.2 an example of plot from HPLC measurement was reported.

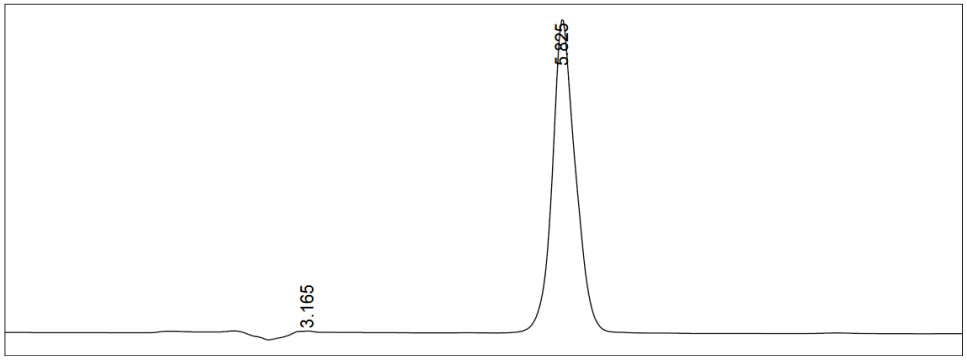

Figure 5.2: Example of HPLC measurement

In Figure 5.3 the results of the dissolution tests were reported as the concentration of TA found into the supernatant of the solutions prepared with different amount of OSA-HA (see *Methods* section) normalized to the water solubility of TA as a function of time. As it can be seen from the figure, after 48 hrs all the solutions reach an equilibrium solubility value. In particular, the value of TA solubility in water was found to be 18 μg/ml according to literature data [21]. In the presence of OSA-HA in the solutions the TA concentration in the supernatant was found to increase as a function of OSA-HA concentration. In detail, in the presence of 0.1% w/v of OSA-HA the observed TA concentration was 4-fold higher compared to TA saturation concentration in water when OSA-HA concentration is 0.5%w/v. These results demonstrate the inclusion capability of OSA-HA towards TA.

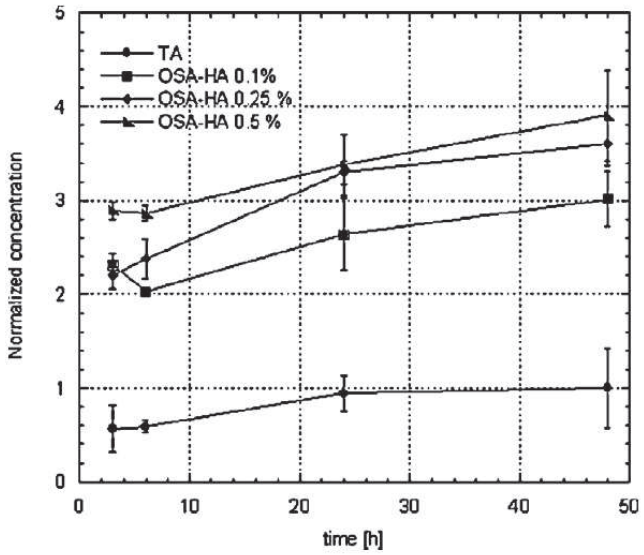

Figure 5.3: Normalised solubilisation profiles of TA.

5.3.2 *Release kinetics*

Experimental and simulated *in vitro* fractional release profiles of TA from OSA-HA platforms in phosphate buffer were shown in figure 5.4. The release of the loaded TA could be sustained for at least 7 days. As shown in the graphs reported in figure 5.4, a 24h-burst effect was noticed in all cases. In particular, the burst fraction was found to be decreasing with increasing OSA-HA concentration and the released drug fractions after 24 h were 0.835, 0.782, 0.695 and 0.571 for TA suspension, from 1, 2.5 and 5.0 mg/mL OSA-HA solutions, respectively.

Moreover, the applied model allowed to discriminate the diffusive and dissolution contributions to drug release. Experimental data were well fit by model equation. In the case of blank experiments (i.e. free TA released from solution loaded in dialysis membrane), the results of the model showed that TA is released from the membrane mainly by diffusion, as expected taking into account the poor solubility of the drug. It must also be underlined that an increase of the concentration of OSA-HA in the membrane led to increasing fractions of TA released by dissolution, as indicated by the increasing values of F_{diss} , (table 5.1).

These results confirm the solubility enhancement of the modified HA towards the hydrophobic TA. Furthermore, it should be noted that the kinetics of diffusion appears to be basically the same, irrespective of the OSA-HA concentration [22]. Actually, k_{diff} values were variable between 0.230 h^{-1} in the case of free TA and 0.198 h^{-1} for the OSA-HA solution at 5.0 mg/mL, as expected in the case of the diffusion of low molecular weight molecules through the hydrated matrix of a polymeric solution.

Therefore, release data clearly show that a combined mechanism, based on parallel dissolution and diffusion, governs TA release from OSA-HA-based solution. The analysis of release profiles reported in Figure 5. shows that, in all cases, diffusion is faster compared to dissolution, *i.e.* that at least initial release phases are governed by diffusion. The dissolution-controlled mechanism of TA released from the inner layer was regarded as secondary, slower release.

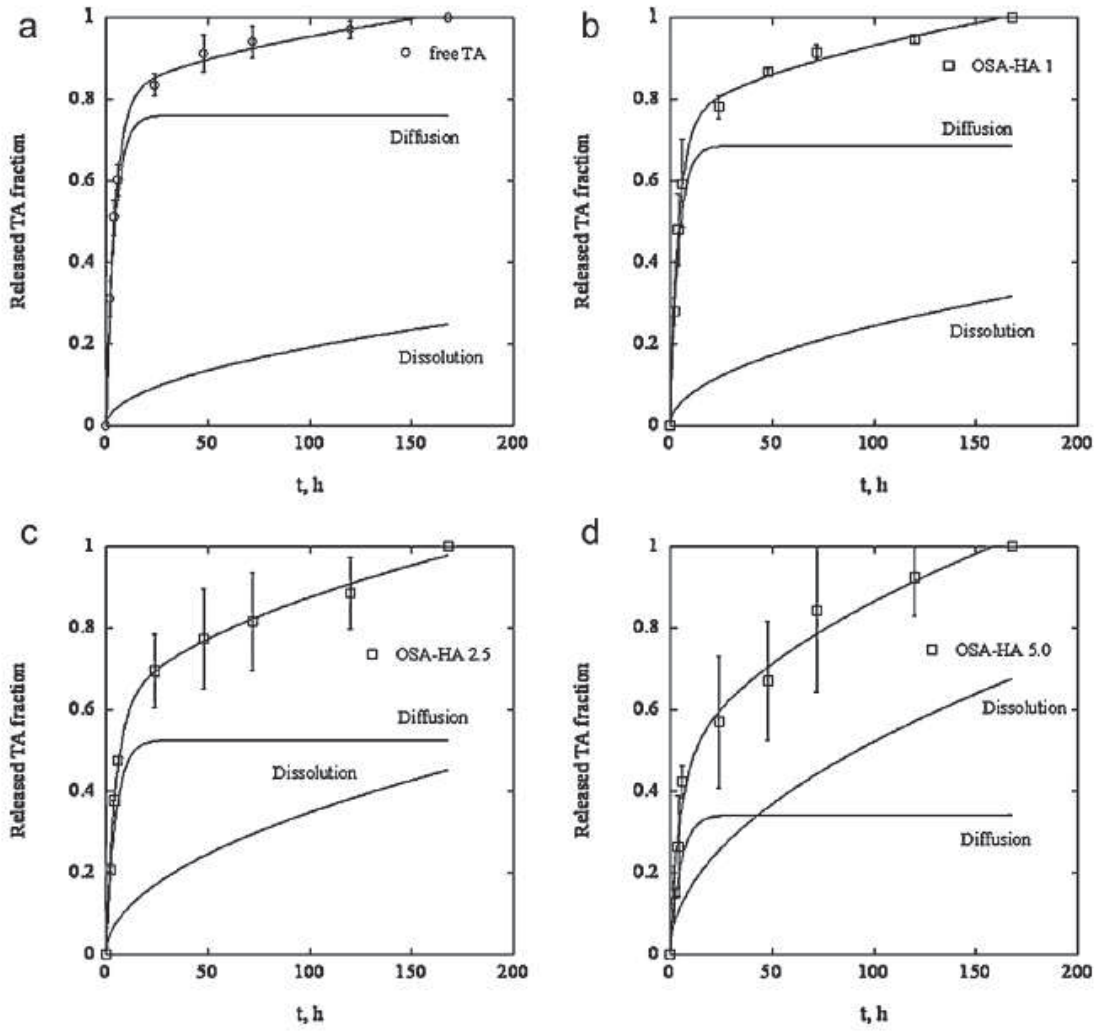

Figure 5.4: TA release profiles from water suspension and OSA-HA solutions at different concentration: (A) TA suspension in water; (B) OSA-HA 0.1 % w/v (C) OSA-HA 0.25 % w/v; (D) OSA-HA 0.5 % w/v. Solid lines represent model simulations. Fitting was performed by Eq.5.3

	Free TA	**OSA-HA 1.0 *mg/mL***	**OSA-HA 2.5 *mg/mL***	**OSA-HA 5.0 *mg/mL***
$F_{diss,\infty}$	0.238 ± 0.078	0.313 ± 0.031	0.473 ± 0.182	0.657 ± 0.272
k_{diss}, $h^{-1/2}$	0.0808 ± 0.0030	0.0783 ± 0.0037	0.0738 ± 0.0055	0.0795 ± 0.0071
k_{diff}, h^{-1}	0.230 ± 0.018	0.241 ± 0.068	0.212 ± 0.100	0.198 ± 0.066

Table 5.1: Model parameters as calculated by fitting experimental release data to Eq. (5.3).

5.4 CONCLUSIONS

In this study it was demonstrated that a novel amphiphilic high molecular weight HA derivative and, in particular, an octenyl succinic anhydride (OSA) modified HA (OSA-HA) is able to self-assemble into micelles, load a hydrophobic drug and release the active molecule with a controlled kinetic mechanism.

REFERENCES

[1] Gatej I., Popa, M., Rinaudo M. Role of the pH on Hyaluronan Behavior in Aqueous Solution . Biomacromolecules, 2005; 6, 61-7.

[2] Lapcık L., De Smedt Jr. S., Demeester J., Chabrecek P.. Hyaluronan: Preparation, Structure, Properties, and Applications. Chemical rewiew, 1998; 98, 2663-84.

[3] Ambrosio L., Borzacchiello A., Netti P. A., Nicolais L. Rheological properties of hyaluronic acid based solutions. Polymeric Materials Science and Engineering, 1998; 79, 244-5.

[4] Ambrosio L., Borzacchiello A., Netti P.A., Nicolais L.. Rheological study on Hyaluronic acid and its derivatives solutions. J. of Macromolecular Science-Pure and Applied Chemistry, 1999; A36 7&8, 991-1000.

[5] Barbucci R., Ruoppoli R., Borzacchiello A., Ambrosio L. Synthesis, chemical and rheological characterisation of new hyaluronic based hydrogels. Journal of Biomaterials Science Polymer Edition, 2000; 11(4), 383-99.

[6] Almond A. Hyaluronan. Cell Mol. Life Sci., 2007; 64, 1591-1596.

[7]Maltese A., Borzacchiello A., Mayol L., Bucolo C., Maugeri F., Nicolais L., Ambrosio L. Novel polysaccharides-based viscoelastic formulations for ophthalmic surgery: rheological characterization. Biomaterials, 2006; 27, 5134-5142.

[8] Borzacchiello A., Mayol L., Ramires P.A., Pastorello A., Di B.C., Ambrosio L., Milella E. Structural and rheological characterization of hyaluronic acid-based scaffolds for adipose tissue engineering. Biomaterials, 2007; 28, 4399-4408.

[9] Mayol L., Quaglia F., Borzacchiello A., Ambrosio L., La Rotonda M.I. A novel poloxamers/hyaluronic acid in situ forming hydrogel for drug delivery: rheological,

mucoadhesive and in vitro release properties. Eur. J. Pharm. Biopharm., 2008; 70, 199-206.

[10] Mayol L., Biondi M., Quaglia F., Fusco S., Borzacchiello A., Ambrosio L., La Rotonda M.I. Injectable thermally responsive mucoadhesive gel for sustained protein delivery. Biomacromolecules, 2011; 12, 28-33.

[11] Benesova K.; Pekar M.; Lapcik L.; Kucerik J. Stability evaluation of n-alkyl hyaluronic acid derivatives by DSC and TG measurement. J. Therm. Anal. Calorim. 2006, 83, 341-348.

[12] Eenschooten C., Guillaumie F., Kontogeorgis G.M., Stenby E.H., Schwach-Abdellaoui K.,. Preparation and structural characterisation of novel and versatile amphiphilic octenyl succinic anhydride-modified hyaluronic acid derivatives. Carbohydrate Polymers, 2010; 79, 597-605.

[13] Borzacchiello A., Mayol L., Schiavinato A., Ambrosio L. Effect of hyaluronic acid amide derivative on equine synovial fluid viscoelasticity. J. Biomed. Mater. Res. A, 2010b; 92, 1162-1170.

[14] Fakhari A., Berkland C. Applications and emerging trends of hyaluronic acid in tissue engineering, as a dermal filler and in osteoarthritis treatment. Acta Biomater., 2013b; 9, 7081-7092.

[15] Gomez J.E., Thurston G.B. Comparisons of the oscillatory shear viscoelasticity and composition of pathological synovial fluids. Biorheology, 1993; 30, 409-427.

[16] Ghosh P., Guidolin D. Potential mechanism of action of intra-articular hyaluronan therapy in osteoarthritis: Are the effects molecular weight dependent? Seminars in Arthritis and Rheumatism, 2002; 32, 10-37.

[17] Pelletier S., Hubert P., Payan E., Marchal P., Choplin L., Dellacherie E. Amphiphilic derivatives of sodium alginate and hyaluronate for cartilage repair: rheological properties. J. Biomed. Mater. Res., 2001; 54, 102-108.

[18] Gerwin N., Hops C., Lucke A. Intraarticular drug delivery in osteoarthritis. Adv. Drug Deliv. Rev., 2006; 58, 226-242.

[19] Nastruzzi C., Esposito E., Cortesi R., Gambari R., Menegatti E. Kinetics of Bromocriptine Release from Microspheres - Comparative-Analysis Between Different In-Vitro Models. Journal of Microencapsulation, 1994; 11, 565-574.

[20] Peppas N.A. Analysis of Fickian and non-Fickian drug release from polymers. Pharm. Acta Helv., 1985; 60, 110-111.

[21] Miro A., d'Angelo I., Nappi A., La M.P., Biondi M., Mayol L., Musto P., Russo R., Rotonda M.I., Ungaro F., Quaglia F. Engineering poly(ethylene oxide) buccal films with cyclodextrin: A novel role for an old excipient? Int. J. Pharm., 2013; 452, 283-291.

[22] Lustig S.R., Peppas N.A. Solute Diffusion in Swollen Membranes .9. Scaling Laws for Solute Diffusion in Gels. Journal of Applied Polymer Science, 1988; 36, 735-747.

-PART 3-

HYALURONIC ACID BASED HYDROGELS FOR REGENERATIVE MEDICINE

CHAPTER 6

Hyaluronic Acid Based Hydrogels For Regenerative Medicine Applications

ABSTRACT

HA hydrogels, obtained by crosslinking HA molecules with divinyl sulfone (DVS) and based on a simple, reproducible and safe process that does not employ any organic solvents, were developed. Owing to an effective purification step, the resulting homogeneous hydrogels do not contain any detectable residual crosslinking agent and are easier to inject through a fine needle.

HA hydrogels were characterized in terms of their viscoelastic and network structural properties. They exhibit a rheological behavior typical of a strong gel and show improved viscoelastic properties by increasing HA concentration and decreasing HA/DVS weight ratio. Furthermore it was demonstrated that processes such as sterilization and extrusion through clinical needles do not imply significant alteration of viscoelastic properties. Moreover the crosslinks appear to compact the network, being a reduction of the mesh size by increasing the crosslinker amount. In vitro and in vivo HA hydrogel degradation tests demonstrated that these new hydrogels show a good stability against enzymatic degradation, that increases by increasing HA concentration and decreasing HA/DVS weight ratio. Finally the hydrogels show a good biocompatibility confirmed by in vitro and in vivo tests.

6.1 INTRODUCTION

Hydrogels thanks to their unique properties such as excellent biocompatibility, high water content and capacity to degrade in safe product, have attracted a great deal of

attention and have been extensively used in several biomedical applications such as regenerative medicine and drug delivery [1-3].

Hyaluronic acid (HA), also referred to as hyaluronan, is a naturally occurring linear polysaccharide composed of repeating disaccharide units of D-glucuronic acid and *N*-acetyl-D-glucosamine linked by β-1-3 and β-1-4 glycosidic bonds [4-8].

HA is a primary component of the extra-cellular matrix of the mammalian connective tissues. It is an important structural element in the skin and is present in high concentration in the synovial joint fluids, vitreous humor of the eyes, hyaline cartilage, disc nucleus and umbilical cord [9-13]. HA plays a major role in several functions in vivo such as lubrification of arthritis joints, viscoelastic properties of soft tissue and it is involved in important cell functions such as cell motility, cell matrix adhesion and cell organization [14-18].

In biological tissues it has a very high molar mass, usually in the order of millions of Daltons, and possesses interesting visco-elastic properties based on its polymeric and polyelectrolyte characteristics [19].

Thanks to its biocompatibility, physical, chemical and biological properties and due to the ease of chemical functionalisation, HA has generated increasing interest among researchers and it is already used in several biomedical applications [20-22].

Clinically, HA is used in soft tissue replacement and augmentation and in surgical procedures and diagnostic. It is employed as a diagnostic marker for many disease states including cancer, rheumatoid arthritis, liver pathologies, and as an early marker for impending rejection following organ transplantation. It is also used for supplementation of impaired synovial fluid in arthritic patients, in aesthetic medicine such as dermal fillers, in soft tissue surgery such as vocal fold augmentation, as scaffold for tissue engineering applications and as a device in several surgical procedures, particularly as antiadhesive following abdominal procedures and as aid in cataract surgery [23-24].

In order to be used for the mentioned application, HA can be obtained from different sources, mainly by extraction from different tissues such as umbilical cord, rooster comb, synovial fluid and vitreous humor; this procedure, however, is expensive and requires an extensive purification of the crude product [25-26]. For these reasons alternatives to the animal extraction of HA were gradually replacing by industrial techniques based on microorganism fermentation. In large industrial quantities, HA is

produced by fermentation of strains of bacteria *Streptococci*. However *Streptococcus* requires an expensive and very difficult fermentation, the use of substantial volumes of organic solvents, and finally the HA product can contain endo- and exotoxins. The HA industrial manufacturing is recently devoted to the fermentation of *Bacillus subtilis* [27] that represents a valid alternative to Streptococcus HA production because it is a non-pathogenic microorganism and the final HA product does not contain any endo- or exotoxins; moreover it's possible to have a better control on HA molecular weight (MW) and also *Bacillus subtilis* grows on minimal media in contrast to Streptococcus that requires more expensive and complex media for growth.

Although HA is an excellent biocompatible material, when native HA is injected in physiological environment, a fast degradation process often occurs because from a side it has a high affinity for water molecules and from the other side it is degraded in vivo by hyaluronidase. For this reason, different strategies such as crosslinking or coniugation, have been used to stabilize HA and obtain a more stable material maintaining at the same time its fundamental properties [28-34]. In the case of crosslinking, HA reacts with a crosslinking agent that is capable of creating covalent bonds between HA chains, instead in the case of coniugation a compound is grafted onto HA chain.

Chemical modifications of HA, by means of both crosslinking or coniugation, generally involve HA carboxyl or hydroxyl groups. Concerning the modification of the carboxylic groups, an example of crosslinker agent used to obtain HA hydrogels is 1-ethyl-3-[3-(dimethylamino)-propyl]-carbodiimide (EDC), one of the preferred among the carbodiimide because of its water solubility [35]. The EDC reacts with the HA carboxylic acid forming an O-acyl isourea-HA intermediate, which in turn react with the chosen amine to form the amide bond. However the O-acyl isourea intermediate is very reactive and can hydrolyze and then rearrange into a stable N-acyl urea by-product. For this reason dimethyl sulfoxide (DMSO) methodologies on the acidic form of the HA have been developed to minimize the EDC hydrolysis [36].

Furthermore different esters and amides of HA, involving carboxyl groups modifications, have been used to form hydrogels for biomedical applications. For example esterification of the carboxyl groups of HA with different alcohol residues resulted in a series of derivatives named HYAFF® [37]. Examples of amides of HA are

HYADD®, obtained derivatizing the polysaccharide backbone with alkylic side chains through amide bonds [38].

As regards to the modifications involving the -OH groups, crosslinked HA hydrogels are obtained using crosslinker agents such as butanediol-diglycidyl ether (BDDE) or divinyl sulfone (DVS) [39]. Furthermore UV-light photocrosslinking hydrogels can be realized through methacrylate–HA conjugates [40], while in situ HA chemical crosslinked hydrogels can be obtained from thiol-modified HA [41].

The modifications methods currently available to crosslink or conjugate HA molecules present some drawbacks. In particular the modification involving HA carboxyl groups can alter the distribution of negative charges along the polymer chain, affecting some fundamental HA biological properties [42]. Furthermore, numerous methods have been developed in organic solvents, such as DMSO or also dimethylformamide (DMF). In this case, the native HA, which is in the form of a sodium salt, needs to be in its acidic form or a tetra-butylammonium salt (HA-TBA) for solubilization in organic solvents and this requires additional steps of physical and chemical treatments that can induce HA chain hydrolysis [43-44].

As regards to the hydrogels obtained by crosslinking reactions, the degree of modification, which is referred to as the crosslinking degree, has a significant effect on the properties of a crosslinked biomaterial, typically in the form of a gel. As the crosslinking density of a gel increases, the distance between the crosslinked segments becomes shorter. When a load is applied, these shorter segments require a greater force to deflect. Thus, increasing the crosslinking density strengthens the overall network, thereby increasing the hardness or stiffness of the gel. However, when the gel comprises all or mostly pendant HA polymer chains, a low crosslinking density network is formed which results in softer gels.

The crosslinking degree strongly affects the injectability of the hydrogel through pharmaceutical needles, a fundamental property to consider in the design of hydrogel to use it for several biomedical applications. In particular a low crosslinking degree determines a soft gel, implying a good injectability, but an high in vivo degradation rate of the gel; on the other side an high crosslinking degree determines an increasing of the gel hardness and so a low injectability profile, but it is required in order to have gels with good mechanical properties and with an increased residence time.

HA concentration is another parameter that influences significantly the injectability profile of the hydrogel. In particular by increasing HA concentration, the hardness or stiffness of the gel increase, so it is necessary to vary opportunely the polymer concentration in order to obtain an hydrogel with specific requirements to be used for biomedical applications.

Furthermore hydrogel injectability depends also from the molecular weight distribution of the polymer that strongly affects the homogeneity of the system.

The aim of this work was to produce HA based hydrogels with improved injectability profile while maintaining the mechanical properties.

The design of HA hydrogels requires to consider many parameters such as HA source, HA concentration, buffer environment for the hydrogel, nature of the crosslinking agent, crosslinking agent/HA weight ratio. However, regardless of these elements, the purity of the HA raw material and the safety of the crosslinking technology are crucial elements in achieving a hydrogel that can be safely administered to patients.

For these reasons in this work HA produced by fermentation of the novel, superior and safe strain, namely *Bacillus subtilis*, has been used to produce hydrogels. This production technology affords a HA product with unique advantageous properties such as reproducible molecular weight. In addition, the higher purity of *Bacillus-subtilis* derived HA compared to the available sources of HA offers the possibility of heat sterilization with minor degradation under given conditions and allows its use with various ingredients without degradation or decrease in viscosity.

Moreover the hydrogels were produced according to the method described in [45] using divinyl sulfone (DVS) as the crosslinking agent and based on a simple, reproducible and safe process that does not employ any organic solvents. Owing to an effective purification step, the resulting homogeneous hydrogels do not contain any detectable residual crosslinking agent. Furthermore the crosslinking reaction with DVS involves hydroxyl groups of HA molecular backbone, avoiding the problems related to the modification reactions involving HA carboxyl groups.

So in this frame the aim was to produce cross-linked HA hydrogels with improved properties, such as higher homogeneity and increased softness compared to the standard DVS crosslinked HA-hydrogels and an easier syringeability. The hydrogels were characterized in terms of viscoelastic properties as function of HA concentration and

HA/DVS weight ratio (w.r.) and network structural parameters. Moreover hydrogel degradation and biocompatibility in vitro and in vivo were studied.

6.2 MATERIALS AND METHODS

6.2.1 *Materials*

HA used in this work is produced by Novozymes Biopharma A/S by fermentation of the novel, superior and safe strain *Bacillus subtilis*. The weight-average molecular weight of HA was determined by size exclusion chromatography combined with multi angle laser light scattering detection (SEC-MALS). Molecular weight of the starting materials was in the range of 0.7 to 1.0 MDa.
DVS was obtained from Merck Gmbh and Sigma Aldrich Co. Hyaluronidase (HAase) from bovine testes was purchased from Sigma Aldrich Denmark A/S (ref H3506). Phosphate buffer saline (PBS) tablets without calcium and magnesium were obtained from MP Biomedicals Inc. (France).

6.2.2 *Hydrogel preparation*

HA was crosslinked according to the method described in [45] and here briefly summarized. The method consists of the following steps: (a) preparation of an alkaline solution of HA; (b) adding DVS to the solution of step (a), whereby HA is crosslinked with the DVS to form a gel; (c) the solution temperature in step (b) is heated to a temperature of 45°C for 180 minutes preferably without stirring.
It was demonstrated that a heating step was beneficial after addition of the DVS to the solution. The hydrogels were prepared with two different HA starting concentrations (5% and 6%) and three different HA/DVS weight ratios (2.5:1, 5:1 and 8:1, which corresponds to crosslinking degrees of 40, 20 and 12.5 w/w% and 80, 40 and 25 mole%, respectively). The hydrogels were prepared by dissolving HA in aqueous NaOH and then adding DVS.

6.2.3 *Viscoelastic and Injectability properties*

Viscoelastic properties of the hydrogels have been evaluated on a rotational rheometer (Gemini, Bohlin Instruments, UK) using a parallel plate geometry (PP30 cell).
Hydrogel was subjected to periodic oscillation in a dynamic experiment (Small amplitude frequency sweep tests) to evaluate the dependence of the viscoelastic parameters, such as the elastic and viscous moduli, G' and G'', upon the frequency.
In dynamic experiment the material is subjected to a sinusoidal shear strain:

$$\Upsilon=\Upsilon_0 \sin(\omega t) \quad (6.1)$$

where Υ_0 is the shear strain amplitude, ω is the oscillation frequency (which can be also expressed as $2\pi f$ where f is the frequency in Hz) and t the time. The mechanical response, expressed as shear stress τ of viscoelastic materials, is intermediate between an ideal pure elastic solid (obeying to the Hooke's law) and an ideal pure viscous fluid (obeying to the Newton's law) and therefore is out of phase respect to the imposed deformation as expressed by:

$$\tau = G'(\omega)\,\Upsilon_0 \sin(\omega t) + G''(\omega)\,\Upsilon_0 \cos(\omega t) \quad (6.2)$$

where G'(ω) is the shear storage modulus or elastic modulus and G"(ω) is the shear loss modulus or viscous.
G' gives information about the elasticity or the energy stored in the material during deformation, whereas G" describes the viscous character or the energy dissipated as heat. In particular, the elastic modulus gives information about the capability of the sample to sustain load and return in the initial configuration after an imposed stress or deformation [46].
The ratio between the viscous modulus and the elastic modulus is expressed by the loss tangent:

$$\tan\delta = G''/G' \quad (6.3)$$

where δ is the phase angle.

The loss tangent is a measure of the ratio of energy lost to energy stored in the cyclic deformation. The phase angle, δ, is equal to 90° for a purely viscous material, 0° for a pure elastic material, and 0°<δ<90° for viscoelastic materials [47].

The frequency range investigated was 0.01Hz-1 Hz. In order to identify the linear viscoelastic response range of the materials, preliminary strain sweep tests were performed on the samples, at the oscillation frequency of 1 Hz. The tests were repeated at least three times on each sample.

The tests have been carried out at the controlled temperature of 25°C by using a thermostatic bath. In order to avoid water evaporation, the humidity of the chamber containing the samples has been controlled by a humidity control accessory.

In order to evaluate the effect of sterilization process on the viscoelastic parameters, the oscillation tests were repeated on sterile samples, which were obtained by autoclaving at standard condtions (121°C, 15 min).

The effect of injection through needle was evaluated by performing the test on injected samples (gauge length, 22G*1" (1") 22G*11/2" (11/2")).

The syringeability was measured on a Texture analyZer (Stable Micro Systems, TA. XT Plus) as the force (in N) needed to inject the hydrogel through a 27G1/2 needle over a distance of 55 mm at a speed of 12.5 mm/min (0.2 mL/min) using 1 mL syringes.

Cross-linked HA hydrogel with HA concentration of 6% and HA/DVS weight ratio of 8:1 was considered and the test was repeated three times.

Moreover the syringeability of DVS crosslinked HA hydrogels prepared according to the patent [45] was compared to that of hydrogels prepared according to traditional methods, for example that not present heating step in the hydrogels preparation.

6.2.4 *Small Angle Neutron Scattering (SANS)*

The SANS studies were performed on samples characterized by HA concentration of 6% and crosslinker percentage of 1% and 10%, using a LOQ beam line with an ISIS pulsed neutron source. The LOQ beam employs neutrons at wavelengths (λ) ranging from 2.2 to 10 Å, which are detected by time-of-flight analysis and recorded with a 64-cm^2 two-dimensional detector placed at 4.1 m from the sample. Such a setup allows collecting data of scattering vector modulus $Q = 4\pi/\lambda \sin(\theta/2)$ in an interval ranging

from 0.006 to 0.32 $Å^{-1}$ [49], where θ is the scattering angle. The samples studies were contained in 1-mm path length, Hellma quartz cells at 25 °C. The experimental raw data were converted on absolute intensity following a previously reported procedure [49].

6.2.5 *In vitro degradation*

In vitro tests were performed to evaluate hydrogel degradation. A stock solution of hyaluronidase was prepared from a starting solution of 100 mg/mL of HAase in PBS (43.900 Units/mL). This solution was diluted to a concentration of 43.9 Units/mL and stored at T= -20°C prior to use. The hydrogel sample was mixed by vortex with an HAase solution in volume ratio of 10:1 to obtain a final enzyme concentration of 4 Units/mL and incubated at T=37° C for different incubation times to analyze the dependence of degradation properties upon time. In order to verify the absence of degradation phenomena due to temperature, a degradation test was carried out on control samples mixed with PBS and incubated at T=37 °C. Rheological oscillation tests were carried out immediately and after 3h, 9h, 16h and 24h. The degradation was evaluated by measuring G'/G'_0 at a frequency of 0.1 Hz as function of time. G'_0 is the G' value just after the mixing with HAase solution.

6.2.6 *Biological properties*

6.2.6.1 *Vitality and Proliferation*

Mouse embryonic fibroblast NIH3T3 cells were cultured in Dulbecco's modified Eagle's medium supplemented with 10% fetal calf serum (Gibco-BRL Life Technologies, Italy) and antibiotics (penicillin G sodium 100 U/mL, streptomycin 100 g/mL, Euroclone) at 37 °C and 5% CO_2.

For seeding on hydrogels, the cells were washed with phosphate-buffered saline (PBS) and incubated with trypsin-EDTA (0,25% trypsin,1m M EDTA, Euroclone), for 5 minutes at 37°C, re-suspended in fresh medium and statically seeded with hydrogel (30.000 cells/cm^2). The cells were cultured for 1 and 4 days.

Cell viability was evaluated by using Alamar Blue (AB) assay. AB was added to the samples (10% v/v of medium) and incubated at 37 °C for 4h.The absorbance of the

samples was measured using an spectrophotometer plate reader (multilabel counter, 1420 Victor, Perkin Elmer) at 570 nm and 600 nm.

AB is an indicator dye that incorporates an oxidation-reduction indicator that changes colour in response to the chemical reduction in growth medium, resulting from cell viability. Data are expressed as the percentage difference in reduction between treated and control cells in viability assay:

Percentage difference between treated and control cells = $(O_2 \times A_1) - (O_1 \times A_2)/ (O_2 \times P_1) - (O_1 \times P_2) \times 100$ (6.4)

where O_1 is the molar extinction coefficient (E) of oxidized alamarBlue® (Blue) at 570nm; O_2 is the E of oxidized alamarBlue® at 600nm; A_1 is the absorbance of test wells at 570nm; A_2 is the absorbance of test wells at 600nm; P_1 is the absorbance of positive growth control well (cells plus alamarBlue® but no hydrogel) at 570nm; P_2 is the absorbance of positive growth control well at 600nm.

For proliferation tests, total DNA content of NIH3T3 cells/hydrogel was assessed at 1,4 days with Quant-iT™ PicoGreen® dsDNA reagent Kit. The PicoGreen dye binds to dsDNA and the resulting fluorescence corresponds to the concentration of dsDNA in solution.The total DNA was extracted from each sample by incubating the cell layer in 500 µl of cell lysis solution (0.2% v/v Triton X-100, 10 mM Tris (pH 7.0), 1 mM EDTA) for 1h-70°C,then followed by three cycles of freeze and thaw;and assayed by following manufacturer ‘s instruction (Molecular Probes, Cat # P-7589). DNA content was determined fluorometrically at excitation wavelength of 480 nm and emission wavelength 528 nm using a microplate reader (Perckin Elmer Victor microplate reader). The relative fluorescence units were correlated with the number of cells present in the hydrogels.

6.2.6.2 *Stem cell differenziation*

The osteogenic differentiation of hMSCs was evaluated by DNA/alkaline phosphatase (ALP) activity measurement. For the DNA/ALP test, at predetermined time point the hydrogels were washed twice with ice-cold PBS, transferred to centrifuge tubes containing 300 mL cell lysis buffer (10mM Tris-HCL, 10mM NaH2PO4/NaHPO4,

130mM NaCl, 1% Triton X-100, and 10mM sodium pyrophosphate; BD Biosciences), and lysed at -4°C for 45 min. After 5 min of centrifugation, total amount of DNA was detected using Pico Green Assay (Molecular Probes), while ALP activity was measured using a biochemical assay (SensoLyte pNPP ALP assay kit; ANASPEC).

6.2.6.3 *In vivo study*

To study in vivo properties HA hydrogels characterized by HA concentration of 5% and HA/DVS w.r. of 5:1 and HA/DVS w.r. of 8:1 were prepared. HA-DVS hydrogels were mixed with physiological saline with a volume ratio of 1:1. After the hydrogels were completely homogenized with a homogenizer (T-18 basic, IKA, Tokyo, Japan) at 8000 rpm for 5 min, 1 mL of the hydrogel suspension was injected into the subcutaneous dorsum of the mice. As a control, non-modified HA solution was used.
Male Sprague-Dawley rats (3 rats/test group) were anesthetized with ketamine hydrochloride (8 mg/kg body weight) and xylazine hydrochloride (1.15 mg/kg body weight). After the injection of HA hydrogels, the rats were sacrificed in 1, 6, and 21 days, and the HA hydrogels were retrieved. General condition of the rat such us body weight and gel implant size were monitored. Furthermore erythema and edema of skin and tissue around injection site were scored.

6.3 RESULTS and DISCUSSION

6.3.1 *Hydrogels viscoelastic and injectability properties*

In figure 6.1 the dependence of the elastic and the viscous moduli upon the oscillation frequency, the so-called mechanical spectra, for the gels obtained crosslinking HA with DVS was reported; in particular as an example the mechanical spectra of hydrogel with a HA concentration of 5% and an HA/DVS weight ratio of 8:1 was reported.

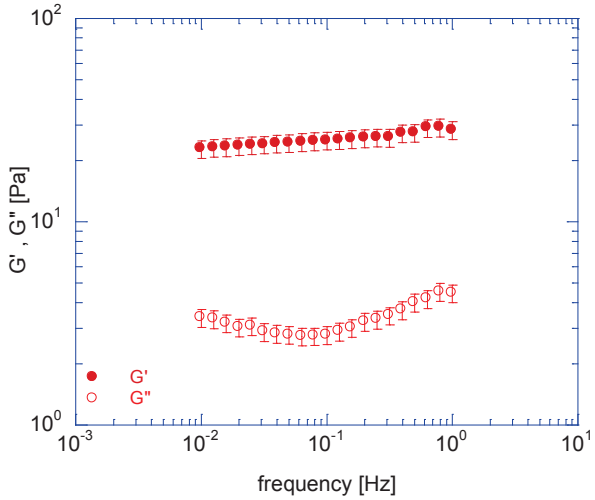

Figure 6.1: Mechanical spectra of samples characterized by HA/DVS 8:1 and [HA]=5%

From the mechanical spectra, it can be noticed that the elastic modulus is one order of magnitude higher than viscous modulus, G' is almost independent of frequency and tan δ is in the range 0.01-0.1. These samples behave as *strong gel* materials.

The overall rheological response is due to the contributions of physical crosslinks, such as electrostatic interactions and hydrogen bonds, chemical crosslinks such as covalent bonds, and to topological interactions among the HA macromolecules (entanglements). The crosslinks and entanglements bring about a reduction of the intrinsic mobility of the polymer chains that are not able to release stress; consequently the material shows a predominant elastic behavior (G'>G") and behaves as a three dimensional network where the principal mode of accommodation of the applied stress is by network deformation.

Changing HA/DVS weight ratio and HA concentration, the gels still behave as strong gels, but their rheological properties differ quantitatively. In table 6.1 the viscoelastic properties for the gels at frequency of 0.1 Hz were reported.

In fig. 6.2 the mechanical spectra of samples prepared at the same HA concentration (5%) and at different HA/DVS weight ratio (2.5:1; 5:1; 8:1) were reported. Comparing the results for the three strong gels, it can be observed that the highest elastic modulus was obtained in the case of samples characterized by a HA/DVS w.r. of 2.5:1. In particular when HA/DVS w.r. is 2.5:1 at a frequency of 0.1 Hz G' is 304.30 Pa, while for the strong gel at HA/DVS w.r. of 5:1. the elastic modulus is 56.20 Pa and for the strong gel at HA/DVS w.r. of 8:1 G' is 25.02 Pa (table 6.1). By doubling the weight

ratio (from 2.5:1 to 5:1), G' is 5.4 times lower while by raising 1.6 times the weight ratio (from 5:1 to 8:1) G' is 2.25 times lower. The decrease of the starting HA/DVS weight ratio leads to gels with improved viscoelastic properties because the elastic modulus is proportional to the number of crosslinking points, that increase with the increasing of the amount of crosslinker.

[HA] [%]	HA/DVS w.r	Viscoelastic properties @ 0.1 Hz			
		G' [Pa]	G'' [Pa]	η* [Pas]	tanδ
5	2.5:1	304.30	16.10	485.20	0.058
	5:1	56.02	3.74	89.36	0.067
	8:1	25.02	2.76	40.10	0.12
6	2.5:1	468.43	17.7	585.48	0.038
	5:1	165.85	9.05	239.17	0.055
	8:1	42.45	3.18	67.76	0.075

Table 6.1: Viscoelastic properties for the gels at frequency of 0.1 Hz

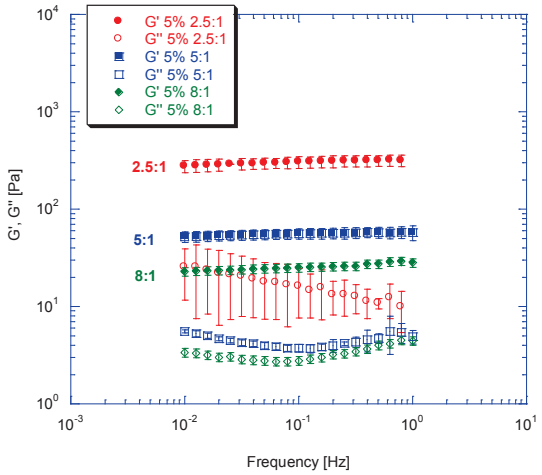

Figure 6.2: Mechanical spectra of samples at different HA/DVS weight ratio (2.5:1; 5:1; 8:1)

Also varying the starting HA concentration, the viscoelastic properties of the gels change significantly. In particular the viscoelastic properties increase with increasing of HA starting concentration for any HA/DVS weight ratio (fig. 6.3a, fig.6.3b, fig.6.3c).

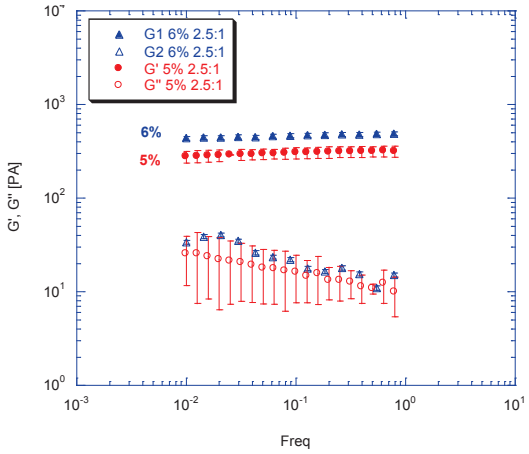

Figure 6.3 a

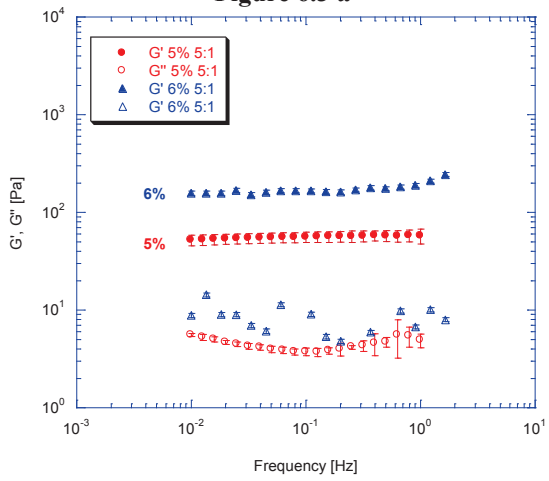

Figure 6.3 b

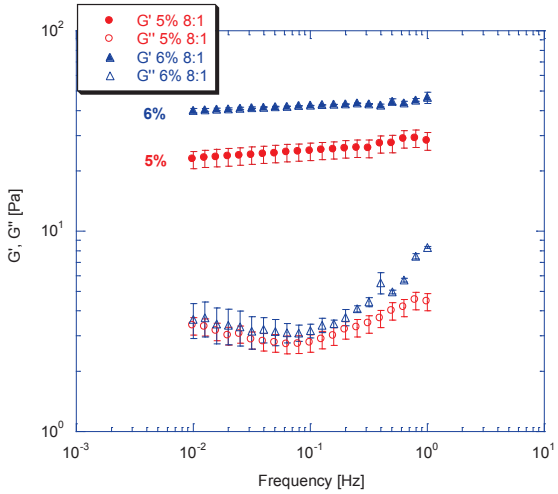

Figure 6.3 c

Figure 6.3: The mechanical spectra of samples at different HA concentrations and HA/DVS weight ratio: 6.3 a) the comparison of the mechanical spectra of samples characterized by [HA]=5% and 6% and HA/DVS weigth ratio of 2.5:1; 6.3 b) the comparison of the mechanical spectra of samples characterized by [HA]=5% and 6% and HA/DVS weigth ratio of 5:1; 6.3 c) the comparison of the mechanical spectra of samples characterized by [HA]=5% and 6% and HA/DVS weigth ratio of 8:1.

In particular for samples prepared with HA/DVS w.r. of 2.5:1, G' is 304.30 Pa when HA concentration is 5%, while it is 1.5 times higher (468.43 Pa) when HA concentration is 6%. For samples characterized by HA/DVS w.r of 5:1 it can be observed that for HA concentration of 5% G' is 56,2 Pa, while for HA concentration of 6% G' is 165,85 Pa that is about 3 times higher. When HA/DVS w.r is 8:1 for HA concentration of 5% G' is 25,02 Pa while for HA concentration of 6% G' is 42,45 Pa that is about 1.7 times higher. By decreasing the weight ratio, the effect of concentration becomes stronger. To analyze the effect of processing such as sterilization and injection through needle on hydrogels, oscillation tests on sterile and not sterile samples, before and after injection were performed.

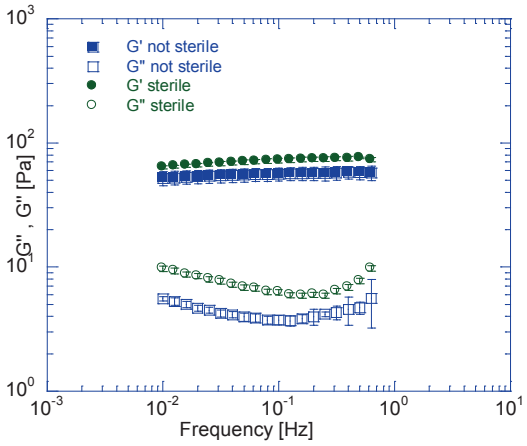

Figure 6.4 a

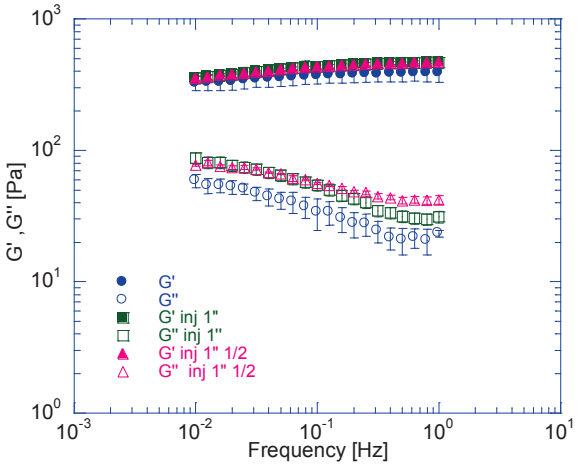

Figure 6.4 b

Figure 6.4: Effect of sterilization and injection on mechanical properties: 6.4a) the comparison of the mechanical spectra of samples before and after sterilization; 6.4 b) the comparison of the mechanical spectra of samples before and after injection through different needles.

In fig. 6.4 a the comparison between the mechanical spectra of the sterile and not sterile samples were reported. There is not statistical significant difference between the dynamic moduli before and after sterilization, so it can be concluded that the sterilization process does not affect the hydrogel viscoelastic parameters. In fig. 6.4 b the mechanical spectra of the sterilized samples are compared before and after the injection through two different needles having different gauge length, G*1" (named 1") and G*1"1/2 (named 1"1/2). It can be noticed that also the injection through the needles does not have effect on the viscoelastic parameters.

In figure 6.5 the comparison between the syringeability of the new DVS cross-linked HA hydrogels (characterized by HA concentration and HA/DVS weight ratios of 8:1), prepared according the patent [45], and that of hydrogels prepared according to traditional methods was shown.

The figure 6.5 shows that the force needed to inject the new hydrogel is lower than hydrogels prepared according to traditional methods.

Furthermore injection profile shows that there is a better stability of the applied injection force in the case of the new hydrogels than those prepared according to traditional methods.

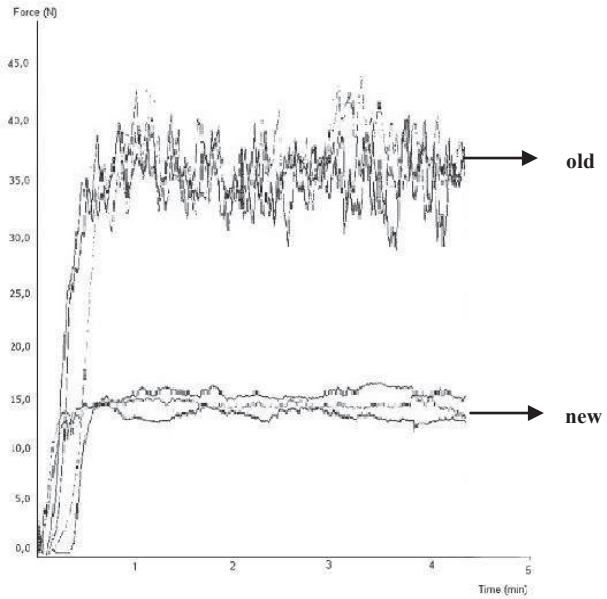

Figure 6.5: Comparision of injectability properties of new crosslinked HA hydrogels (new) and hydrogel prepared with traditional methods (old)

Since the stability of injection force is index of the sample homogeneity, the results demonstrated that the new hydrogels were more homogeneous than those obtained with traditional methods and were easier to inject through a fine needle.

6.3.2 *Network Structural Parameters*

The values of the elastic modulus can be used to estimate the parameter of the network structure [50].

As G is proportional to the number of entanglements [47], the elastic modulus can be expressed through:

$$G \cong R \cdot T \cdot z \tag{6.5}$$

where RT is the thermal energy and z is the number of the entanglements points or crosslinking point expressed in mol/volume.

The parameter z can be calculated by:

$$z \approx \frac{c}{M_e} \tag{6.6}$$

where c is the polymer concentration and M_e is the average molecular weight of the polymer segments between two entanglements.

Substituting in eq.(6.5), Me can be estimated by the following equation:

$$M_e \cong \frac{R \cdot T \cdot c}{G} \tag{6.7}$$

To calculate G by means of eq.(6.7), it has to be assumed the validity of the rubber elasticity theory and that the temporary network of gel–like material is presumed to behave as does vulcanized rubber upon stimulus of a time scale shorter than the life time of the entanglement network [51].

As the “dangling ends”, which are the polymer chain segments attached to the network by only one entanglement point, do not contribute to the G value, because they cannot store elastic energy, a correction is needed in eq.(6.7) [51]:

$$G \cong \frac{R \cdot T \cdot c}{M_e}\left(1 - 2\frac{Me}{M_n}\right) \tag{6.8}$$

where M_n is the number average molecular weight.

Using the "equivalent network model" [52], it is possible to give an estimation D_N which is the average distance between the entanglements points or crosslinking points, in a idealized "equivalent network":

$$D_N = \sqrt[3]{\frac{6 \cdot M_e}{\pi \cdot c \cdot A}} \tag{6.9}$$

where A is the Avogadro's number.

In table 6.2 the results in terms of D_N and M_e were reported. It can be noticed that the highest M_e (238292 g/mol) and highest D_n (38 nm) were displayed by sample having the lowest starting concentration and the lower density of crosslinker (HA concentration of 5% and a HA/DVS w. r. of 8:1). Indeed the sample that shows the lowest M_e (61213) and a Dn of 24 nm, is characterized by the highest starting concentration and the highest crosslinker amount (HA concentration of 6% and a HA/DVS w. r. of 2.5:1).

[HA] [%]	**HA/DVS w.r**	**G* [Pa]**	**Me (g/mol)**	**D_N (nm)**	**Degradation level [%]**
5	2.5:1	304.30	97104	26	42
	5:1	56.02	208107	34	69
	8:1	25.02	238292	38	77
6	2.5:1	468.43	61213	24	35
	5:1	165.85	110457	31	68
	8:1	42.45	203958	38	72

Table 6.2: Network parameters for HA-DVS crosslinked hydrogels

* *value of the elastic modulus at 0.1 Hz*

6.3.3 *SANS results*

Figure 6.6 reports the scattering intensities $I(Q)$ for HA hydrogels, without crosslinks and at 1% and 10% of crosslinks.

Analysis of HA crosslink-free sample reveals a quite flat profile, suggesting a very weak network. Indeed, the scattering should arise from the polymer chains that, because of the low concentration and the high level of solvation, is observed to appear flat. The situation is different in the presence of crosslinks. According to the mean-field theory of polymers in a good solvent [51, 53-54], scattering profile can be described in terms of the mesh size formed by crosslinks. It arises from the thermal fluctuations of the polymer concentration and is related to the average distance between crosslinks (the mesh size ξ): in this case in the region where $q\xi << 1$ the scattering intensities $I(Q)$ can be well described by a Lorentzian function:

$$I(Q) = \frac{I^0}{1 + Q^2\xi^2} \tag{6.10}$$

where I^0 is the limit value of the intensity at zero Q, related to the number of crosslinks per unit of volume.

Equation 6.10 has been fitted to the experimental data, and the fitting curves are reported in figure 6.6 together with the experimental data. From the least square analysis the average mesh size, ξ has been extracted and reported in table 6.3.

Crosslink percentage	$\xi(\mathrm{nm})$
1%	223±5
10%	94±6

Table 6.3: Mesh size ξ obtained for HA hydrogels at different crosslinks percentage, in D_2O, estimated from the fitting of equation 6.10.

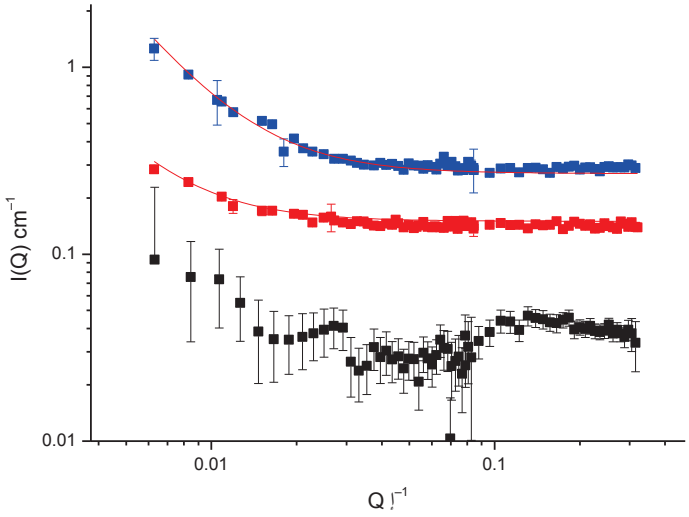

Figure 6.6: Scattering intensities $I(Q)$ obtained at 25°C for HA hydrogel samples: (□) without crosslinks, (□) 1% and (□) 10% of crosslinks. Lines correspond to fitting of equation 6.10 to experimental data.

As it can be observed, the crosslinks appear to compact the network, being the mesh size reduced of a factor 2 when their number is increased from 1% to 10%.

6.3.4 *In vitro degradation properties*

In order to evaluate hydrogels degradation, in vitro tests were performed. In figures 6.7a and 6.7b the degradation test results were reported. In figure 6.7a a comparison between the elastic modulus spectra evaluated at different degradation times, for the sample characterized by a HA concentration of 5% and a HA/DVS weight ratio of 5:1, was shown. From the results, it can be noticed that, at any frequency, G' decreases with the increase of degradation time, meaning that in presence of HAase, the degradation occurs.

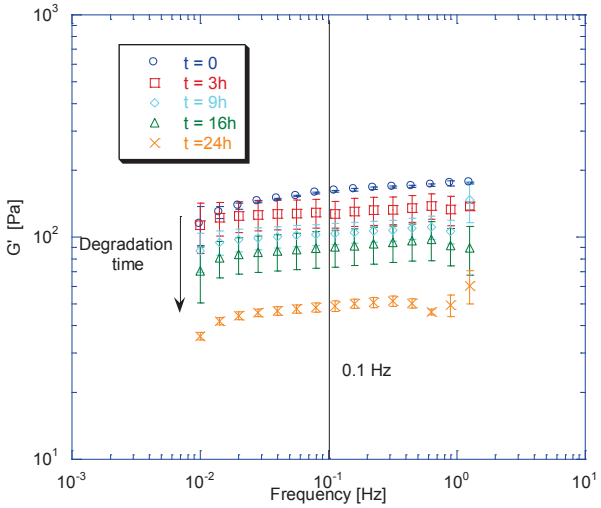

Figure 6.7 a

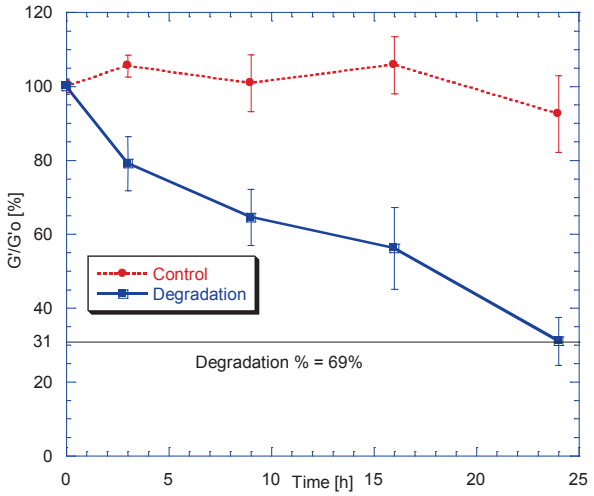

Figure 6.7 b

Figure 6.7: In vitro degradation results: fig 6.7 a) the comparison of between the elastic modulus spectra evaluated at different degradation time (0, 3, 9, 16, 24 h); fig. 6.7 b) The evaluation of the percentage G'/G'_o in function of time.

The evaluation of the ratio G'/G'_0 at frequency 0.1Hz in function of time, for an example sample, was reported in figure 6.7b; in particular this figure shows a degradation curve and a control curve, where the degradation curve indicates a quantitative evaluation of the percentage of degradation for each time, and the control curve shows that in absence of HAase, no degradation was observed. For this sample after 24 h of incubation, the percentage of degradation level is about 70%.

Table 6.2 shows a summary of degradation tests in which the degradation percentage for each sample after 24 h of incubation was reported. It can be noticed that by increasing HA concentration of the hydrogel from 5% to 6%, the percentage of degradation level

decreases; keeping constant HA concentration and decreasing the HA/DVS weight ratio, the hydrogel shown a decreasing of the percentage of degradation level up to 35%.

6.3.5 *Biological properties*

6.3.5.1 *In vitro study*

The direct cytotoxicity evaluation results on bulk hydrogels were shown in figure 6.8. In this graph, the percentage difference in reduction of Alamar Blue between hydrogels and control versus time was reported. The vitality of cells in contact with hydrogels is in the range 70 - 90% compared to negative control, after 24 hours. After 4 days of contact the vitality of the samples increases up to 100- 120%. The assay was stopped at 4 day because the cell proliferation was terminated by contact inhibition.

In order to evaluate the proliferation of cells, the results of the PICO green test were reported in fig. 6.9 and expressed as the number of cells alive on the hydrogels after 1 and 4 days.

From fig.6.8-6.9 it can be concluded that the vitality and proliferation of cells placed in contact with the hydrogel is greater than control cells. This behaviour was shown for both HA concentrations, 5% and 6%, and for all considered HA/DVS weight ratio, 2.5:1, 5:1, 8:1. The in vitro tests demonstrate that the hydrogels considered here show a good cellular response and the presence of DVS is not cytotoxic to cells.

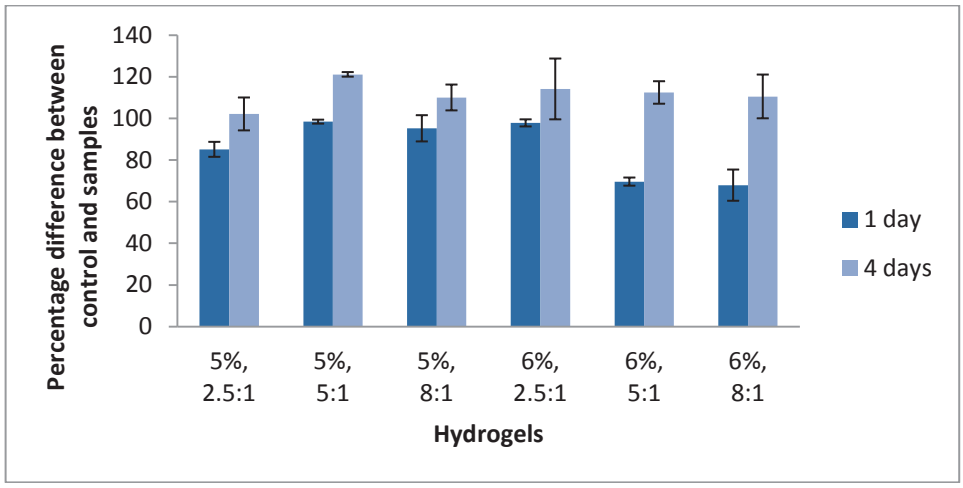

Figure 6.8: Vitality tests: percentage of reduction of Alamar Blue between hydrogel and controls. The hydrogels are characterized by different HA concentrations (5% and 6%) and different HA/DVS weight ratio (2.5:1, 5:1, 8:1).

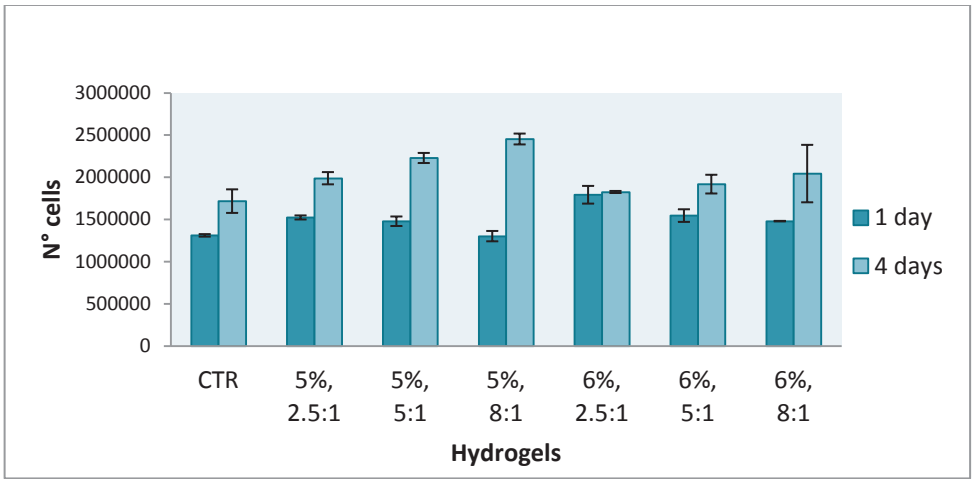

Figure 6.9: Proliferation tests after 1 and 4 days; the hydrogels are characterized by different HA concentrations (5% and 6%) and different HA/DVS weight ratio (2.5:1, 5:1, 8:1).

6.3.5.2 *Stem cells differentiation*

The stem cell differentiation was evaluated by the determination of the ratio between the quantity of ALP and the quantity of DNA after that the cells were placed in contact with the hydrogels for 7, 14 and 21 days. The results were reported in table 6.4.

From the biological results it can be noticed that for all samples the trend of ALP ng/DNA ng is the same: the values of ALP ng/DNA ng present a peak after 14 days that the mesenchimal stem cells were put in contact with the hydrogels.

Starting HA concentration	HA/DVS Weight ratio	ALP ng/DNA ng 7days	ALP ng/DNA ng 14days	ALP ng/DNA ng 21days
6%	2.5:1	9.85	14.53	5.45
6%	5:1	7.56	13.52	3.3
6%	8:1	10.01	15.33	5.22
5%	2.5:1	7.68	9.25	4.05
5%	5:1	6.42	7.52	2.71
5%	8:1	8.31	9.82	3.02
MSC VI (CTR)		6.51	8.25	2.45

Table 6.4: Biological properties in presence of osteogenic medium

Varying the starting HA concentration, the biological properties change. In particular for any weight ratio the values of ALP ng/DNA ng, when the HA concentration is 6%, are higher than that when the HA concentration is 5%. So the presence of HA influences positively the activity of the cells.

6.3.5.3 *In vivo study*

From in vivo study it results that there was a comparable body weight gain for all the rat groups, no evidence of erythema or inflammation around HA hydrogels (figures 6.10 - 6.11) in any groups and slight swelling of the gel implant following injection.

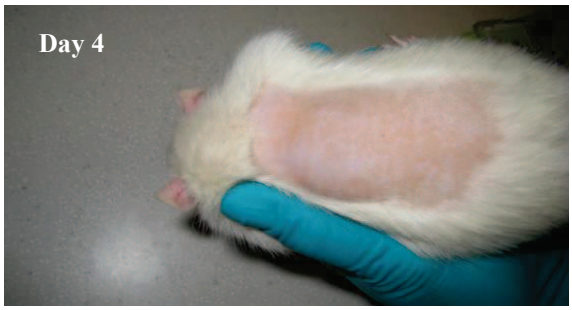

Figure 6.10: visual observation 4 days after the injection of a moderately crosslinked HA implant

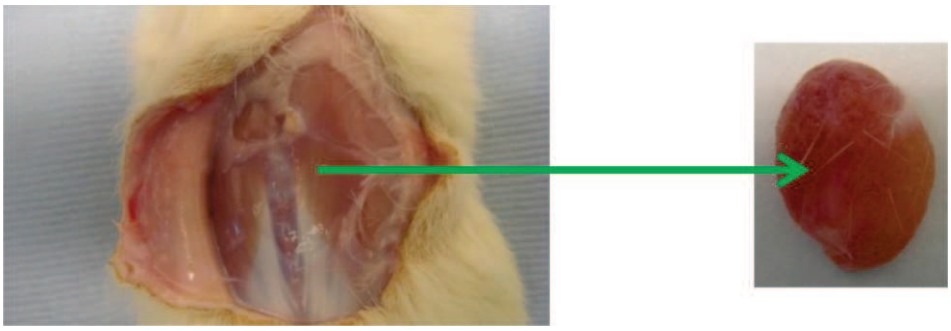

Figure 6.11: Removal of moderately crosslinked HA hydrogel at day 21

Residence time of the hydrogel is a function of the crosslinking degree. Non-modified HA is resorbed 1 day after injection; crosslinked HA hydrogels at HA/DVS w.r. of 5:1 and HA/DVS w.r. of 8:1 are still present at the injection site at day 21 (figure 6.12).

The remarkable difference in the residence time between non modified HA and HA crossliked hydrogels demonstrated that the chemical crosslinking was an effective way to increase the stability against enzymatic degradation of HA.

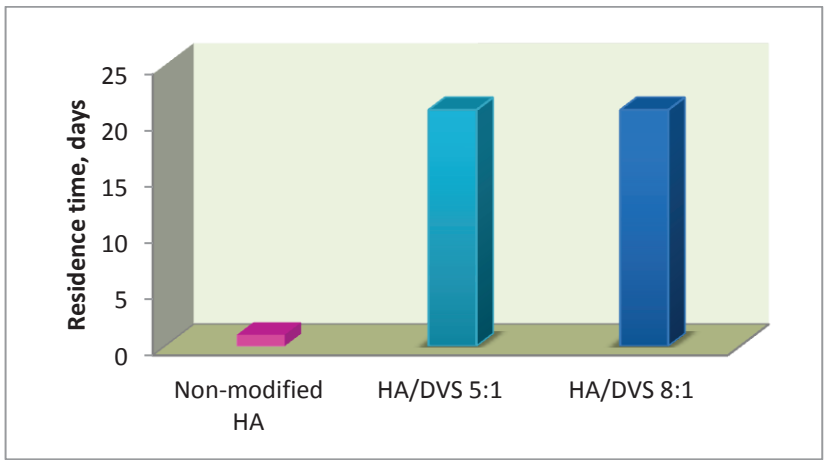

Figure 6.12: Residence time for non modified HA, crosslinked HA hydrogels at HA/DVS w.r. of 5:1 and HA/DVS w.r. of 8:1

6.4 CONCLUSIONS

HA-DVS crosslinked hydrogels based on a simple, reproducible and safe process that does not employ any organic solvents, were developed. Owing to an effective purification step, the resulting transparent and homogeneous hydrogels do not contain any detectable residual crosslinking agent and are easier to inject through a fine needle. These hydrogels exhibit a rheological behavior typical of a strong gel and show improved viscoelastic properties by increasing HA concentration and decreasing HA/DVS weight ratio. Furthermore it was demonstrated that processes such as sterilization and extrusion through clinical needles do not imply significant alteration of viscoelastic properties. From the SANS tests it resulted that the crosslinks appear to compact the network, being a reduction of the mesh size by increasing the crosslinker amount. In vitro and in vivo HA hydrogel degradation tests demonstrated that these new hydrogels show a good stability against enzymatic degradation, that increases by increasing HA concentration and decreasing HA/DVS weight ratio. Finally the hydrogels show a good biocompatibility confirmed by in vitro and in vivo tests.

REFERENCES

[1] Hoffman A. S. Hydrogels for biomedical applications. Advanced Drug Delivery Reviews, 2012; 64, 18–23.

[2] Borzacchiello A., Mayol L., Ambrosio L., Garskog O., Dahlqvist A.. Rheological Characterization of Vocal Folds after Injection Augmentation in a Preliminary Animal Study, J. of Bioactive and Compatible Polymers, 2004; 19, 331-341.

[3] Jia X., Yeo Y., Clifton R. J., Jiao T., Kohane D. S., Kobler J. B., Zeitels S. M., Langer R. Hyaluronic Acid-Based Microgels and Microgel Networks for Vocal Fold Regeneration. Biomacromolecules 2006; 7, 3336-3344.

[4] Gatej I., Popa M.,and Rinaudo M. Role of the pH on Hyaluronan Behavior in Aqueous Solution. Biomacromolecules 2005; 6, 61-7.

[5] Lapcık L., De Smedt Jr. S., Demeester J., Chabrecek P. Hyaluronan: Preparation, Structure, Properties, and Applications. Chemical rewiew 1998; 98, 2663-84.

[6] Ambrosio L., Borzacchiello A., Netti P. A., Nicolais L. Rheological properties of hyaluronic acid based solutions. Polymeric Materials Science and Engineering, 1998; 79, 244-5.

[7] Ambrosio L., Borzacchiello A., Netti P. A., Nicolais L., Rheological study on Hyaluronic acid and its derivatives solutions. J. of Macromolecular Science-Pure and Applied Chemistry, 1999, A36 7&8, 991-1000.

[8] Barbucci R., Ruoppoli R., Borzacchiello A., Ambrosio L. Synthesis, chemical and rheological characterisation of new hyaluronic based hydrogels. Journal of Biomaterials Science Polymer Edition, 2000; 11(4), 383-99.

[9] Onheit Gary D. M, Yle K, Oleman M. C. Hyaluronic acid fillers. Dermatologic Therapy, 2006; 19, 141–50.

[10] Borzacchiello A., Netti P. A, Ambrosio L., Nicolais L., Hyaluronic acid derivatives mimic the rheological properties of vitreous body. New Frontiers in Medical Sciences: Redefining Hyaluronan, Elsevier: Amsterdam, 2000; 195-202. ISSN: 0531-5131.

[11] Borzacchiello A., Ambrosio L., Network formation of low molecular weight hyaluronic acid derivatives, Journal of Biomaterials Science Polymer Edition, 2001; 12(3), 307-16, ISSN 09020-5063.

[12] Barbucci R., Lamponi S., Borzacchiello A., Ambrosio L., Fini M., Torricelli P., Giardino R. Hyaluronic acid hydrogel in the treatment of osteoarthritis, Biomaterials 2002; 23(23), 4503-13. ISSN: 0142-9612.

[13] Xin X., Borzacchiello A., Netti P. A., Ambrosio L., Nicolais L., Hyaluronic Acid Based Semi Interpenetrating Materials, J. Biomater. Sci. Polymer Edn, 2004; 15(9), 1223-36.

[14] Mori M., Yamaguchi M., Sumitomo S., Takai Y. Hyaluronic-based biomaterials in tissue engineering. Acta Histochem. Cytochem, 2004; 37 (1), 1-5.

[15] Borzacchiello A., Mayol, L., Gaerskog, O., Dahlqvist, A., Ambrosio, L. Evaluation of injection augmentation treatment of hyaluronic acid based materials on rabbit vocal folds viscoelasticity. Journal of Materials Science: Materials in Medicine 2005; 16(6), 553-7.

[16] Borzacchiello A., Mayol L., Ramires P.A., Di Bartolo C., Pastorello A., Ambrosio L. Milella E., Structural and rheological characterization of hyaluronic acid-based scaffolds for adipose tissue engineering, Biomaterials 2007; 28, 4399–408.

[17] Fusco S., Borzacchiello A., Miccio L., Pesce G., Rusciano G., Sasso A., Netti P. A. High frequency viscoelastic behaviour of low molecular weight hyaluronic acid water solutions. Biorheology, 2007; 44, 403-18.

[18] Borzacchiello A., Mayol L., Schiavinato A., Ambrosio L., Effect of hyaluronic acid amide derivative on equine synovial fluid viscoelasticity. Journal of biomedical materials research, 2010; Part A 92(3), 1162-70.

[19] Volpi N., Schiller J., Stern R., Soltés L. Role, Metabolism, Chemical Modifications and Applications of Hyaluronan. Current Medicinal Chemistry, 2009; 16, 1718-1745.

[20] Gustafson S., Hyaluronan in drug delivery. The chemical, biology and medical application of the hyaluronan and its derivatives, 1998; 72, 291-304.

[21] Kogan G., Soltes L., Stern R., Gemeiner P. Hyaluronic acid: a natural biopolymer with a broad range of biomedical and industrial applications. Biotechnol Lett 2007; 29, 17–25.

[22] Hemmrich K., von Heimburg D., Rendchen R., Di Bartolo C., Milella E., Pallua N. Implantation of preadipocyte-loaded hyaluronic acid-based scaffolds into nude mice to evaluate potential for soft tissue engineering, Biomaterials, 2005; 26(34), 7025-7037.

[23] Kablik J., Monheit G. D., Yu L., Chang G., Gershkovich J. Comparative Physical Properties Of Hyaluronic Acid Dermal Fillers. Dermatol Surg 2009; 35, 302–312.

[24] Dahlqvist A., Garskog O., Laurent C., Hertegard S., Ambrosio L., Borzacchiello A. Viscoelasticity of rabbit vocal folds after injection augmentation, Laryngoscope, 2004; 114(1), 138-42.

[25] Widner B., Behr B., Von Dollen S., Tang M., Heu T., Sloma A., Sternberg D., DeAngelis P.L., Weigel P.H., Brown S. Hyaluronic acid production in bacillus subtilis. Appl. Environ. Microbiol., 2005; 71, 3747-3752.

[26] O'Regan M., Martini I., Crescenzi F., De Luca C., Lansing M. Molecular mechanisms and genetics of hyaluronan biosynthesis. Int J Biol Macromol, 1994; 16(6), 283-286.

[27] Borzacchiello A., Ambrosio L. Network formation of low molecular weight hyaluronic acid derivatives. Journal of Biomaterials Science Polymer Edition, 2001; 12(3), 307-316.

[28] Price R. D., Berry MG, Navsaria H.A. Hyaluronic acid: the scientific and clinical evidence. Journal of Plastic, Reconstructive & Aesthetic Surgery, 2007; 60, 1110-1119.

[29] Ambrosio L., Borzacchiello A., Netti P. A., Nicolais L. Rheological study on hyaluronic acid and its derivative solutions. Journal of macromolecular science, part a: pure and applied chemistry, 1999; 36 (7-8), 991-1000.

[30] Monheit G.D., Coleman K.L. Hyaluronic acid fillers. Dermatologic Therapy, 2006; 19, 141–150.

[31] Matarasso S.L., Carruthers J.D., Jewell M.L. Consensus recommendations for soft-tissue augmentation with nonanimal stabilized hyaluronic acid (Restylane). Plastic & Reconstructive Surgery, 2006;117 (3), 3S–34S.

[32] Tezel A., Fredrickson G.H. The science of hyaluronic acid dermal fillers. J Cosmet Laser Ther, 2008; 10, 35–42.

[33] Laurent U.B.G., Reed R.K. Turnover of hyaluronan in the tissues. Adv Drug Deliv Rev, 1991; 7, 237–56.

[34] Almond A. Hyaluronan. Cell Mol Life Sci 2007; 64, 1591–6.

[35] Oh E., Park K., Kim K.S., Kim J., Yang J., Kong J., Lee M.Y., Hoffmanc A.S., Hahna S. K. Target specific and long- acting delivery of protein, peptide, and nucleotide therapeutics using hyaluronic acid derivatives, Journal of Controlled Release, 2010; 141(1), 2–12.

[36] Schneider A., Picart C., Senger B., Schaaf P., Voegel J., Frisch, B. Layer-by-layer films from hyaluronan and amine-modified hyaluronan, Langmuir, 2007; 23(5), 2655–2662.

[37] Pelletier S., Hubert P., Payan E., Marchal P., Choplin L., Dellacherie E. Amphipilic derivatives of sodium alginate and hyaluronate for cartilage repair: Rheological properties. J Biomed Mater Res, 2001; 54,102–108.

[38] Bellini D., Topai A. Amides of hyaluronic acid and the derivatives thereof and a process for their preparation, WO2000001733 A1. 1999.

[39] Liu Y., Zheng Shu X., Prestwich G.D. Biocompatibility and stability of disulfide-crosslinked hyaluronan films. Biomaterials, 2005; 26, 4737-4746.

[40] Baier Leach J., Bivens K.A., Patrick C.W.Jr., Schmidt C.E. Photocrosslinked hyaluronic acid hydrogels: natural, biodegradable tissue engineering scaffolds. Biotechnol.Bioeng., 2003; 82, 578-589.

[41] Shu X.Z., Liu Y., Luo Yi, Roberts M.C., Prestwich G.D. Disulfide Cross-Linked Hyaluronan Hydrogels. Biomacromolecules, 2002; 3, 1304-1311.

[42] Banerji S., Wright A.J., Noble M., Mahoney D.J, Campbell I.D, Day A.J., Jackson D.G. Structures of the Cd44-hyaluronan complex provide insight into a fundamental carbohydrate-protein interaction, Nat Struct Mol Biol., 2007; 14(3), 234-239.

[43] Bergman K., Elvingson C., Hilborn J., Svensk G., Bowden T. Hyaluronic acid derivatives prepared in aqueous media by triazine-activated amidation. Biomacromolecules, 2007; **8**(7), 2190–2195.

[44] Pelletier S., Hubert P., Lapicque F., Payan E., Dellacherie E. Amphiphilic derivatives of sodium alginate and hyaluronate: Synthesis and physico-chemical properties of aqueous dilute solutions, Carbohydrate Polymers, 2000; 43(4), 343–349.

[45] Longin F., Schwach-Abdellaoui K.. Method of cross-linking hyaluronic acid with divinylsulfone, US Patent No. 0338100, 2013.

[46] Ferry JD. Viscoelastic Properties of Polymers. Wiley, New York (1970).

[47] D'Errico G., De Lellis M., Mangiapia G., Ortona O., Fusco S., Borzacchiello A., Ambrosio L. Structural and mechanical properties of UV photocrosslinked poly(N-vinyl-2- pyrrolidone) hydrogels. Biomacromolecules, 2008; 9 (1), 231-40.

[48] Balazs E.A., Leshchiner A. Crossliked gels of hyaluronic acid and products containing such gels, U.S. Pat. No. 4,582,865, 1984.

[49] Heenan R. K., Penfold J., King S. M.. SANS at Pulsed Neutron Sources: Present and Future Prospects. Journal of Applied Crystallography, 1997; 30, 1140-1147.

[50] De Smedt S.C., Dekeyser P., Ribitsch V., Lauwers A., Demeester J. Viscoelastic and transient network properties of hyaluronic acid as a functionof the concentration. Biorheology, 1993; 30, 31-41.

[51] Flory P.J., Principles of Polymer Chemistry, Cornell University Press, Ithaca, N.Y., 1953.

[52] Schurz J., Rheology of polymer solutions of the network type. Progress in Polymer Science, 1991; 16(1), 1-53.

[53] de Gennes P.G., Scaling Concepts in Polymer Chemistry, Cornell University Press, Ithaca, N.Y., 1979.

[54] Koberstein J.T., Picot **C.,** Benoit H. Light and neutron scattering studies of excess low-angle scattering in moderately concentrated polystyrene solutions**.** Polymer, 1985; 26, 673-681.

-SUMMARY AND OUTLOOK-

CHAPTER 7

Summary and outlook

7.1 Summary

This project was aimed to provide biocompatible hyaluronic acid (HA) based systems for applications in regenerative medicine and drug delivery.

The choice of HA as starting material for the production of advanced biomaterials was due to the fact that it have attracted a great deal of interest among the researchers for its peculiar properties particularly suitable for the preparation of interesting biocompatible systems (see Chapter 1).

In particular in the first part of this thesis HA coated biodegradable nanoparticles as novel drug carriers for tumor targeting were developed. Nanoparticles were prepared by a single emulsion technique and shown a spherical shape and a size ranging from 170 to 300 nm (see Chapter 2). The amphiphilic nature of these nanostructured devices, characterized by a inner hydrophobic core and a hydrophilic shell, allowed to obtain a drug encapsulation efficiency of 61.2% and in vitro sustained Irinotecan release up to 24 days (see Chapter 3).

In the second part of this thesis novel self-associative nanostructured soft carriers based on an amphiphilic hyaluronic acid derivative were developed. The new syntetized amphiphilic HA derivative is an octenyl succinic anhydride (OSA) modified HA, obtained through a simple reaction in an aqueous medium involving exclusively HA hydroxyl groups. This derivative was able to self assemble into micelles characterized by a spherical shape and diameter around 100 nm. In the perspective of using these novel devices as viscosupplementation products, the rheological properties were evaluated and it was demonstrated that OSA-HA solutions could be suitable tools to be used in viscosupplentation therapy, exhibiting a viscoelastic behavior similar to that of synovial fluid (see Chapter 4). Furthermore thanks to the presence of hydrophobic

domains along the molecule backbone, these nanosized structures were able to load a hydrophobic drug, triamncinolone, usually used for the treatment of joint diseases, and release it with a controlled kinetic (see Chapter 5).

In the third part of this thesis stable structures at macroscale obtained crosslinking HA molecules to form injectable hydrogels for regenerative applications were developed.

HA hydrogels, produced crosslinking HA molecules with divinyl sulfone (DVS), were based on a simple, reproducible and safe process that does not employ any organic solvents. Owing to an effective purification step, the resulting homogeneous hydrogels do not contain any detectable residual crosslinking agent and are easier to inject through a fine needle. HA hydrogels were characterized in terms of their viscoelastic and network structural properties. They exhibit a rheological behavior typical of a strong gel and show improved viscoelastic properties by increasing HA concentration and decreasing HA/DVS weight ratio. Furthermore it was demonstrated that processes, such as sterilization and extrusion through clinical needles, do not imply significant alteration of viscoelastic properties. In vitro and in vivo HA hydrogel degradation tests demonstrated that these new hydrogels show a good stability against enzymatic degradation, that increases by increasing HA concentration and decreasing HA/DVS weight ratio. Furthermore *in vitro* and *in vivo* studies demonstrated that these materials are biocompatible and non-toxic, and show a long *in vivo* residence time (see Chapter 6).

7.2 Future work

In the perspective of using HA coated biodegradable nanoparticles for concrete applications in cancer therapy and OSA-HA nanogels for the treatment of joint diseases, it could be necessary to obtain a better control of their polydispersity. Furthermore future work will be devoted to confirm the validity of these systems with *in vitro* and *in vivo* studies.

Finally the HA based hydrogels will be further investigated for various drug delivery and tissue engineering applications.

APPENDIX

I. CONFERENCES

- 4th China-Europe Symposium on biomaterials in regenerative medicine, Sorrento, Italy 1-4 July 2013.

- XXV Symposium of the European society for biomaterials, 8-12 September 2013, Madrid (SPAIN).

II. PUBBLICATIONS

II.1 Posters

- A. Borzacchiello, L. Russo, B. M. Malle, M. Mellergaard, K. Schwach-Abdellaoui, L. Ambrosio. Development of a new cross-linked hyaluronic acid derived from bacillus subtilis towards biomedical applications. Advances in Polimer based Materials Capri, Italy 29 Maggio - 1 Giugno 2011

- A. Borzacchiello, L. Mayol, M. Biondi, C. Serri, L. Russo, L. Ambrosio, Biodegradable nanoparticles coated by hyaluronic acid for delivery of chemotherapeutic drug, 4th China-Europe Symposium on biomaterials in regenerative medicine, Sorrento, Italy 1-4 July 2013.

II.2 Oral presentations

- A. Borzacchiello, L. Mayol, M. Biondi, L. Russo, J. Roubroeks, B. M. Malle, K. Schwach-abdellaoui, L. Ambrosio, Novel amphiphilic HA derivatives for hydrofhobic drug delivery, 4th China-Europe Symposium on biomaterials in regenerative medicine, Sorrento, Italy 1-4 July 2013.

- A. Borzacchiello, L. Mayol, M. Biondi, L. Russo, B. M. Malle, K. Schwach-abdellaoui, J. Roubroeks, Novel amphiphilic HA derivatives: potential solubilizing and controlling the hydrophobic drug release, XXV Symposium of the European society for biomaterials, 8-12 September 2013, Madrid (SPAIN)

- L. Mayol, M. Biondi, C. Serri, L. Russo, A. Borzacchiello, L. Ambrosio, M. I. La Rotonda, Hyaluronic Acid-coated biodegradable naanoparticles for tumor targeting, XXV Symposium of the European society for biomaterials, 8-12 September 2013, Madrid (SPAIN).

II.3 ARTICLES AND BOOK CHAPTERS

Portions of this thesis have been adapted from the following article and book chapters that were cowritten by the author:

- L. Mayol, M. Biondi, L. Russo, B. M. Malle, K. Schwach-Abdellaoui, A. Borzacchiello. Amphiphilic Hyaluronic Acid derivatives towards the design of micelles for the sustained delivery of hydrophobic drugs. *Carbohydrate Polymers,* 2014, 102, 110– 116.

- L. Russo, M. A. Autiello, B. M. Malle, K. Schwach-Abdellaoui, A. Borzacchiello Hyaluronic acid: regenerative medicine and drug delivery. *Encyclopedia of Biomedical Polymers and Polymeric Biomaterials*, edited by Taylor & Francis. *Publication planned in August 2014.*

- A. Borzacchiello, L. Russo, S. Zaccaria, L. Ambrosio. Physical And Chemical Hyaluronic Acid Hydrogels And Their Biomedical Applications. *Polysaccharide hydrogels: characterization and biomedical applications* edited by Pietro Matricardi, Franco Alhaique and Tommasina Coviello. Pan Stanford publishing. *In press.*

Other papers cowritten by the author not included in this thesis:

- S. Santoro, L. Russo, V. Argenzio, A. Borzacchiello. Rheological properties of cross-linked hyaluronic acid dermal fillers. *J Appl Biomater Biomech* 2011; 9, 2, 127-136.

Other book chapters cowritten by the author not included in this thesis:

- L. Russo, S. Zaccaria, M. A. Autiello and A. Borzacchiello. Hydrogels for biomedical applications. *Biomedical Composites Materials Manufacturing and Engineering,* edited by J. Paulo Davim. De Gruyter, 2013, Chapter 8, 141-168.

- A. Borzacchiello, L. Russo, L. Ambrosio. Hyaluronic acid based hydrogels at micro and macro scale. *Natural Biomaterials for Advanced Devices and Therapies,* Wiley book edited by Rui Reis and Numo Neves. *In press.*

- A. Borzacchiello, M.A. Autiello, L. Russo, L. Nicolais. Novel biomimetic design for composite materials. *Encyclopedia of Composites* Wiley book edited by Luigi Nicolais and Assunta Borzacchiello (2^{nd} Edition), 2012, 3, 2016-2023.

II.4 Articles in preparation

- M. Biondi, L. Mayol, L. Russo, C. Serri, A. Borzacchiello, L. Ambrosio. Hyaluronic Acid-Coated Biodegradable Nanoparticles For Tumor Targeting.

- L. Russo, B. M. Malle, M. Mellergaard, K. Schwach-Abdellaoui, A. Borzacchiello. Development of a new cross-linked hyaluronic acid derived from bacillus subtilis towards regenerative medicine.

- L. Russo, B. M. Malle, M. Mellergaard, K. Schwach-Abdellaoui, A. Borzacchiello. Optimization of a fermentation derived biopolymer for applications as bioadhesive systems.

III. TEACHING

III.1 Assistentship in bachelor's courses

Biomaterials, bachelor's course of Biomedical Engineering, University of Naples Federico II. March 2011-June 2011.

III.2 Co supervision

- Master's thesis in Biomedical Engineering University of Naples Federico II, *Caratterizzazione E Ottimizzazione Di Adesivi A Base Di Polimeri Naturali Per Applicazioni Biomedicali*. Candidate: Luigi Brancato Matr. 080 / 274, academic year 2010-2011.

- Bachelor's thesis in Biomedical Engineering University of Naples Federico II, *Idrogeli Polimerici Per Applicazioni Biomedicali*. Candidate: Alessia Cristiano Matr. N36/345, academic year 2011/2012.

- Bachelor's thesis in Biomedical Engineering University of Naples Federico II, *Caratterizzazione Ed Ottimizzazione Di Adesivi Chirurgici A Base Di Albumina*. Candidate: Michela Costabile Matr. 691/894, academic year 2011/2012.

- Master's thesis in Biomedical Engineering University of Naples Federico II, *Nanocarrier A Base Di Acido Ialuronico Anfifilico Per Il Rilascio Controllato Di Farmaco*. Candidate: Luisa Di Donato Matr. M54/016, academic year 2011/2012.

- Master's thesis in Biomedical Engineering University of Naples Federico II, *Nanocarriers A Base Di Acido Ialuronico Per Applicazioni Biomedicali*. Candidate: Celeste Manfredonia Matr. M54/9, academic year 2012/2013.

- Bachelor's thesis in Biomedical Engineering University of Naples Federico II, *Nanoparticelle A Base Di Acido Ialuronico Per Applicazioni Biomedicali*. Candidate: Mirco Frosolone Matr. 691/497, academic year 2012/2013.

ACKNOWLEDGEMENTS

This thesis has been much more of the results that have been presented, it has been for me a maturation process at different levels and it would not have been possible without the help and support of many people.

I would like to thank first of all Eng. Assunta Borzacchiello to gave me the opportunity to work on this challenging thesis project.

I am sincerely and particularly indebted to Laura Mayol and Marco Biondi for their precious guidance and advice, and for providing me with useful tips.

I would like to express my gratitude to Prof. Paolo A. Netti who accepted to be my tutor.

I am grateful to the people of Novozymes Biopharma, who collaborated with me in part of this project.

A special thank goes to Birgitte M. Malle and Khadija Schwach-Abdellaoui. Their professionality and expertise provided me with valuable help and support.

I also thank Johannes Roubroeks, Sara Poulsen and Martin Mellergaard with whom scientific discussions were always very stimulating.

I would like to thank Cristina del Barone to perform the acquisition of TEM micrographs of my nanoparticles and Massimiliano Porzio to help me in HPLC measurements. I also thank Stefania Zeppetelli which was of great help with my cell culture experiments, both in practical and interpretation issues.

I would like to thank all the people at the Department of Materials and Production Engineering at the University of Naples. First of all I would like to thank my dear friend Daniela, you are a really crazy and perhaps I adore you for this. Thanks to Mauro, I was a nuisance, I know it! Thanks for listening me always. Thanks to Antonio for giving me moments of carefreeness.

A special thanks to my dear friend Tinie, thanks for your wise tips, both professional and personal. Although you are in the other part of the world, I felt you so close. Thanks for being so nice and kind with me, always.

Thanks to Sabrina, we worked together only in the last year of this walk, but it was so easy to grow fond of you. With you I tasted the beauty of working together, sharing the same goal. You were much more important than you can imagine, now I have faith in people again. Thank you to be a friend and not only a colleague.

I would like to thank Mariagrazia for supporting me as only a “mother” can do, and for giving me useful advice for my personal life as only a friend can do.
A special thank to Giorgio, your advices was so important for me. Thanks to Luigi for putting up with me in our travels back home.
I also thank Luigi, Michele, Valentina, Rosaria, Giuseppe, Roberto, Alfredo, Ugo, Teresa, Marica, Marietta, Ines, Diogo, Mario, each one of you gave me something.
Moreover I would like to thank all the people of faculty of Farmacy, in particular Carla, Virginia, Sara, Simona, Fiammetta, Giovanni and Vittorio for welcoming me and making me feel at home.
I would also like to thank the security guards of our new institute IPCB-CNR, Antonino e Massimo, for their extreme and daily kindness.
I could not thank all the people who shared my life outside the lab over these last years.
I thank all my friends and especially Ilaria, Francesca, Teresa, Nicola e Biagio, because I know they are always there if I need them. A special thanks goes to my family for its unlimited support. Thanks to my mom, for visceral love that you give me every day, always ...and to my dad for the values you taught me.
Thanks to my brother Francesco, you've always been a model for me. Thanks to my brother Attilio, for tolering my hysteria and amusing me for our crap.
Thanks especially to Diletta. No one like you was able to live down everything and completely disconnect with reality, almost as if it were a magic ... inviting me into your world " with the exclusive", giving me your love so unconditional and pure ... Thank you my little…
Also thanks to Gabriel. You do not know yet speak, but you can not imagine how great it can be the power of a small smile.
And finally, thanks to Giovanni. The fruit of this work for much I owe it to you ... as I would have done without you,... no more of you I was able to understand me so deeply, to support me always and to put up with me in my moments of hysteria (and in these three years there have been many!) ... Thank you for always believing in me, not only in these three years, but since I was little more than a child...you've always been there to support me in every disappointment and rejoice with me for every little success.
You are an essential element in my life... indispensable...Thanks for everything, Giovannidilè!
And it is paradoxical to think that all started with this sentence...
"Wings commence to beating"

Well ... " I hope!"